Dictyostelium cell-fate bias is regulated antagonistically by the Retinoblastoma orthologue RblA and the cyclin-dependent kinase Cdk1

Kimchi-Audrey Strasser

A Thesis

in the Department

of

Biology

Presented in Partial Fulfillment of the Requirements
For the Degree of
Doctor of Philosophy (Biology) at
Concordia University
Montreal, Quebec, Canada

February 2012

CONCORDIA UNIVERSITY
SCHOOL OF GRADUATE STUDIES

This is to certify that the thesis prepared

By: Kimchi-Audrey Strasser

Entitled: *Dictyostelium* cell-fate bias is regulated antagonistically by the Retinoblastoma orthologue RblA and the cyclin-dependent kinase Cdk1

and submitted in partial fulfillment of the requirements for the degree of

Doctor of Philosophy (Biology)

complies with the regulations of the University and meets the accepted standards with respect to originality and quality.

Signed by the final examining committee:

	Chair
Dr. Gerald Weeks	External examiner
Dr. Peter Pawelek	External to Program
Dr. Christopher Brett	Examiner
Dr. Vladimir Titorenko	Examiner
Dr. Reginald Storms	Examiner
Dr. Adrian Tsang	Thesis supervisor

Approved by

_____
Chair of Department or Graduate Program Director

05.04.2012

_____
Dean of Faculty

ABSTRACT

Dictyostelium **cell-fate bias is regulated antagonistically by the Retinoblastoma orthologue RblA and the cyclin-dependent kinase Cdk1**

Kimchi Strasser, Ph.D.

Concordia University, 2012

A *Dictyostelium* cell chooses its fate based on the time of its last division prior to the initiation of development. At the onset of development, freshly-divided cells tend to form the stalk of the fruiting body while late-G2 cells become the reproductive spores. How the phases of the cell cycle are linked to cell-type differentiation is unknown. To address this issue, we targeted for analysis two key cell-cycle regulators, Cdk1 and the Retinoblastoma orthologue RblA.

Using RNA-blot analysis and reporter-gene studies, we showed that *cdk1* is expressed shortly before mitosis then again during mid-development. We also generated a series of doxycycline-inducible *cdk1* mutants. Cells expressing *cdk1*Y15F were blocked in mitosis and displayed defects in spindle assembly, suggesting that Cdk1 dephosphorylation on tyrosine15 is a pivotal step in the G2/M transition of *Dictyostelium*. Those expressing *cdk1*T14A were smaller than the control strain, implying that Cdk1T14 phosphorylation is one mechanism by which *Dictyostelium* coordinates cell growth with cell division. When given the choice between becoming spores or stalk cells, Cdk1T14A cells opted for the stalk fate. Importantly the developmental phenotype was rescued when *cdk1*T14A was expressed in RblA-deficient cells. By comparing the transcriptional profiles of wild-type and RblA-deficient cells, we found that RblA-repressed genes

associated with cell proliferation. These genes were expressed in late G2 then again in mid-development.

Collectively our findings support a model in which RblA and Cdk1 play opposing roles in the cell cycle. In this model RblA prevents cell-cycle progression by repressing mitosis and S-phase genes. Repression is relieved in late G2 and genes such as *cdk1* are activated, thereby allowing cells to advance through the cell cycle. The antagonistic relationship between Retinoblastoma and Cdks is not new; it has long been established in other model systems. The novelty of our findings is that RblA and Cdk1 also influenced development. We found that cells with an active Cdk1 (or lacking a functional RblA) at the onset of development were ushered to the stalk pathway. This is important since it implies that these cell-cycle regulators are part of the intrinsic signalling pathway responsible for initial cell-type choice in *Dictyostelium*.

Acknowledgements

I thank my advisor Adrian Tsang, our close collaborator Harry MacWilliams, my committee members Vladimir Titorenko and Reginald Storms, Pascale Gaudet, Dictybase, Gerry Weeks for the *cdk1* cDNA, Annette Müller-Taubenberger for the actin1 antibody, Ralph Gräf and Jonathan Chubb for the fluorescent vectors, the Deutscher Akademischer Austausch Dienst for a scholarship, my family, and Matt and Nat for putting things into perspective.

To Harry

Table of Contents

Contribution of Authors

Dr. Adriano Ceccarelli made the *Dictyostelium rblA* disruptant.

Dr. Gareth Bloomfield constructed the microarray and analysed the resulting data.

Vineet Dua prepared RNA from the cell-cycle experiment for mRNA-Seq.

Dr. Asa MacWilliams designed and wrote the mRNA-Seq software.

Dr. Harry K. MacWilliams analysed the mRNA-Seq data.

Dr. Harry K. MacWilliams developed the macros for visualizing the mRNA-Seq data in Excel.

Dr. Harry K. MacWilliams generated the Cdk and cyclin phylogenetic trees.

Dr. Harry K. MacWilliams developed the *Dictyostelium* tetON system.

Dr. Harry K. MacWilliams photographed the PCNA-fluorescent cells.

List of Figures

List of Tables

List of Abbreviations

A: Alanine

act: Actin

APC: Anaphase promoting complex

AX: Axenic

β-gal: beta-galactosidase

bp: Base pairs

BrdU: Bromodeoxyuridine

BsR: blasticidin resistant

C: Celsius

Cdk: Cyclin dependent kinase

Dd: *Dictyostelium discoideum*

DIF: Differentiation inducing factor

DNA: Deoxyribonucleic acid

dNTP: Deoxyribonucleotide triphosphate

ecmA: Extracellular matrix A

F: Phenylalanine

FACS: Fluorescence activated cell sorter

G1: Gap 1

G2: Gap 2

G418: Geneticin

Gfp: Green fluorescent protein

KK2: Potassium phosphate buffer

L: Litre

M: Molar

M phase: Mitosis

mRNA: messenger RNA

mRNA-Seq: mRNA sequencing

neoR: Neomycin (G418) resistant

PCNA: Proliferating cell nuclear antigen

PCR: Polymerase chain reaction

qRT-PCR: Quantitative real-time PCR

Rb: Retinoblastoma

Rfp: Red fluorescent protein

RNA: Ribonucleic acid

Rnr: Ribonucleotide reductase

rpm: Rotations per minute

S. pombe: Schizosaccharomyces pombe

S. cerevisiae: *Saccharomyces cerevisiae*

T: Threonine

rtTA: Reverse tetracycline transactivator

term: Terminator

tet: Tetracycline response element

Y: Tyrosine

1. INTRODUCTION

To generate a multicellular organism, a single cell must grow, divide, and differentiate although these events are not restricted to any particular order. In certain species, for instance, fertilization is immediately followed by successive rounds of chromosome duplication and cell division (Gilbert 2006). This produces a mass of cells that is similar in size to the original egg. Only later in development do these cells go on to grow and acquire specialized functions. Cells of the nervous system serve as another example. Here certain cell types withdraw from the cell cycle then undergo differentiation while others are committed to a particular fate prior to cell-cycle arrest. Others still migrate, proliferate, and express tissue-specific genes in parallel (Galderisi et al 2003). Regardless of whether growth and development occur simultaneously or independently, the proper formation of organs and tissues from pluripotent stem cells requires a tight coupling of proliferation to differentiation, since terminally differentiated cells do not divide. Case in point, re-entry into the cell cycle after terminal differentiation denotes a hallmark of cancer (Hanahan and Weinberg 2000, Hartwell and Kastan 1994). Although a lot is known about the molecules that regulate cell proliferation, much remains unclear about the role of cell-cycle proteins with respect to differentiation.

1.1 The phases of the cell cycle

Most cell cycles are divided into four phases including two gaps, designated as G1 and G2, which bracket a S phase for DNA synthesis and M phase or mitosis for chromosome segregation. DNA synthesis starts at multiple sites on the chromosomes known as replication origins. The origins are primed for replication during the early G1

phase of the cell cycle by the pre-replication complex (Lodish 2000). This involves the sequential assembly of multiple proteins at the origins including the origin recognition complex, the ATP-binding protein Cdc6, the DNA replication factor Cdt1, and the mini–chromosome maintenance hexamer complex. The mini-chromosome maintenance complex is a helicase that unwinds the DNA during S phase to allow polymerases to copy the opened strands (Nieduszynski et al 2005). For many cell types, entry into S phase signifies a commitment to completing the cell cycle and dividing (Blagosklonny and Pardee 2002).

In eukaryotic cells, nuclear division is restricted to a brief period of the cell cycle known as mitosis. This phase of the cell cycle is marked by the condensation of the duplicated chromosomes which then align at the metaphase plate (or the equator) of the cell. At this stage, Cdc20 activates the anaphase promoting complex, a ubiquitin ligase that targets specific proteins for proteolysis by the proteasomes (Kimata et al 2008). One major substrate of the anaphase promoting complex is Securin whose destruction is needed for the cells to transit from metaphase into anaphase (Uhlmann et al 2000). Securin is recognized and flagged for destruction by the anaphase promoting complex via the D box composed of the amino acid sequences RXXLXXXXN where R is an arginine, X is any amino acid, L is a leucine, and N is an asparagine and the KEN box where K and E are lysine and glutamic acid, respectively (Holt et al 2008). These motifs are found in other substrates of the anaphase promoting complex (Glotzer et al 1991, Pfleger and Kirschner 2000). The degradation of Securin releases Separase, the protease responsible for dissolving the bonds that hold the sister chromatids together (Musacchio and Salmon 2007). Once chromatid cohesion is eliminated, the two separate chromatids are then free

to move in opposite directions through the action of kinesin motors (Rogers et al 2004). As the chromosomes move near the poles, a contractile ring, composed of actin and myosin bundles, pinches the cell in half through a process known as cytokinesis (Pines and Rieder 2001). Cleavage produces two cells, each of which contains a full set of chromosomes.

The G1 and G2 gaps intercalate S phase and mitosis to give the cells time to grow. They also serve as important regulation points or checkpoints (Hartwell and Weinert 1989) where cells can arrest before entering the next cell-cycle phase. There are two major checkpoints in the cell cycle. The first, known as Start in yeast (van den Heuvel 2005) or the Restriction point in animal cells (Blagosklonny and Pardee 2002), is at the G1/S transition. Here some cells can also leave the cell cycle to become quiescent, to differentiate, or to undergo senescence (Morgan 1995). A second major checkpoint arrests the cells at G2/M transition in the presence of incompletely replicated or damaged DNA (Weinert et al 1994). Entry into both S-phase and mitosis is controlled by cyclin-dependent protein kinases (Doree and Hunt 2002).

1.2 Cdks and cell-cycle control

The cyclin-dependent protein kinase (Cdk) family consists of proline-directed serine/threonine kinases that are linked to multiple cellular processes, the most notable being cell-cycle control. A single Cdk known as the cell division control 2 (Cdc2) protein in *Schizosaccharomyces pombe* or its counterpart Cdc28 in *Saccharomyces cerevisiae* regulates the yeast cell cycle (Malumbres and Barbacid 2009). Four Cdks (Cdk1, 2, 4, and 6) normally control the mammalian cell cycle but targeted disruption in mice shows that only Cdk1 is essential (Figure 1) (Barriere et al 2007, Santamaria et al

2007, Satyanarayana and Kaldis 2009). Additionally, HeLa cells depleted of the *cdk*1 transcript using RNA interference arrest at the G2/M checkpoint (Harborth et al 2001). Cdk7, 8, 9, 10, and 11 participate in various aspects of transcriptional control (Malumbres and Barbacid 2009) whereas Cdk12 and Cdk13 are required for RNA splicing (Chen et al 2006, Chen et al 2007). Interestingly the Cdk family tree stretches to include Cdk5, a protein kinase that shares high similarity with other cyclin-dependent kinases (Hellmich et al 1992) but whose function is linked primarily to development. Specifically, Cdk5 accumulates in post-mitotic neurons in the developing brain where it is involved in cell-cycle arrest and differentiation (Nikolic et al 1996, Tsai et al 1993). This kinase is essential for proper development since null mice die at birth with severe neurological defects (Tanaka et al 2001).

By definition, a monomeric Cdk subunit is devoid of enzymatic activity until partnered with a cyclin**.** In mammalian cells three D-type, two E-type, two A-type, and three B-type cyclins are involved in cell-cycle regulation. These ten cyclins are encoded by genes that are regulated in a cell-cycle dependent manner, meaning that they are expressed only at specific times during the cell cycle (Malumbres and Barbacid 2009). According to classical models, extracellular signals induced the transcription of D-type cyclins in G1 (Deshpande et al 2005). As they accumulate, D cyclins preferentially bind to Cdk4/6 to form active kinases which, in turn, allow for the synthesis of E and A-type cyclins (Harbour et al 1999). This is achieved by inhibiting Retinoblastoma, the inhibitor of S phase (discussed below in Section 1.3). Cyclin E-Cdk2 complexes are involved in the G1/S transition whereas Cyclin A-Cdk2 function during the G2 period (Hochegger et al 2008). Cyclin B is produced later in the cell cycle and pairs up with Cdk1 to control

entry into mitosis (Riabowol et al 1989). Like the Securins, the cell-cycle cyclins are marked for destruction by the anaphase promoting complex (Glotzer et al 1991). Ubiquitin-cyclin conjugates are then captured by the proteasomes and degraded into peptides of seven to eight amino acids in length which can be further processed into free amino acids (Lodish 2000). Since cyclins are essential for Cdk function, this results in kinase inactivation to allow the cells to reset the cell cycle (Ciechanover 1994, Ciechanover et al 2000). Thus intermittent waves of cyclin synthesis and degradation turn the Cdks on and off during the cell cycle to provide cells with a basic level of regulatory control. Cdks are also regulated by phosphorylation and through their interactions with cyclin-kinase inhibitors.

Mutational analyses targeting conserved amino acid residues in the cell-cycle Cdks have been used to identify the sites involved in kinase regulation. To activate a Cyclin-Cdk complex, a phosphate group must be added to the conserved threonine160 residue (threonine 161 in some cell types) (Krek et al 1992). The enzyme responsible for threonine 160 phosphorylation is the cyclin-activating kinase (Fisher and Morgan 1994). Like its substrates, the cyclin-activating kinase is a Cyclin-Cdk complex made up of a catalytic subunit Cdk7 (also known as Mo) paired with Cyclin H. The complex also requires the protein Ménage a trios (Mat1) for assembly (Fisher et al 1995). In addition to its role in Cdk activation, the cyclin-activating kinase forms part of the general transcription factor IIH which is involved in the initiation of transcription (Kaldis 1999).

Cdk1 and possibly also Cdk2 kinase activity is downregulated by the addition of a phosphate group on threonine14 and tyrosine15 (Atherton-Fessler et al 1994, Fleig and Gould 1991, Gould and Nurse 1989, Morgan 1995). The two highly conserved residues

are located in the ATP binding loop (or active site) at the amino termini of Cdks (De Bondt et al 1993). The inhibitory phosphorylations are controlled by the membrane bound Myt1 kinase that preferentially targets threonine14 and the nuclear Wee1 kinase that phosphorylates tyrosine15 exclusively (Liu et al 1997, Liu et al 1999, McGowan and Russell 1993, Mueller et al 1995, Russell and Nurse 1987). Cdk dephosphorylation is achieved by the simultaneous inactivation of Wee1 and Myt1 and the activation of the Cdc25 phosphatase (Kumagai and Dunphy 1991, Lammer et al 1998, Millar et al 1991, Morgan 1995, Russell and Nurse 1986). Cyclin B-Cdk1 complexes enhance their own activity by phosphorylating and activating Cdc25, and inactivating Myt1 and Wee1 by phosphorylation (Hoffmann et al 1993) to promote rapid mitotic entry.

Replacing the threonine at position 14 with an alanine and the tyrosine at position 15 with a phenylalanine in Cdk1 allows cells to escape the G2/M checkpoint (Fletcher et al 2002, Hemerly et al 1995, Krek and Nigg 1991, Krek et al 1992, Norbury et al 1991, Sgarlata and Perez-Martin 2005). The phenotypic consequences vary depending on the organisms and the experiments used to characterize the mutant but include chromosome hypercondensation and impaired mitotic spindle assembly, elevated histone H1-directed kinase activity, reduced cell size, and the absence of cytokinesis, all together implying cell-cycle arrest in mitosis. In the fungal phytopathogen *Ustilago maydis,* induced expression the *cdk1*T14AY15F affects cell growth and spore formation suggesting that Cdk1 may be important for the normal development of this fungus (Sgarlata and Perez-Martin 2005). The impact of the T14AY15F mutation on development has not been described in other systems probably because it also affects cell viability (Gould and Nurse 1989, Lundgren et al 1991, Sgarlata and Perez-Martin 2005).

Schizosaccharomyces pombe cells expressing the Cdk1 single Y15F mutation show similar signs of premature mitosis (Krek et al 1992) but the phenotype is less severe in HeLa cells (Krek and Nigg 1991). The T14A mutation is recessive in yeast; when the gene is expressed at natural levels in a *cdc2* null background the mutant cells are smaller than the wild-type control (Den Haese et al 1995). A different effect has been described in mammals. Overexpression of Cyclin B together with Cdk1T14A allows HeLa cells to enter mitosis even after exposure to DNA-damaging levels of ionizing radiation, suggesting that this phosphorylation site is important in the G2/M checkpoint (Fletcher et al 2002).

Cyclin-dependent kinase inhibitors play an important role in Cdk regulation and cell-cycle control. There are two classes of cyclin-dependent kinase inhibitors: the inhibitors of CDK4 (INK4) family and the Cdk- interacting protein/Kinase inhibitory protein (Cip/Kip) family. The INK group including INK4a, INK4b, INK4c and INK4d specifically inhibit Cyclin D-Cdk4/6 activity by binding to the Cdk monomers (reviewed in (Ciemerych and Sicinski 2005). Mice lacking INK4a, b, or c are viable but develop a variety of tumours emphasizing the importance of INK proteins in maintaining cell-cycle arrest. The Cip/Kips p21, p27, and p57 function by forming inactive ternary complexes with Cyclin-Cdk1 or Cyclin-Cdk2 (Nakayama et al 2004, Pagano et al 1995, Toyoshima and Hunter 1994). Paradoxically p21 and p27 also act as scaffolds for Cyclin D-Cdk4/6 assembly and in so doing, release Cyclin E-Cdk2 complexes from inhibition (Sherr and Roberts 1999). The activity of cyclin-dependent kinase inhibitors is modulated during the cell cycle through transcriptional repression and ubiquitin-mediated degradation by the proteasomes (Pagano et al 1995).

Cyclin-dependent kinase inhibitors are also involved in differentiation. In the African clawed frog *Xenopus laevis*, a rise in p27 during embryogenesis correlates with muscle development. Cells progressively commit to becoming myofibers through a signalling cascade involving the basic helix-loop-helix transcription factor MyoD. p27 interacts with MyoD to activate muscle-specific genes whereas targeted depletion of p27 with short anti-sense oligonucleotides prevents cells from differentiating into muscle (Vernon and Philpott 2003). A similar situation is seen in the nervous system where p27 expression increases in cells destined to form primary neurons. Here the protein functions by stabilizing neurogenin, another helix-loop-helix transcription factor, whose key function is to promote the neural phenotype (Ma et al 1996). Ectopic expression of p27 increases the number of primary neurones in the neural plate while cells lacking the protein proliferate and fail to differentiate (Vernon et al 2003). Collectively, these finding suggest that at least some of the cyclin-dependent kinase inhibitors are needed to specify cell identity, and they do so in a manner that it distinct from their role as cell-cycle regulators.

In G2 and early mitosis, active Cyclin-Cdk1 complexes phosphorylate over 70 substrates carrying the minimal consensus sequence S/T-P (where S/T is a serine or a threonine and P is a proline) to elicit processes such as nuclear envelop breakdown and chromosome condensation (Malumbres and Barbacid 2005). After metaphase Cdk1 activity is turned off, resulting in chromosome decondensation, nuclear envelope reassembly, and cytokinesis (Malumbres and Barbacid 2009).

1.3 Retinoblastoma

Retinoblastoma and the closely related proteins, p107 and p130, are important

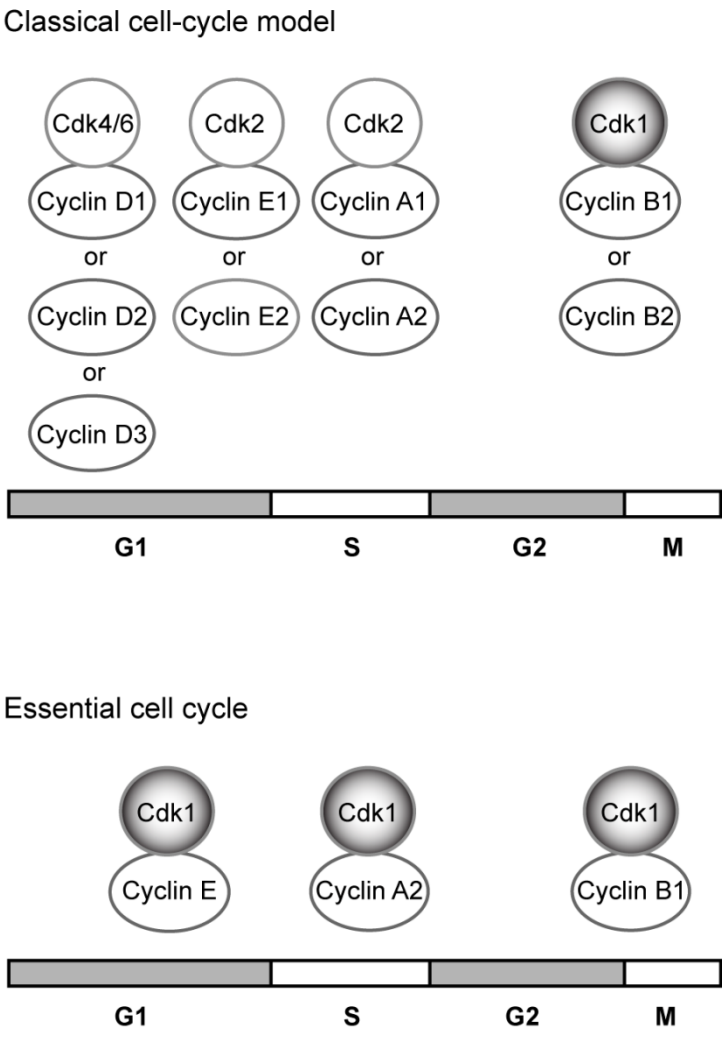

Figure 1. Mammalian cell-cycle regulation by Cdks

In classical models, Cdk4 and Cdk6 pair with the D-type cyclins (including D1, D2 and D3) to control exit from G1. Cdk2 binds to Cyclins E and A for entry and progression through S phase while active CyclinB-Cdk1 complexes govern the G2/M transition. Recent studies show that the majority of Cdks and cyclins are not essential. Targeted disruption of the cell-cycle cyclins in mouse germline cells reveals that cyclinA1, cyclin B2, and the D-type cyclins are dispensable. Similarly, mice lacking Cdk2, Cdk4, and Cdk6 proliferate normally showing defects only in specific cell types implying that, like the yeast cell cycle, Cdk1 alone can control the mammalian cell cycle by binding to a minimum number of cyclins (adapted from Malumbres and Barbacid 2009, Santamaria et al 2007).

regulators of the cell cycle (Cobrinik 2005). Together, they form a family known as the pocket proteins because they contain a central, pocket-shaped domain that allows them to interact with other proteins (Münger 2003). The pocket proteins act as transcriptional repressors to inhibit DNA synthesis by targeting the E2F-family of transcription factors. E2Fs fall into two classes: E2F1, E2F2, and E2F3a are known to activate transcription while E2F3b, E2F4, E2F5, and E2F6 are transcriptional repressors (Figure 2) (Cobrinik 2005). In the hypophosphorylated state, Retinoblastoma binds to the activator E2Fs to silence transcription and to prevent the cells from entering S phase (Figure 3). Mitogenic signals stimulate the production of D-type cyclins which go on to form complexes with Cdk4 and Cdk6. Mounting levels of active Cyclin D-Cdk4/6 initiate the phosphorylation of Retinoblastoma to destabilize the Retinoblastoma-E2F associations. Once released, the activator E2Fs can stimulate transcription by binding to promoters motifs upstream of so-called E2F-responsive genes (Rabinovich et al 2008). Most E2Fs bind to these promoter regions in association with a dimerization partner, DP1 or DP2 (Bandara et al 1993, Dimova and Dyson 2005, Helin et al 1993, Krek et al 1993). In many instances, the binding of E2Fs1-3a correlates with histone acetylation by chromatin modifying enzymes (Cobrinik 2005) and transcriptional activation. Early E2F transcriptional targets include E-type cyclins which combine with Cdk2 to phosphorylate and fully inactivate Retinoblastoma (Botz et al 1996, Geng et al 1996, Ohtani et al 1995). Other E2F-responsive cell-cycle genes include those encoding enzymes for dNTP biosynthesis such as ribonucleotide reductase, components of the pre-replication complex such as Cdc6, and histones to package the replicated DNA into chromatin (Ewen 2000, Gutierrez 2005).

As mentioned above, interphase Cdks phosphorylate and downregulate

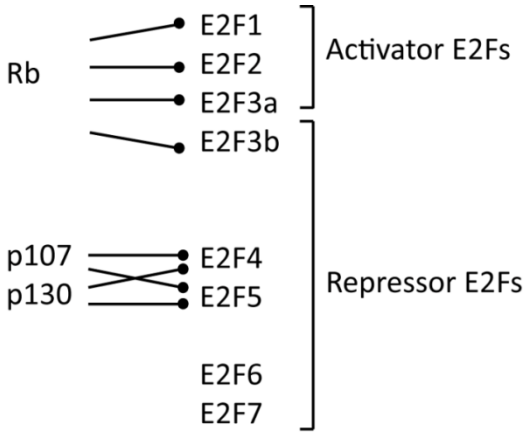

Figure 2. Interaction between the pocket proteins and E2F transcription factors

In mammals there are three pocket proteins: Retinoblastoma, p107, and p130. Retinoblastoma preferentially binds to activator E2Fs: E2F1, E2F2, and E2F3a. p130 and p107 bind to the repressor E2Fs E2F4 and E2F5. E2F6 and E2F7 form pocket-protein independent repressor complexes (adopted from Cobrinik 2005).

Retinoblastoma activity to turn on the expression of cyclins. The cyclins go on to activate more Cdks to favour cell proliferation. The action is reciprocated by Retinoblastoma which inhibits Cdks directly by repressing their transcription and indirectly by stabilizes cyclin-kinase inhibitors. Specifically Retinoblastoma binds to and sequesters the S-phase kinase-associated protein Skp, an F-box ubiquitin ligase that targets the cyclin-kinase inhibitor, p27, for degradation (Ji et al 2004). In the absence of Skp, p27 accumulates and binds to Cdk2. This keeps Cdk2 in an inactive state and prevents the cell from proliferating. Therein lies the antagonistic relationship between Retinoblastoma and Cdks.

Although the pocket proteins are usually associated with S phase, recent studies have shown that they also regulates the expression of genes needed for mitosis (Cobrinik 2005). In mammals, this involves a multi-subunit repressor complex known as the DREAM (DP, Rb-like, E2F, and MuvB). DREAM contains the pocket protein p130 or p107, the repressor E2F4 along with its dimerization partner DP1, and a core of five synthetic multi-vulval class B (MuvB) proteins: LIN9, LIN37, LIN52, LIN54, and the Retinoblastoma-binding protein 4. During the G1 phase, DREAM binds to the promoters of G2/M-specific genes at the cell-cycle genes homology region (CHR) to repress transcription. The interactions between members of the DREAM complex are dynamic and as cells advance through the cell cycle p130/p107 and E2F4-DP1 are released in exchange for MybB. The new Myb MuvB-core (MMB) complex functions as a transcriptional activator of 'late' cell-cycle genes including *cycB* and *cdc25* (Muller et al 2011). In *Drosophila melanogaster* DREAM complexes appear to play a different role by inactivating differentiation-specific genes in proliferating cells (Kornejak et al 2004).

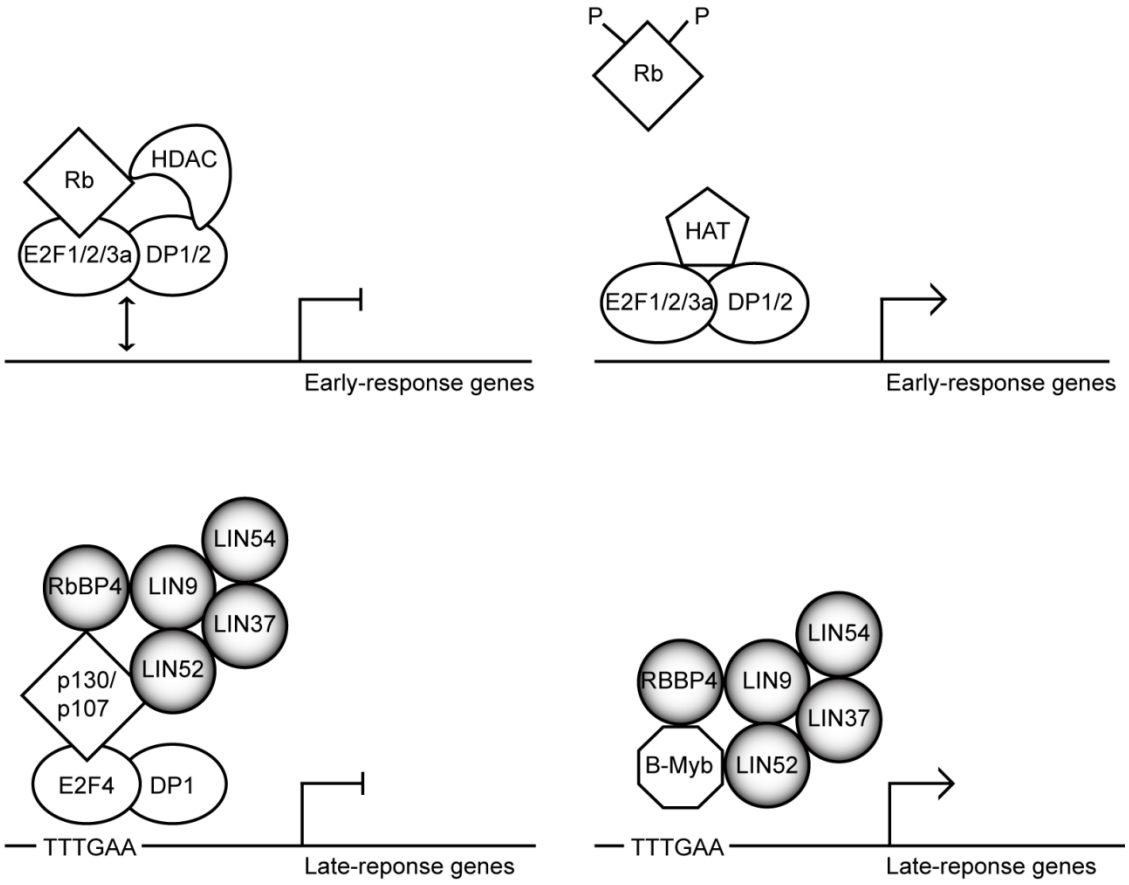

Figure 3. Alternative pocket protein complexes contribute to the repression of E2F responsive genes

In early G1, Retinoblastoma binds to activator E2Fs 1-3 at or sequestered away from the promoter regions of 'early' E2F-target genes. Retinoblastoma recruits various chromatin remodelling enzymes including type I histone deacetylases (HDACs) resulting in chromatin compaction and transcriptional repression. In late G1, Retinoblastoma is phosphorylated and dissociates from E2Fs. The binding of E2F1-3a at E2F-responsive promoters correlates with the recruitment of histone acetyltransferases (HATs), the restoration of histone acetylation, and transcriptional activation. The DREAM complex (which contains the pocket protein p130 or p107, the repressor E2F4 along with its dimerization partner DP1, a core of five MuvB proteins: LIN9, LIN37, LIN52, LIN54, and the Retinoblastoma-binding protein 4 or RbBP4) binds to the CHR promoter elements resembling the sequence TTTGAA found upstream of 'late' response genes such as *cdc25*, *cdc2*, and *cycB1*. The complex has repressor functions. In S phase or G2, E2F4-DP1 and p130/p107 are exchanged for B-Myb to form the MMB transcriptional activator complex. The arrangements do not necessarily reflect actual protein-protein interactions (adapted from Cobrinik 2005, Muller et al 2011).

Beyond the cell cycle, Retinoblastoma also functions as an important regulator of differentiation. Evidence comes from Retinoblastoma-null mice that die *in utero* shortly after conception with abnormalities in muscle tissue, blood cells, and nerves (Zacksenhaus et al 1996). In the precursors of these cells, *Rb* is normally expressed at high levels (Jiang et al 1997, Szekely et al 1992). There, the Retinoblastoma protein induces the expression of lineage-specific genes by interacting with different transcription factors including the myocyte enhancer factor-2 **(**MEF2), neurogenic differentiation 1 (NeuroD1), and CCAAT-enhancer-binding proteins (c/EBPs) (Batsche et al 2005, Chen et al 1996, Cole et al 2004, Gu et al 1993, Iavarone et al 2004, Novitch et al 1999, Thomas et al 2001, Toma et al 2000). Retinoblastoma also binds to MyoD to specify the muscle cell fate (Gu et al 1993) much like the cyclin-kinase inhibitor p27. Hence Retinoblastoma serves as another example of a protein controlling both the cell cycle and differentiation.

1.4 *Dictyostelium discoideum* as a model system

Due to genetic redundancy, studies on components of the cell cycle with respect to differentiation can be challenging. In mouse models, for example, cells lacking Retinoblastoma will compensate for the loss by overexpressing p107 (Sage et al 2003). Also, many Cdks are non-essential in most tissues (Santamaria et al 2007, Satyanarayana and Kaldis 2009). In the absence of one or more Cdks, the remaining Cdks will assume the role of the missing protein(s) to regulate the cell cycle; the same holds true for the cyclins (Satyanarayana and Kaldis 2009). Thus null cells only reveal functions that cannot be assumed by other proteins. Difficulties are compounded by the fact that some cell-cycle proteins are maternally derived (Gilbert 2006) and that genetic deletions of

essential cell-cycle regulators, such as *cdk1* in mice, result in early embryonic death before a developmental role can be ascribed (Satyanarayana and Kaldis 2009). Such limitations may be overcome in developing systems that contain a non-redundant set of cell-cycle proteins commonly found in metazoans.

Although budding yeast (*S. cerevisiae*) and fission yeast (*S. pombe*) are the single-celled eukaryotes of choice for cell-cycle studies, they lack homologues of the Retinoblastoma-E2F tumour suppressor pathway. The slime mold *Dictyostelium discoideum* offers an excellent model to study cell-cycle regulation and differentiation because it readily switches from a unicellular to a multicellular state. Unfortunately relatively little is known about the *Dictyostelium* cell cycle. This is probably because it is considered to be atypical. In *Dictyostelium* the G1 phase is very short or absent (Weijer et al 1984). Still the *Dictyostelium* genome codes for an orthologue of the canonical G1 regulator, Retinoblastoma, as well as the transcription factors E2F and the E2F-dimerization partner DP (MacWilliams et al 2006), and a few members of the DREAM complex. The single *Dictyostelium* Retinoblastoma orthologue, called Retinoblastoma-like or RblA, shares sequence homology with all three members of the pocket proteins in mammals (MacWilliams et al 2006). *Dictyostelium* also has 12 cyclin-dependent kinases but only one Cdk (Cdk1) belongs to the cell-cycle class (Figure 4) (Goldberg et al 2006). It is expressed during growth and in mid development (Luo et al 1995, Parikh et al 2010) and a cloned copy rescues a *S. cerevisiae* temperature sensitive cdc28 strain (Michaelis and Weeks 1993). The inhibitory phosphorylation sites in Cdk1 are conserved although they are shifted from threonine14 and tyrosine15 to threonine20 and tyrosine21 (hereafter referred to as T14 and Y15 for clarity). The genome also encodes at least three cell-cycle

cyclins including Cyclin A, B, and D (Figure 5) (Luo et al 1995, MacWilliams et al 2006), the putative Cdk1 negative regulator Wee1 (Goldberg et al 2006), and the Cdk1 activator Cdc25 (Mayanagi et al 2004). Database searches at http://www.dictybase.org/ reveal that the *Dictyostelium* genome encodes homologues of several other regulators of the mammalian and yeast cell cycles (Table 1). The cyclin-dependent kinase inhibitors are one exception; *Dictyostelium* has no INK4s or Cip/Kips recognizable by sequence homology. Along with this elementary set of cell-cycle proteins, *Dictyostelium* also has a relatively simple developmental program. Unlike the cell cycle, however, development in *Dictyostelium* has been extensively studied (Bonner 2009).

1.4.1 *Dictyostelium* differentiation

During differentiation, cells alter their morphology and take on new functions. So is the case for *Dictyostelium* cells when exhausted of nutrients. A series of coordinated events allows the free-living amoebae to aggregate into a multicellular organism (Figure 6).

At the start of development, individual cells communicate with each other through the periodic production and secretion of cyclic adenosine 3′, 5′-monophosphate (cAMP). Neighboring cells respond to the pulse of cAMP by moving towards the source and successively producing bursts of the chemoattractant. As a consequence, the signal is propagated outwards causing the mass movement of up to 100 000 cells. Guided by waves of cAMP, the amoebae unite into streams that converge at a central point to give rise to a cohesive mound. The structure is then extended upwards by a dominant tip and collapses to the ground to form a migrating slug (Gaudet et al 2008). At this point of the

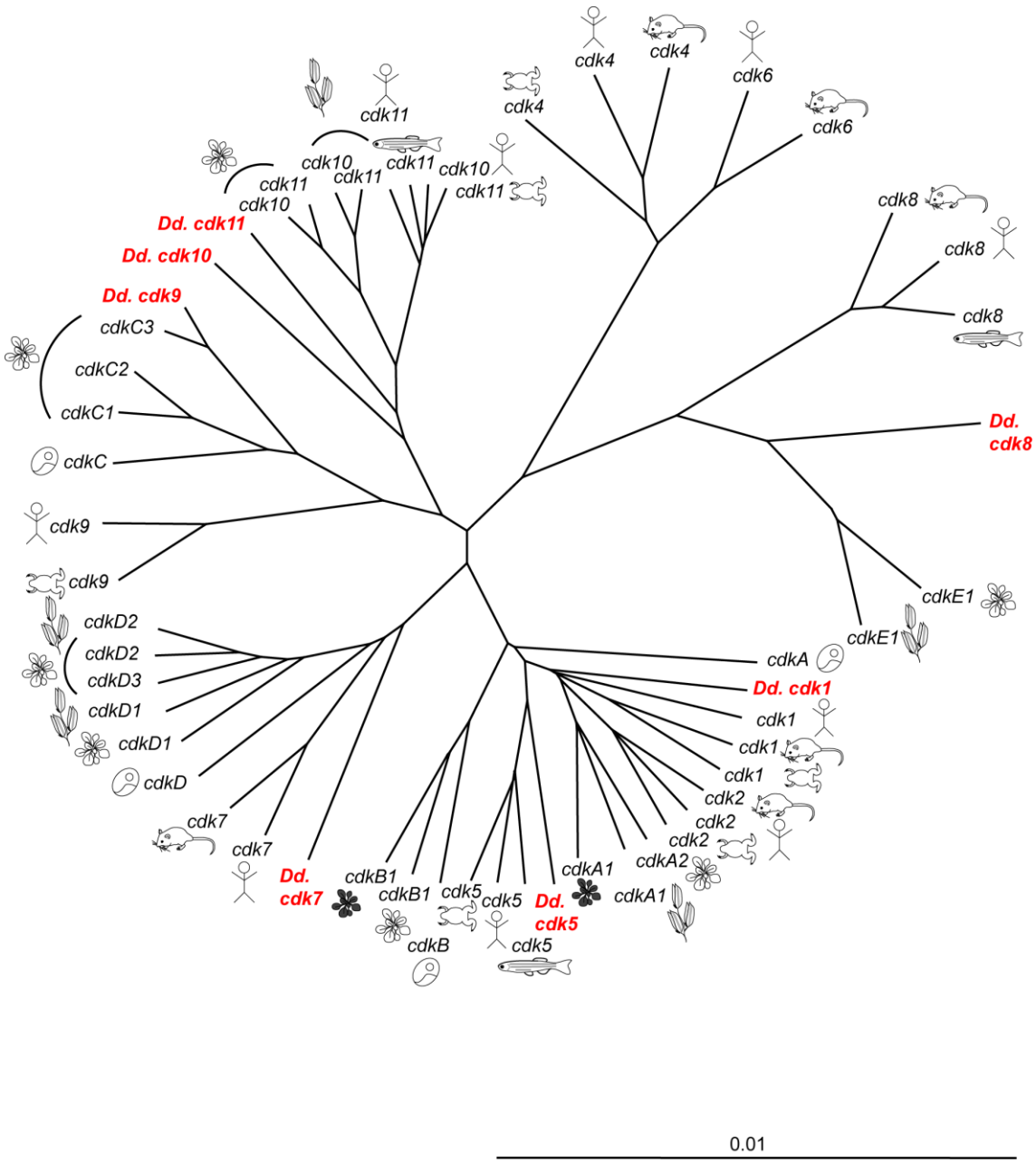

Figure 4. The cyclin-dependent kinase (*cdk*) gene family

Only the 11 Cdks that have been extensively studied are included here. Sequences aligned using DIALIGN and unrooted diagrams generated using TreeView. *Homo sapiens*, *Mus musculus*, *Xenopus laevis*, *Danio rerio*, *Arabidopsis thaliana*, *Nicotania tabacum*; *Oryza sativa*; *Ostreococcus tauri.* Shown in red are *Dictyostelium discoideum* (*Dd.*) Cdks (adapted from H.K. MacWilliams, unpublished results).

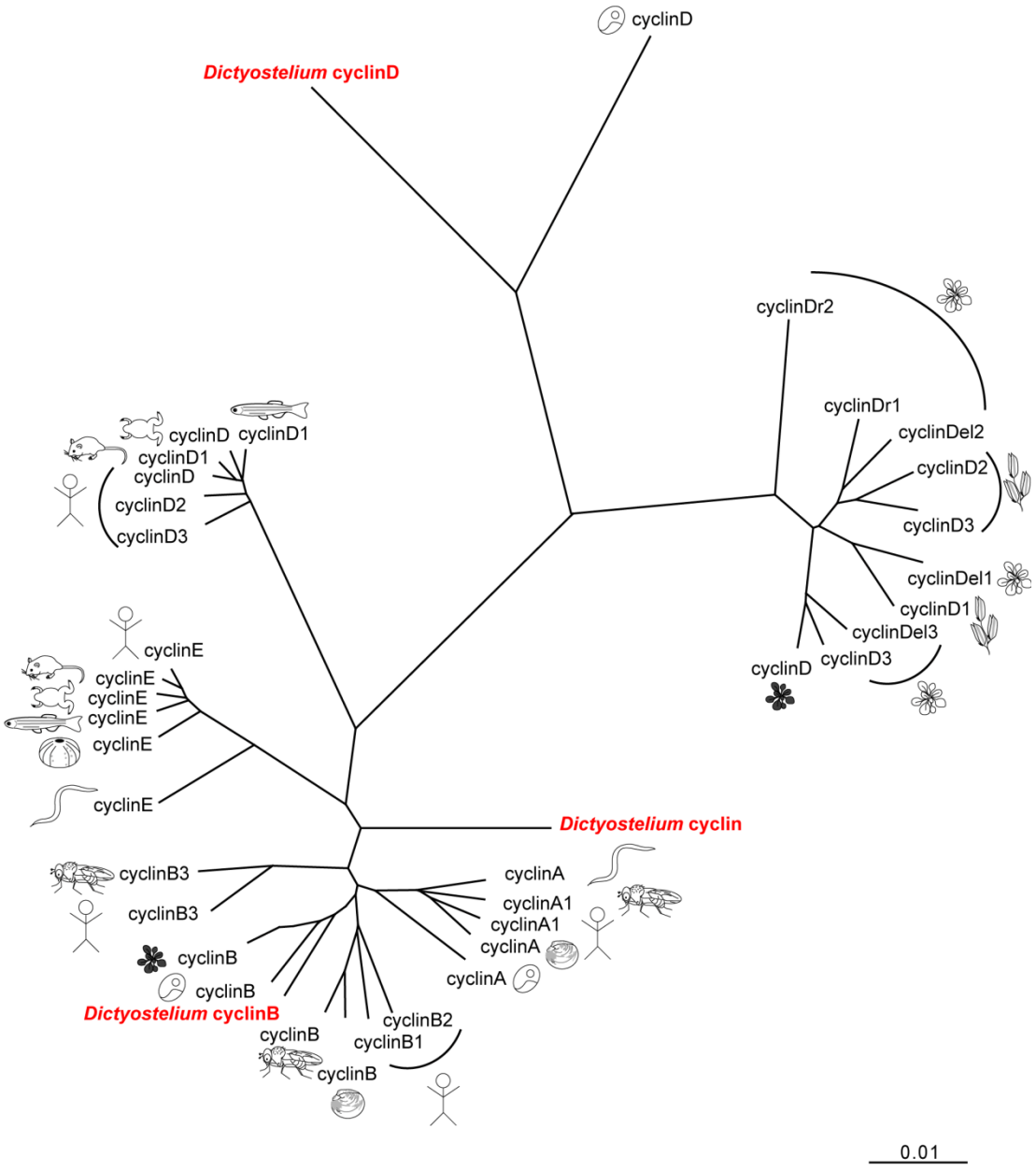

Figure 5. The cyclin gene family

The *Dictyostelium* genome encodes homologues of cyclin B, cyclin D and possibly cyclin A. It also contains cyclins C, H, K, and L but they are not considered to be cell-cycle cyclins. Sequences aligned using DIALIGN and unrooted diagrams generated using TreeView. *Homo sapiens*, *Mus musculus*, *Xenopus laevis*, *Danio rerio* (zebrafish), *S. purpuratus,* clam, *Caenorhabditis elegans*, *Drosophila melanogaster* *Arabidopsis thaliana*, *Nicotania tabacum*, *Oryza sativa*, *Ostreococcus tauri* (adapted from H.K. MacWilliams, unpublished results).

Table 1. Cell-cycle genes in *Dictyostelium discoideum*

	Gene	Description	HOMOLOGUE(S) Human	Yeast	Fly
Cell cycle control	*cdk1*	Predicted to activate S/G2 cyclins Cyclin A, B, and D	CDK1 CDK2	CDC28 PHO85	Cdc2 Cdc2c
	cks1	Orthologue of cyclin-dependent kinases regulatory subunit	CKS1	CKS1	Cks30A Cks85A
	plk	Plays a role in mitosis and localizes to the centrosomes	PLK1	CDC5	Polo
	aurK	Associates with the mitotic spindle and plays a key role in mitosis (Li et al 2008)	Aurora kinase	IPL1	Aurora
	wee1	Similar to *S. pombe* Wee1, inhibitor of mitosis through phosphorylation of Cdc2	Wee1-like	SWE1	Wee1-like
	cycA	Predicted to interact with the cyclin-dependent kinase Cdk1; contains a KEN box for degradation by APC/Cdh1	Cyclin A		
	cycB	Predicted to interact with the cyclin-dependent kinase Cdk1 (Luo et al 1995)	Cyclin B1, 2, and 3	Cyclin 1, 2, 3, and 4	Cyclin A, B, B3
	cycD	Similar to metazoan and plant type G1 cell-cycle cyclins; highest similarity to algal Cyclin D; predicted to interact with Cdk1	Cyclin D	Cln	Cyclin D
	cdc25	Similar to mammalian dual specificity protein phosphatases cdc25B and C, involved in G2/M through dephosphorylation of Cdc2 on T14 and Y15	CDC25A, B, C	MIH1	M-phase inducer phospha-tase
Transcriptional network	*rb (rblA)*	Putative orthologue of Retinoblastoma (Rb); inhibits progression from G1 to S phase through interactions with the E2F transcription factors (MacWilliams et al 2006)	RB, p107, p130		RBF, RBF2
	e2f	Transcription factor E2F	E2F2		dE2F1, 2
	dp (tfdp2)	E2F dimerization partner 2; binds to E2F to activate the expression of cell-cycle genes	Dp-2		dDP
	lin54	Play a role in chromatin remodelling or transcriptional repression; putative member of DREAM complex	Tesmin (MTL5)		Lin54
	lin9	Putative member of DREAM complex	LIN9		Mip130
	mybO	Putative myb transcription factor	Gon-4		dmyb

	rbbD	Putative Retinoblastoma-like binding protein; putative member of DREAM complex	RBBP4		CAF1p55
Pre-replication complex	*cdc6*	Putative orthologue of cell-division control protein 6	CDC6	CDC6	DmCdc6
	cdc45	Required for the initiation of chromosomal DNA replication	CDC45	CDC45	CDC45L
	orcA-F	The origin-recognition complex (ORC); plays a role in the initiation of DNA replication	ORC1-6	ORC1-6	Orc1-6
	Mcm 2-7	Similar to Mcm2-7 hexamer complex that binds to chromatin as a part of the pre-replication complex	MCM 2-7	MCM 2-7	Mcm 2-7
Chromatin disassembly	*spt16*	Similar to SPT16 of the FACT complex that acts to reorganize nucleosomes; involved in mRNA elongation, DNA replication, and repair	SPT16	SPT16	Spt16
	ssrp1	Orthologue of the SSRP1; component of the FACT complex; involved mRNA elongation, DNA replication, and repair	SSRP1	POB3	Ssrp1
Replication fork	*Gins 1-4*	Conserved replication complex GINS, which is essential for initiation of DNA replication in *X. laevis*	PSF1-4	PSF1-4	Psf1-4
	polα 1-4	DNA polymerase alpha; required for the initiation of DNA replication	DNA poly-merase α	DNA poly-merase α	DNA poly-merase α
	polδ 1-3	DNA polymerase delta; required for chromosomal DNA replication	DNA poly-merase δ	DNA poly-merase δ	DNA poly-merase δ
	wrnip1	Orthologue of Werner helicase-interacting protein 1, a modulator for initiation or reinitiation events during DNA polymerase δ-mediated DNA synthesis	WRNIP1	MGS1	
	polε A&B	Similar to DNA polymerase epsilon in yeast and vertebrates; involved in DNA replication, DNA repair, and cell-cycle checkpoint control	DNA poly-merase ε	DNA poly-merase ε	DNA poly-merase ε
	lig1	DNA ligase; required for the ligation of Okazaki fragments during lagging-strand DNA synthesis	DNA ligase1	DNA ligase1	DNA ligase1
	pcna	Proliferating cell nuclear antigen (Muramoto and Chubb 2008)	PCNA	PCNA	PCNA, PCNA2
	rfc1-5	Replication factor C	RFC1-5	RFC1-5	Gnf1

Provision of nucleotides	*rnrA*	Ribonucleotide reductase large subunit	RNR large subunit	RNR R1	Rnr large subunit
	rnrB-1	Ribonucleotide reductase small subunit (MacWilliams et al 2001)	RNR subunit M2 B	RNR chain 1	Rnr subunit M2
	thyA	Thymidylate synthase; *de novo* biosynthesis of pyrimidine deoxyribonucleotides	Thymi-dylate synthase	Thymi-dylate synthase	Thymi-dylate synthase
	dtymk	Thymidylate kinase; *de novo* biosynthesis of pyrimidine deoxyribonucleotides	Thymi-dylate kinase	Thymi-dylate kinase	CG5757
Histone biosynthesis	*H1, 2A&B, 3&4*	Histones (Stevense et al 2011)	Histones	Histones	Histones
	slbp	Histone RNA hairpin-binding protein	Histone RNA hairpin-binding protein		Histone RNA hairpin-binding protein
Chromatin assembly	*nasp*	Histone chaperone required for DNA replication	Nuclear auto-antigenic sperm protein		NASP homol-ogue
	CAF1 a&b	Putative chromatin assembly factor 1	CAF	POP2	Pop2
	asf1	Anti-silencing function 1; conserved nucleosome assembly factor and histone chaperone protein	ASF1A &B	ASF1	Asf1
Sister chromatid cohesion	*STAG*	Required for sister chromatid cohesion in eukaryotes	Stromal antigen	LD-34181p	Cohesin subunit SSC3
	nipped -B	The *Drosophila* protein plays a structural role in chromatin and is involved in sister-chromatid cohesion	Nipped-B	Sister-chromatid cohesion protein2	Nipped-B
	rad21	Involved in chromosome cohesion during the cell cycle and DNA repair	RAD21	sister chromatid cohesion protein1	Rad21
	pds5	Similar to human precocious dissociation of sisters protein; sister-chromatid cohesion protein	PDS5	PDS5	Pds5
	eco1	Establishment of cohesion; acetyl-	ESCO1&	ECO1	N.acetyl-

		transferase required for chromatid cohesion during DNA replication	2		transferase eco
	nek2	Never in mitosis kinase; involved in the formation of microtubule-organizing centers	Nek2	KIN3	Nek2
	sun1	Mediates attachment between centrosome and nucleus, associates the centromeres with the centrosome, and stabilizes genome during mitosis (Schulz et al 2009)			Klaroid
	CP91	Centrosomal protein 91 kDa (Schulz et al 2009)			
	CP75	Centrosomal protein 75 kDa (Schulz et al 2009)			
	dcc1	Involved in sister-chromatid cohesion establishment	DSCC1	DCC1	CG11788
Chromosome condensation	*pich*	Polo-interacting checkpoint helicase	ERCC6-like		
	smc1-6	Structural maintenance of chromosome; functions in chromosome dynamics	SMC	SMC	Smc
Centromere	Cenp 68	Localizes to the centromeres (Schulz et al 2009)			
	hcpA& B	Localizes to the centromeres and plays a role in growth and mitosis	Chromo-box protein homol-ogue		Hetero-chromatin protein 1
	spc25	Interacts with Ndc80 in the attachment of microtubules to kinetochores	Spc25	SPC25	Spc25
	ndc80	A subunit of the kinetochore complex involved in microtubule binding and the spindle-assembly checkpoint	NDC80	NDC80	Ndc80
Spindle checkpoint	*anapc (apc)*	Anaphase-promoting complex, a cell-cycle regulated ubiquitin-ligase that controls progression through the cell - cycle	APC	APC	Apc
	mad2	Mitotic spindle-assembly checkpoint protein	MAD2L2		MAD2-like
	bub1& 3	Putative mitotic-checkpoint proteins	BUB1 beta	MAD3	Bub1-related kinase
	cdc20	Activator of the APC, required for metaphase/anaphase transition; directs ubiquitination of mitotic cyclins	CDC20	CDC20	FI02843p

	ube2c	Involved in the destruction of cyclins during mitosis	UBE2C	UBE2 18kDa	Ube2c
	mps1	Monopolar spindle kinase, a threonine/tyrosine kinase involved in regulating of the onset of mitosis	TTK	MPS1	Altered disjunc-tion
	espl1	Highly similar to caspase-like protease also called Separase which plays a central role in sister-chromatid segregation in yeast	Separase	ESP1	Separase
Cyto-kinesis	*icpA*	*Dictyostelium*-null mutant has defects in cytokinesis, chromosome segregation, and spindle organization	INCENP	Sli15p	Incenp

Partial list of genes encoding proteins with known or suspected functions in the cell cycle. Genes were found by searching the database at http://www.dictybase.org/. References are provided for *Dictyostelium* genes (or their protein products) experimentally shown to be cell-cycle regulated under the Description column.

developmental program, the cells have already begun to adopt different characteristics (Figure 7). Cells occupying the anterior region of the slug express the extracellular matrix (*ecmA*) gene which encodes a component of the stalk tube (Gaudet et al 2008). They are predisposed to forming the stalk cells while those located in the posterior region of the slug are more of a spore nature (Figure 7) (MacWilliams and Bonner 1979). Approximately 10% of the cells distributed throughout the rear of the slug are known as 'anterior-like' because of their similarities to the prestalk cells (Jermyn and Williams 1991, Sternfeld and David 1982). If the prestalk region is excised, the anterior-like cells move forward to regenerate the missing segment while some of the prespore cells re-differentiate into anterior-like cells (Sternfeld and David 1982). In embryos this phenomenon is known as regulative development (Gilbert 1997). Hence, although a *Dictyostelium* cell may be stalk- or spore-like at this stage of development, it has not yet lost the ability to form the different cell types.

About 18 hour after the onset of development, the cells commit to a particular fate and terminally differentiate. A slug becomes motionless and retracted with its anterior end raised as the prestalk cells at the front force their way through the cell mass. As more and more cells from the apical region plunge downwards, those that were originally at the back of the slug are hoisted upwards to form a fruiting body (Loomis 1996).

Genes involved in terminal differentiation are expected to be expressed during the last few hours of development, at a time when the cells commit to the spore or stalk-cell fate. The expression of an entire suite of terminal-differentiation genes appears to depend on the *Dictyostelium* homologue of the serum response factor, *srfA*. SRF is a transcription factor that controls the expression of genes involved in differentiation

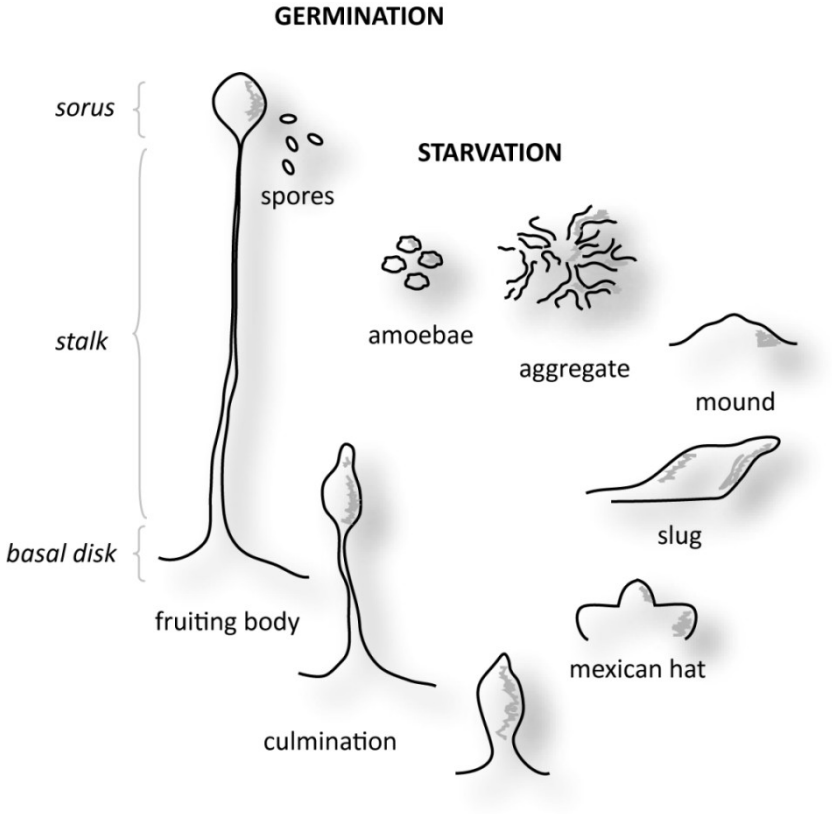

Figure 6. The *Dictyostelium discoideum* life cycle

When fed bacteria or liquid media *Dictyostelium* amoebae grow as single cells. If the food source is exhausted or removed, the cells aggregate and differentiate. Within 24 hours, morphogenesis leads to a simple, multicellular fruiting body consisting of dormant spores mounted on a tapered stalk. The stalk consists of dead, vacuolated cells. It serves to lift the spore mass, facilitating their dispersal to richer environments where they can germinate into amoebae. The spores are contained in the sorus which is bound to the stalk during culmination by the upper and lower cups. The mature fruiting body is supported by a basal disk that anchors it to the substratum (adapted from Gaudet 2008).

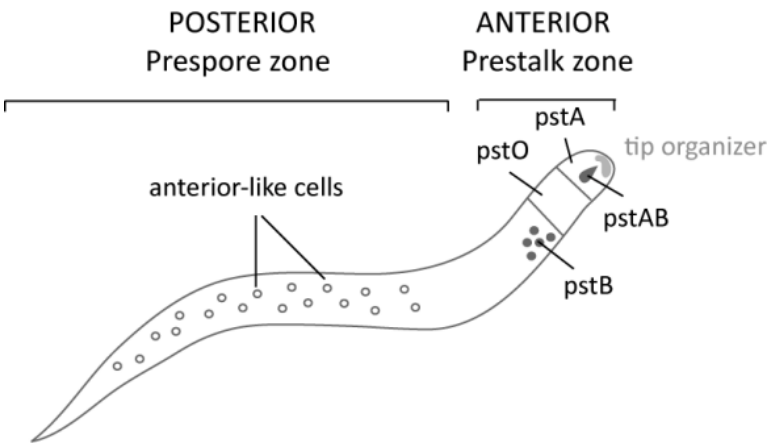

Figure 7. The anatomy of a *Dictyostelium* slug

Prestalk and prespore cells are located in distinct zones of the slug. The anterior region consists of prestalk cells differentiating into stalk cells. The prestalk region is subdivided into parts: the pstB cells which will form the outer basal disk, the prestalkO (pstO) cells which contribute to the upper cup in the late culminant, the prestalkA (pstA) region, just in front of the pstO cells, the pstAB cone, and the tip organizer which is responsive to light and heat. Prespore cells are located in the posterior region. This region also contains 'anterior-like' which are similar to the prestalk cells (adopted from Gaudet et al 2008).

(Escalante and Vicente 2000). In *Dictyostelium, srfA* null cells develop into spores with reduce viability suggesting that SrfA is important for spore maturation. Microarray analyses on wild-type and *srfA* null cells identified 22 SrfA-target genes (Escalante et al 2004). Half of these were detected at low levels during the early stages of development and activated strongly during terminal differentiation. More recently, an mRNA-sequencing study on developing wild-type cells produced a long list of candidate terminal-differentiation genes (Parikh et al 2010). Their transcriptional profiles are available on the *Dictyostelium* gene-expression database dictyExpress (Rot et al 2009). The most strongly upregulated genes, induced only after the early culminate stage (18 hours of development) are listed in Table 2. Many are pseudogenes meaning that they are expressed but do not code for functional proteins (Pink et al 2011). The data set also includes genes that are similar to high copy suppressor of STATalpha. (*hssA*), a gene expressed exclusively in cells of the stalk pathway (Vicente et al 2008) and others which are involved in spore germination. Given that Retinoblastoma controls the expression of lineage-specific genes (Batsche et al 2005, Chen et al 1996, Cole et al 2004, Gu et al 1993, Iavarone et al 2004, Novitch et al 1999, Thomas et al 2001, Toma et al 2000), it is likely that some of the *Dictyostelium* genes identified in these studies are induced during late development by RblA.

1.4.2 *Dictyostelium* differentiation and the cell cycle

Although each *Dictyostelium* cell has the potential to become a stalk cell or a spore, pathway choice is guided by the time lapse between nutrient removal and the last mitosis. When starved, cells that are undergoing mitosis or those that have recently divided usually form part of the stalk. There is a switch from the stalk to the spore

pathway in mid-G2 so that cells that are in the late G2-phase of the cell cycle at the onset of development are most likely to become spores (Araki et al 1994, Araki and Maeda 1998, Gomer and Firtel 1987, MacWilliams et al 2001, McDonald and Durston 1984, Ohmori and Maeda 1987, Weeks and Weijer 1994, Weijer et al 1984, Wood et al 1996, Zimmerman and Weijer 1993). The mechanism tying the phases of the cell cycle to initial cell-type choice is unclear but a few models have been proposed. One model is based on the idea that cell-type bias is driven by a cell's sensitivity to the secreted morphogen differentiation inducing factor-1 (DIF-1) (Thompson and Kay 2000a). DIF-1 is a chlorinated alky phenone that promotes stalk-cell differentiation and inhibits spore formation (Kay and Jermyn 1983). Responsiveness to DIF-1 changes during the cell cycle and is highest in cells that are in mitosis (Thompson and Kay 2001). Another model holds that a *Dictyostelium* cell exits the cell cycle at a specific point in late G2 to develop. Within a population of starving, asynchronously growing cells (i.e. cells in various phases of the cell cycle) some enter development early, as measured by the expression of early differentiation markers such as the cAMP receptor cAR1 (Abe and Maeda 1994), while others develop later by virtue of their distance to the exit point. However, cells that develop more rapidly are stalky under some conditions (Maeda and Maeda 1974, Wang et al 1988) but sporey under others (Araki et al 1994, Huang et al 1997) suggesting that developmental rate and initial cell-type choice are not directly linked.

One attribute thought to be important for a developing *Dictyostelium* cell is its size (Araki and Maeda 1998, Muramoto and Chubb 2008). Cell size is correlated to the cell cycle since a cell that has recently divided is smaller than a cell in late G2 which has had time to grow. It has been proposed that size differences could affect cell mobility and

Table 2. Terminal Differentiation Genes in *Dictyostelium discoideum*

Gene/ID	Description	Cell-type enrichment
DDB_G0293344	Partial tRNA-specific retrotransposon TRE5-C	none
DDB_G0269508	Conserved in Dictyostelids; structural similarity to nuclear transport factor	stalk
DDB_G0284451	Pseudogene	none
DDB_G0267278	ORF1 encoding a protein of unknown function of the putative DNA transposon DDT-A	none
DDB_G0268408	Pseudogene similar to a family of *D. discoideum* genes including DDB_G0267968 and DDB_G0268554	none
DDB_G0268150	Pseudogene similar to a small family of *Dictyostelium* genes	none
DDB_G0268324		stalk
DDB_G0268326		stalk
DDB_G0269320	Pseudogene similar to a family of *Dictyostelium discoideum* genes including DDB_G0292008 and DDB_G0283487	none
DDB_G0269536		stalk
DDB_G0269806		none
DDB_G0270852	Partial ORF2 of tRNA-specific retrotransposon TRE3-C	none
DDB_G0271026	Partial ORF2 of tRNA-specific retrotransposon TRE3-C	none
DDB_G0271560		spore
DDB_G0274235		none
DDB_G0276061		spore
DDB_G0276123		none
DDB_G0277717		none
DDB_G0282443		none
DDB_G0284787		none
DDB_G0285121		stalk
DDB_G0286113	Pseudogene; fragment, similar to DDB_G0269802	none
DDB_G0287051		none
DDB_G0288765		none
DDB_G0291338	Mitochondrial protein	stalk
DDB_G0292170		spore
DDB_G0292228		none
DDB_G0292614		none
DDB_G0293316	Related to the *hssA* genes	stalk
DDB_G0294164	ORF1 encoding GAG and protease proteins of retrotransposon Skipper	none
DDB_G0294198		none
DDB_G0294254	ORF2 encoding reverse transcriptase (RT) and integrase (IN) proteins retrotransposon Skipper	none
DDB_G0295693	Similar to DDB_G0285143	none

DDB_G0288397		spore
DDB_G0275433	Similar to *D. purpureum* protein	stalk
DDB_G0285443	Related to the *hssA* genes	none
DDB_G0271756	Related to the *hssA* genes	none
DDB_G0285567	Related to the *hssA* genes	none
DDB_G0274335		stalk
DDB_G0270004		none
DDB_G0286675	Related to the *hssA* genes	spore
gerA	Germination protein p109	stalk
DDB_G0285273	Highly conserved protein containing AhpC/TSA domain	none
DDB_G0285569		spore
DDB_G0288489		spore
DDB_G0287561	NADH:flavin oxidoreductase/NADH oxidase domain-containing protein	spore
DDB_G0285737	Related to hssA genes	none
DDB_G0287501	Similar to polyketide synthases	none
gerB	Germination protein p109	stalk
DDB_G0274337		spore
DDB_G0289359		none
DDB_G0276687	Related to the *hssA* genes	spore
DDB_G0278553	Small amoebozoan gene family; absent in other organisms	spore
DDB_G0281757		stalk
DDB_G0279023	Contains a predicted signal peptide, putative transmembrane domain, and serine-rich region similar to bacterial SASA repeat	none
DDB_G0293890	Related to *hssA* genes	none
DDB_G0285289		spore
DDB_G0277709		stalk
DDB_G0286887		spore
DDB_G0268858	Contains a predicted signal peptide	none
DDB_G0272298		spore
DDB_G0279545	Similar to bacterial short-chain dehydrogenase/reductase family proteins	spore
DDB_G0282681	Putative pseudogene; fragment, similar to DDB_G0267600, DDB_G0267598	none
DDB_G0271780	Zinc-containing alcohol dehydrogenase (ADH)	spore
DDB_G0289245		stalk
DDB_G0282455		stalk
aslD-1	Similar to acetyl-CoA synthetase	spore
DDB_G0282439		spore
eIF4e3	Orthologue of the eukaryotic initiation factor EIF4E3	stalk
DDB_G0292254		spore
DDB_G0273111		none
iliH	CAZy family GH9; catalyses the hydrolysis of glucosidic linkages; induced by *Legionella pneumophila* infection	stalk

DDB_G0293060		spore
DDB_G0290419		stalk
gerC	Germination protein p109	spore
sinN137	Related to *hssA* genes	stalk
DDB_G0278537		stalk
DDB_G0270594		none
DDB_G0273155	Zinc-containing alcohol dehydrogenase (ADH)	stalk
DDB_G0278231		spore
DDB_G0286203		none
DDB_G0282441		none
cotE	Contains cysteine-rich and mucin-like repeats; contains a signal peptide	spore
DDB_G0292826		spore
DDB_G0288829		spore
DDB_G0279355		spore
DDB_G0292824		stalk
DDB_G0279541		spore
DDB_G0274317		stalk
DDB_G0292822		spore
DDB_G0280337		stalk
DDB_G0288323		stalk

Genes expressed exclusively after 18 hours of development. Genes identified using dictyExpress (Rot et al 2009).

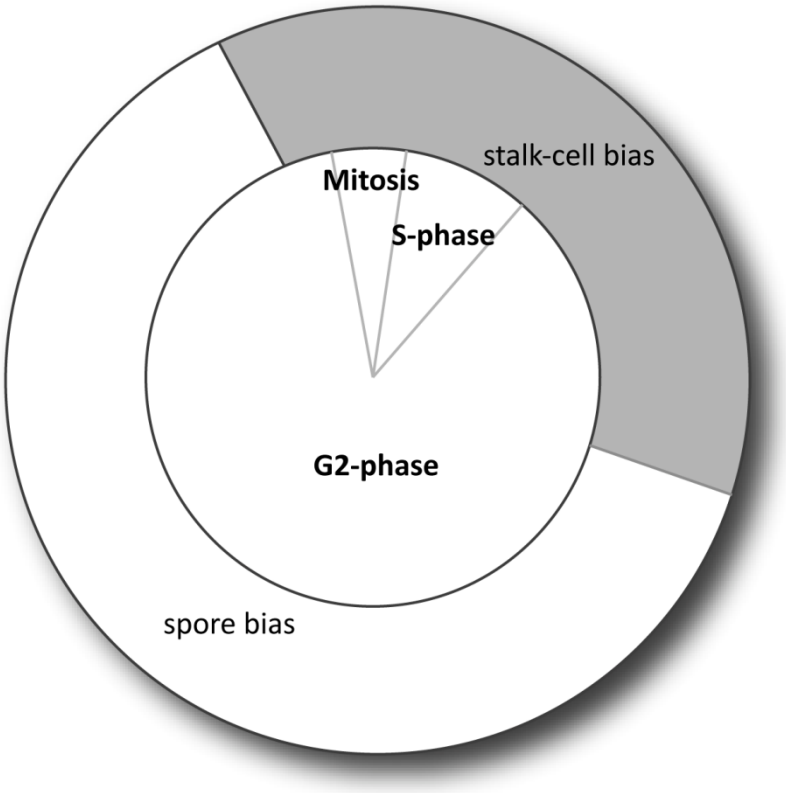

Figure 8. Cell-fate bias is linked to the phases of the cell cycle

Cells that are in the late G2-phase of the cell cycle when starved are most likely to differentiate into spores. Cells that are undergoing mitosis or those that have recently divided are assigned to the stalk pathway (Araki et al 1994, Araki and Maeda 1998, Gomer and Firtel 1987, MacWilliams et al 2001, McDonald and Durston 1984, Ohmori and Maeda 1987, Weeks and Weijer 1994, Weijer et al 1984, Wood et al 1996, Zimmerman and Weijer 1993).

positioning within the developing aggregate where diffusible factors would, in turn, steer cell identity (Meinhardt 1983, Thompson and Kay 2000b). Indeed, *Dictyostelium rblA*-deficient cells are smaller than normal and show a strong stalk-cell preference (MacWilliams et al 2006). Glucose-starved cells or nutrient-depleted stationary-phase cells also have a tendency to become stalk cells (Soll et al 1976, Thompson and Kay 2000a). Late stationary-phase cells, however, are known to increase in size over time (Soll et al 1976) suggesting that size alone is not what predisposes cells toward a certain fate.

Evidence suggests that a *Dictyostelium* cell divides after entering development. In growing cells, two replication-related genes (ribonucleotide reductase and *rblA*) are expressed periodically during the cell cycle. Their mRNA transcript levels drop when the cells are starved but rise again during mid-development (MacWilliams et al 2001, MacWilliams et al 2006). Also histone H1-directed kinase activity increases during mid-development and this is dependent on the cell-cycle cyclin Cyclin B (Luo et al 1995). Recently, Muramoto and Chubb monitored cell-cycle activity in multicellular slugs by using a fluorescently tagged replication factor (proliferating cell nuclear antigen) and time-lapse microscopy (Muramoto and Chubb 2008). Frame-by-frame investigations on developing cells show clear cell division and nuclear DNA synthesis. So even though conditions are not conducive to growth, it appears as though at least some of the cells within a developing population advance through the cell cycle. This final round of cell division may be important for restricting cells to the spore fate (Araki and Maeda 1998).

1.5 Rationale

The *Dictyostelium* genome encodes recognizable homologues of almost all of the mammalian cell-cycle regulators but only a few have been empirically shown to be cell-cycle genes (see Table1 for references). Some accumulate during the G2 phase of the cell cycle (MacWilliams et al 2001, MacWilliams et al 2006) while others encode proteins that show cell-cycle dependent re-localization within the cell shortly before mitosis (Muramoto and Chubb 2008, Schulz et al 2009). Another relevant observation is that *Dictyostelium* cells arrest in late G2 in response to DNA-damaging agents (Muramoto and Chubb 2008). Although this strongly suggests the presence of a G2/M checkpoint in the *Dictyostelium* cell cycle, the current literature does not provide information on the proteins that regulate this transition.

The main goals of this study were (1) to expand our understanding of the *Dictyostelium* cell cycle and (2) to clarify the role of the cell cycle in development. We reasoned that if the molecular components of the cell cycle were involved in cell-type biases, then these biases would be altered in the presence of cell-cycle mutants. With this in mind, we generate a series of Cdk1 mutants lacking the inhibitory phosphorylation site(s) including the Cdk1 threonone14-to alanine (T14A) mutant, the Cdk1 tyrosine15-to-phenylalanine (Y15F) mutant, and the double mutant Cdk1T14AY15F lacking both phosphorylation sites. Considering that substitution of the tyrosine for a phenylalanine is cytotoxic (Gould and Nurse 1989), each mutated gene was placed under the control of an inducible promoter known as the tetracycline-responsive element (tet). This promoter is part of the tetON expression system, a vector that is induced by doxycycline (Urlinger et al 2000). The reverse tetracycline transactivating element (Urlinger et al 2000), which binds to the tet in the presence of doxycycline to induced expression, was cloned into the

same vector backbone. This allowed us to select for positive transformants using one antibiotic. A similar, dual TetOn vector has been used to successfully induced gene expression in *Dictyostelium* cells (Veltman et al 2009). To assess vector-derived gene expression, we fused a codon-optimized tandem affinity purification tag (Puig et al 2001) downstream of *cdk1*, away from the presumptive catalytic site. Each recombinant vector was introduced independently into the *Dictyostelium* laboratory strain Ax2. This enabled us to examine the effects of the Cdk1 mutants in a wild-type background.

The neomycin-resistance cassette, one of the few antibiotic markers used to select for positive *Dictyostelium* transformants, induces spore-related characteristics (Schulkes et al 1995). This can be problematic in experiments designed to determine the differentiation preference of a cell wherein cell-type bias is measured with respect to the untransformed, parental strain. The tetON system allowed us to perform these experiments using a single strain. By comparing cells in the induced and uninduced states, we were able to study the effects of the *cdk1* mutations on cell-type bias in an otherwise genetically identical background.

Although the Retinoblastoma/E2F/DP pathway is conserved in most eukaryotes it appears to have been lost in the yeast phylum. *Dictyostelium* is one of the most primitive organisms with a Retinoblastoma-related protein. Cells of a null mutant grow more slowly and are smaller than the wild-type control (MacWilliams et al 2006). This phenotype is surprisingly mild given the importance of Retinoblastoma in cell-cycle control. We wanted to better define the role of RblA in the *Dictyostelium* cell cycle. Since Retinoblastoma exerts control over the cell cycle primarily at the level of transcription, we used mRNA-sequencing to further characterize the RblA mutant.

A picture emerges of a cell cycle in which Cdk1 and RblA act as opposing molecules to control cell proliferation. Our findings improve our understanding of the *Dictyostelium* cell cycle and provide new insights into the mechanism linking the phases of the cell cycle to cell-type differentiation.

2. MATERIALS AND METHODS

2.1 Strains

Strains generated in this study were named according strain nomenclature guidelines set forth by *Dictyostelium* Community Organizing Committee. The format is the following:

gene-/[promoter]:gene(substitution):marker

where

- represents a null mutant
/ represents a compound mutant
[ ] represents the promoter gene
( ) indicates a substitution
: represents a fusion between two genes

A complete description of each strain acquired or generated in this study is provided in Table 3.

2.2 Media

Strains were maintained in HL5 media (Watts and Ashworth) with 25 units of penicillin and 25 μg ml^{-1} streptomycin (SIGMA; stock solution of 10000 units penicillin and 10 mg streptomycin ml^{-1}). For the glucose mixing experiments, 1 L HL5 medium without glucose was prepared, divided into two equal volumes of 0.5 L, autoclaved, then 86 mM D-glucose (Roth; stock solution of 1.55 M prepared in water and sterilized by filtration) was added to one of the bottles. This bottle was labelled G+. The same volume of filter-sterilized water was added to the second bottle which was labelled G-.

Table 3. Strains acquired or generated in this study

Strain name	Description	Genotype	source
Ax2	Axenic lab strain	axeA2, axeB2, axeC2	(Watts and Ashworth 1970) via Coukell group York University
rblA-	*rblA* disruptant mutant	*rblA*-, axeA2, axeB2, axeC2, bsR	(MacWilliams et al 2006)
[cdk1]:UBI:gal	Transcriptional reporter; Ax2 expressing lacZ encoding an unstable beta-galactosidase under the control of the *cdk1* promoter	axeA2, axeB2, axeC2, [cdk1]: UBI:lacZ, neoR	this study
rblA- /[cdk1]:UBI:gal	Transcriptional reporter; *rblA* disruptant expressing lacZ encoding an unstable beta-galactosidase under the control of the *cdk1* promoter	*rblA*-, axeA2, axeB2, axeC2, [cdk1]: UBI:lacZ, bsR, neoR	this study
[cycB]:UBI:gal	Transcriptional reporter; Ax2 expressing lacZ encoding an unstable beta-galactosidase under the control of the cyclinB promoter	axeA2, axeB2, axeC2, [cycB]: UBI:lacZ, neoR	this study
rblA- /[cycB]:UBI:gal	Transcriptional reporter; *rblA* disruptant mutant expressing lacZ encoding an unstable beta-galactosidase under the control of the cyclinB promoter	*rblA*-, axeA2, axeB2, axeC2, [cycB]: UBI:lacZ, bsR, neoR	this study
[tet]:*cdk*1:TAP	*cdk1* wild-type overexpressor tagged with TAP at the carboxy terminus under the control of the doxycycline inducible expression system in AX2	axeA2, axeB2, axeC2, [tet]:*cdk1*:TAP	this study
[tet]:*cdk1*(T14A): TAP	*cdk1*(T14A) overexpressor tagged with TAP at the carboxy terminus under the control of the doxycycline inducible expression system in AX2	axeA2, axeB2, axeC2, [tet]:*cdk1* (T14A): TAP, neoR	this study
[tet]:*cdk1*(Y15F): TAP	*cdk1*(Y15F) overexpressor tagged with TAP at the carboxy terminus under the control of the	axeA2, axeB2, axeC2, [tet]:*cdk1*	this study

	doxycycline inducible expression system in AX2	(Y15F): TAP, neoR	
[tet]:*cdk1*(T14A-Y15F):TAP	*cdk1*(T14AY15F) overexpressor tagged with TAP at the carboxy terminus under the control of the doxycycline inducible expression system in AX2	axeA2, axeB2, axeC2, [tet]:*cdk1* (T14AY15F): TAP, neoR	this study
rblA-/[tet]:*cdk1*(T14A):TAP	*cdk1*(T14A) overexpressor tagged with TAP at the carboxy terminus under the control of the doxycycline inducible expression system in *rblA*-	*rblA*-, axeA2, axeB2, axeC2, [tet]:*cdk1* (T14A): TAP, neoR, bsR	this study
[tet]:*cdk1*(Y15F): TAP/ GFP:*tubA*	*cdk1*(Y15F) overexpressor tagged with TAP at the carboxy terminus under the control of the doxycycline inducible expression system in AX2 marked with GFP:alpha tubulin	axeA2, axeB2, axeC2, [tet]:*cdk1* (Y15F): TAP, GFP:*tubA*, neoR, bsR	this study
[tet]:*cdk1*(Y15F): TAP/ RFP:*pcna*	*cdk1*(Y15F) overexpressor tagged with TAP at the carboxy terminus under the control of the doxycycline inducible expression system in AX2 marked with RFP:PCNA	axeA2, axeB2, axeC2, [tet]:*cdk1* (Y15F): TAP, RFP:*pcna,* neoR, bsR	this study
[tet]:*cdk1*(Y15F): TAP/ *CP224*:GFP	*cdk1*(Y15F) overexpressor tagged with TAP at the carboxy terminus under the control of the doxycycline inducible expression system in AX2 marked with CP224:GFP	axeA2, axeB2, axeC2, [tet]:*cdk1* (Y15F): TAP, *CP224*:-GFP, neoR, bsR	this study

2.3 Construction of a *Dictyostelium* tandem affinity purification (TAP) tag

A tandem affinity purification (TAP) tag with codons optimized for *Dictyostelium* was generated by polymerase-chain reaction (PCR)**.** The TAP tag consists of three modules: The calmodulin binding peptide (CBP), followed by the tobacco etch virus cleavage site, and protein A at the very end (Puig et al 2001). Protein A allows the fusion protein complex to bind to IgG beads. The partially purified complex is recovered using the tobacco etch virus protease. The complex goes through another round of purification by binding reversibly to calmodulin-coated beads.

Attempts at using conventional PCR for TAP assembly failed, producing short fragments but never the full-length product (results not shown). As an alternative, we used thermodynamically balanced inside-out PCR for gene synthesis (Gao et al 2003). With this method, the N-terminal half of the gene was coded by a set of overlapping forward primers and the C-terminal half by a group of overlapping reverse primers. Using the computer program DNAWorks (Hoover and Lubkowski 2002), 24 oligonucleotides were designed for assembly into a C-terminal TAP tag (Figure 9). The use of an automated program for primer design was beneficial, producing primers with uniform melting temperatures and a minimum tendency to form hairpins or misprime. In some instances, however, the primers were optimized by reducing or extending the computer-generated sequences to include a 3' GC clamp. The numbers and concentrations of primers that produced the desired PCR product were determined by iterative trials. We found that assembly worked best using two primer pairs at a time with 20 to 40 nM of template. Accordingly, the 583 bp full-length TAP tag was assembled in 6 separate PCR

Figure 9. PCR-based synthesis of the *Dictyostelium* C-terminal TAP tag

Forward (f) primers are blue in colour and reverse (r) primers red. Alternate lower and upper cases are used to delineate one primer from the next. Some primers were optimized by shortening ( ) or extending (^) the DNAworks computer-generated sequences.

reactions using the following parameters: Denaturation at 95 °C for 2 minutes, during which time 2.5 units of Expand Long (Roche) polymerase were added to avoid mispriming. This was followed by 25 cycles of 95 °C for 15 seconds, 55 °C for 1 minute, and 68 °C for 1 minute followed by a final extension at 68 °C for 10 minutes. After each PCR reaction, the synthetic gene fragment was resolved on a 1.7% agarose gel in 1xTBE (89 mM Tris base, 89 mM boric acid, 2 mM EDTA, pH 8.0; Tris base and boric acid from ROTH, EDTA from SERVA) and gel-purified (Qiagen QIAquick Gel Extraction Kit) prior to serving as template for the subsequent extension reaction. For cloning purposes, unique *Spe*I and *Xho*I sites were included upstream and downstream of the TAP tag, respectively. Using the sites, the tag was introduced into the plasmid pBluescript for sequence verification prior to fusing it downstream of *cdk*1.

2.4 Vectors

Vectors generated in this study were named according to the Dictybase molecular genetics constructs nomenclature guidelines. Specifically, promoter regions are separated from coding sequences by a slash (/). Coding sequences are separated by a dash (-) (http://www.dictybase.org/Dicty_Info/nomenclature_guidelines.html).

2.4.1 Reporter constructs

For reporter gene constructs, the *cdk*1 promoter region from -1209 to 31 was amplified using the primers 5'- CTCTAGATGATTTAGGGGTATAATATTTGG -3' that introduced an upstream *Xba*I site and 5'-TGGATCCTTGATATCTTGATAAACCTCC -3' that overlapped the ATG codon and introduced a downstream *Bam*HI site. The 1248 bp fragment was used to replace the *rnr*B promoter in the vector *rnr*B::ilegal (Gaudet *et al*., 2001) to make cdk1/UBI-lacZ (Figure 10). In this reporter construct the *cdk1* promoter

drives the expression of a fragment of a ubiquitin (UBI) gene from *S. cerevisiae* attached to lacZ by a linker sequence (MacWilliams et al 2001). This modified lacZ encodes a labile beta-galactosidase with a half-life of approximately 30 minutes (MacWilliams et al 2001). For *cyc*B, the sequence -1969 to 89 was amplified using 5'-CTCTAGATCAACAAATCCATCATTTCC-3' and 5'-TATGGATCCTGGTACTTTGTTTTCATCC-3' then cloned upstream of unstable beta-galactosidase as described above to make the reporter construct cycB/UBI-lacZ.

2.4.2 Site-directed mutagenesis of *cdk1* cDNA by PCR

The *cdk*1 cDNA (a gift from G. Weeks) was subcloned from a pGEX backbone into the *Bgl*II and *Spe*I sites of pBluescript KS (+) (Stratagene) to make pBluescript(*cdk*1). Specific base substitutions were introduced in *cdk*1 using site-directed mutagenesis PCR (Ho et al 1989). Three mutagenic PCR primer-pairs were designed to introduce base substitutions in *cdk1* (Table 4). In the first PCR reaction, the N-terminal half of the gene was amplified with the ´universal´ primer and the desired *cdk*1 mutagenesis reverse primer while the C-terminal region was amplified separately with the corresponding *cdk*1 mutagenesis forward primer and the ´reverse´ primers. For the first amplification reactions, 50-100 ng of the vector pBluescript(*cdk*1) and 2.5 units of *PfuTurbo*® DNA polymerase (Stratagene) were used. PCR conditions were: Denaturation at 95°C for 5 minutes, 20 cycles of 95°C for 30 seconds, annealing at 40°C for 30 seconds, and extension at 72°C for 3 minutes, followed by 72°C for 10 minutes (Mastercycler gradient, Eppendorf). The PCR products were individually treated with the restriction endonuclease *Dpn*I (New England Biolabs Inc.), cleaned, quantified, and mixed in equimolar amounts for the final amplification. For this PCR reaction the

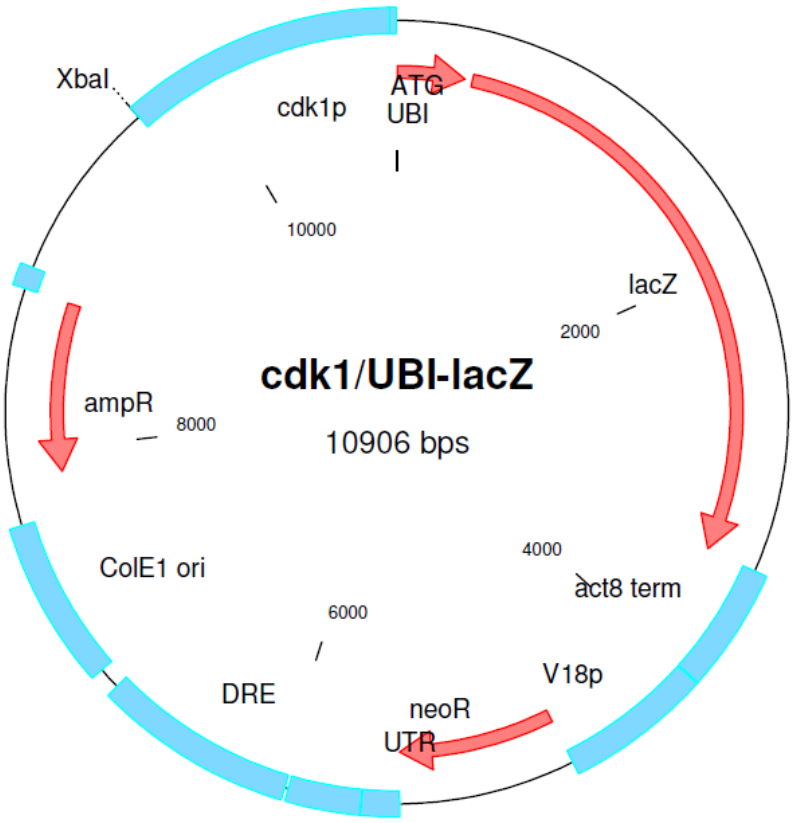

Figure 10. The cdk1/UBI-lacZ reporter construct.

UBI-lacZ encoding an unstable beta-galactosidase is under the control of the *cdk1* promoter; transcription is terminated at the actin8 (act8) terminator sequence. The vector also contains the ampicillin resistance (ampR) and the neoR cassettes for selection in *E.coli* and *Dictyostelium*, respectively. The neoR gene encodes neomycin phosphotransferase, an enzyme which confers resistance to neomycin. It is driven by the promoter of the ribosomal protein gene V18 allowing for transformation in non-axenic strains; transcription ends at the 3' untranslated region (UTR) of transposon5 and terminator sequence. The *Dictyostelium* repetitive element (DRE) targets integration to sites 50 +/- 4 bp upstream of tRNA genes which leads to more homogeneous expression and decreases spontaneous plasmid loss (Marschalek et al 1992, Winckler 1998). cdk1/UBI-lacZ replicates automonously in *E. coli* from the ColE1 ori. Location of features**:** ubiquitin fragment and linker sequence 3-351, lacZ 390-3444, terminator from actin 8 gene 3452-3996, V18 promoter 4001-4644, neoR 4645-5439, 3´UTR from transposon5 5440-5940, DRE 6834-5956**,** ColE1 ori 6934-7669, ampR 8736-7876, *cdk1* 9660-10903.

Table 4. Primers for site-directed mutagenesis PCR.

Primer name	length (nts)	Tm (ºC)	GC content (%)	Sequence (5´-3´)
universal	21	70.3	50	CGACGTTGTAAAACGACGGCC
reverse	23	65.8	50	AGCGGATAACAATTTCACACAGG
*cdk1*T14A fwd	22	63.3	45	GGTGAAGGT**G**CCTATGGTAAAG
*cdk1*T14A rev	22	63.3	45	CTTTACCATAGG**C**ACCTTCACC
*cdk1*Y15F fwd	22	60.3	50	GGTGAAGGTACCT**T**TGGTAAAG
*cdk1*Y15F rev	22	60.3	50	CTTTACCA**A**AGGTACCTTCACC
*cdk1*T14AY15F fwd	22	65.5	57	GGTGAAGGT**G**CCT**T**TGGTAAAG
*cdk1*T14AY15F rev	22	65.5	43	CTTTACCA**A**AGG**C**ACCTTCACC

Primer pairs are grouped together. fwd stands for forward and rev for reverse. Point mutation(s) are in bold font.

external primers 'universal' and 'reverse' were used at a concentration of 0.1 μM. The fusion products were cloned back into pBluescript KS (+) for sequence verification by automated sequencing.

pBluescript(*cdk*1) was treated with *Bgl*II and *Spe*I and ligated into the corresponding sites of a pGEM derivative (constructed by H.K. MacWilliams). The codon optimized *Dictyostelium* TAP tag was ligated downstream of *cdk*1 using the sites *Spe*I and *Xho*I. Finally, the first few amino acids of *cdk*1 including the ATG initiation codon, missing from the original cDNA (Michaelis and Weeks 1992), were reconstituted with the synthetic oligonucleotide 5´-GATCTATGGAATCAGATGGAGGTTTAT CAAGAT-3´.

For inducible expression, TAP-tagged *cdk*1 was cloned under the control of the tetracycline response element (tet) using the restriction enzyme sites *Bgl*II and *Xho*I. The reverse tetracycline transactivator (rtTA) was inserted into the *Bgl*I/*Nhe*I sites to generate tet/*cdk1*-TAP-rtTA, a single vector bearing both elements of the tetON system selectable with the antibiotic geneticin (Figure 11)(H.K. MacWilliams, unpublished).

2.5 Gene Transformation

Reporter constructs and doxycycline-inducible vectors were introduced into cells using the calcium chloride precipitation and glycerol shock method (Nellen et al 1984). Following an overnight incubation in non-selective HL5 medium, the cells were harvested by centrifugation and suspended in 0.5 ml of *Klebsiella aerogenes*. These bacteria serve as a food source for *Dictyostelium* (Fey et al 2007). The cell suspension was spread uniformly onto KK2 agar (1.5% agar in 20 mM potassium phosphate, pH 6.2) containing 100 μg ml^{-1} geneticin (GIBCO; 20 mg ml^{-1} stock in water) then incubated at

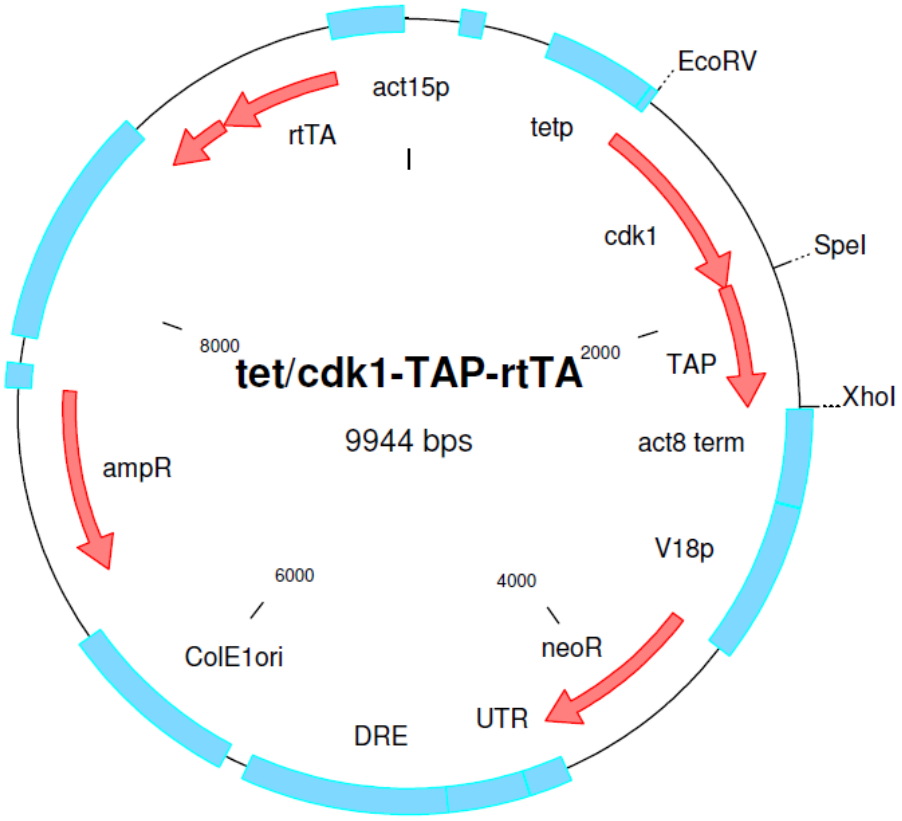

Figure 11. The *Dictyostelium* doxycycline-inducible vector tet/*cdk1*-TAP-rtTA

The reverse tetracycline transcriptional activator (rtTA) is constitutively expressed from the *Dictyostelium* actin15 promoter (act15p). In the presence of doxycycline, rtTA binds to the tetracycline-response elements located within the inducible promoter (tetp) to activate the transcription of *cdk1*-TAP.The tandem affinity purification tag (TAP) for protein complex purification is fused to the 3' of *cdk1*; transcription is terminated at the actin8 terminator (act8 term) sequence. The vector also contains the neomycin (neoR) and ampicillin resistance (ampR) cassettes for selection in *Dictytostelium* and *E.coli*, respectively. The *neoR* gene is driven by the promoter of the ribosomal protein gene V18 (V18p) allowing for transformation in non-axenic strains; transcription ends at the 3' untranslated region (UTR) of transposon 5 and terminator sequence. The *Dictyostelium* repetitive element (DRE) targets integration to sites 50 +/- 4 base-pairs upstream of tRNA genes which leads to more homogeneous expression and decreases spontaneous plasmid loss (Marschalek et al 1992, Winckler 1998). tet/*cdk1*-TAP-rtTA replicates automonously in *E. coli* from the ColE1 ori. Restriction enzymes recognition sites for subcloning are shown. Location of features**:** tetp 585-1016, *cdk1* 1020-1910, TAP 1900-2472, act8 term 2482-2872, V18 promoter 2877-3520, neoR 3521-4315, 3´UTR from transposon5 and terminator 4316-4819, DRE 5645-4817, ColE1 ori 6480-5745, ampR 7547-6687, transactivator 9029-8733, rtTA 9605-9032, act15p 9924-9622.

22ºC until clones were visible which took about five days. Spores from clonal isolates that had formed on the bacterial lawns were inoculated separately in HL5 medium containing 20 μg ml^{-1} of geneticin.

Fluorescent vectors including gfp-*tubA* (Koonce et al 1999), *CP224*-gfp (a centrosomal protein fused upstream of green-fluorescent protein) (Graf et al 2000), or rfp-*pcna* (Muramoto and Chubb 2008) were transformed into [tet]:*cdk1*(Y15F):TAP cells using a modified version of the electroporation protocol (Knecht and Pang 1995). In detail, 50 μg of vector DNA were ethanol precipitated, resuspended in 10 μl H50 buffer (20mM HEPES, 50 mM KCl, 10 mM NaCl, 1 mM $MgSO_4$, 5 mM $NaHCO_3$, 1 mM NaH_2PO_4, pH 7.0; HEPES from Sigma, $NaHCO_3$ from Merck, NaH_2PO_4 from SERVA, all other chemicals from ROTH), and stored on ice. Cells ($5x10^6$) were washed twice in 25 ml of ice-cold H50 buffer then resuspended in 100 μl of H50. The DNA and the cells were combined and transferred to an ice-cold electroporation cuvette (BioRad; 0.1 cm gap). Cells were electroporated twice at 0.85 kV, 25 μF, and a parallel resistance of ∞ using a BioRAD electroporator (GenePulser® II). The cells were transferred from the cuvette into a 100 mm Petri dish (SARSTEDT) containing 10 ml HL5 medium. Clones were selected the following day by adding 10 μg ml^{-1} geneticin and 10 μg ml^{-1} blasticidin (Life Technologies™; 5 mg ml^{-1} stock solution in water).

2.6 Culture conditions

Ax2 cells transformed with the reporter construct cdk1/UBI-lacZ or cycB/UBI-lacZ were maintained in HL5 medium containing 20 μg ml^{-1} geneticin. For *rblA*-deficient cells carrying reporter constructs, 10 μg ml^{-1} blasticidin was also included in the growth medium.

Doxycycline-inducible strains were grown in HL5 medium with 20 μg ml^{-1} geneticin. [tet]:*cdk1*(Y15F):TAP cells transformed with the fluorescent vectors were cultured in HL5 with 10 μg ml^{-1} geneticin and 10 μg ml^{-1} blasticidin. For induction the tetracycline analogue doxycycline (SIGMA; 20 mg ml^{-1} stock prepared in water) was added to a final concentration of 20 μg ml^{-1}. To remove the doxycycline, cells were washed twice in KK2 buffer (20 mM potassium phosphate, pH 6.2) then resuspended in conditioned medium (McDonald and Durston 1984) or buffer. We noted that the Y15F slow-growth phenotype was lost after several generations and so [tet]:*cdk1*(Y15F):TAP and [tet]:*cdk1*(T14AY21F):TAP cells were regularly cloned on *Klebsiella aerogenes* lawns then tested for growth by plating them with bacteria onto KK2 agar with doxycycline (20 μg ml^{-1}) and without. Clonal isolates that showed growth in the absence of doxycycline and no growth in the presence of doxycycline were used for further analysis.

Cells grown in HL5 medium without glucose were passaged at $1x10^5$ cells ml^{-1} then maintained in exponential growth at densities below $5x10^5$ cells ml^{-1}.

2.7 Cell counts and size measurements

Cell counts and size measures were taken in triplicate every twenty to thirty minutes using a Coulter counter (Beckman-Coulter Z2 particle analyser) by diluting 100 μl of culture in 0.7% sodium chloride solution containing 5 mM EDTA. The size data – in the form of distribution graphs and tabular listings – was stored on a standard PC and visualized using the Coulter® Accucomp® software version 3.01a. The threshold size for mitosis was calculated by averaging the sizes of wild-type and uninduced cells listed in Table 5.

2.8 Bromodeoxyuridine incorporation

Bromodeoxyuridine labelling and staining was exactly as described (MacWilliams et al 2001) using a 0.8 ml aliquot of cells and 100 µM bromodeoxyuridine (SIGMA; 10mM stock solution prepared in water and filter-sterilized). Bromodeoxyuridine-positive cells were counted automatically using a custom-written ImageJ macro (H.K. MacWilliams, unpublished).

2.9 Developmental conditions

To initiate development, cells were washed twice in sterile KK2 buffer then resuspended in 2.5 ml of sterile KK2. The cell suspension was dispersed on a nitrocellulose membrane (Whatman BA85; 82 mm diameter disks) overlaid on two layers of pre-cut 3MM Whatman (~82mm diameter) moistened with KK2. The excess buffer flowing out of the sides of the membrane was removed with scrap pieces of 3MM Whatman then the membrane was transferred onto a freshly prepared KK2 agar plate using forceps. To prevent drying, two layers of 3MM Whatman were taped-down to the lid of the Petri dish and moisten with KK2. The closed Petri dishes were stored in a moist chamber. For mRNA-sequencing, aggregates were harvested from the nitrocellulose membranes at the early culminant stage just after the spore mass lifted off the substrate; this occurred at about 18 hours in the Ax2 strain and 15 hours in the *rblA* disruptant.

2.10 Whole-mount histochemical detection of beta-galactosidase activity

For reporter assays, the circular nitrocellulose membrane containing the washed cells was cut into eight equal pieces (like those of a pie). At the desired developmental stage, a piece of the membrane was placed cells facing upwards onto a piece of Whatman moistened with fixing solution composed of 0.1% glutaraldehyde (SIGMA; 4% stock)

and 2% Tween-20 (SIGMA) in Z buffer (60 mM Na_2HPO_4, 40 mM NaH_2PO_4, 10mM KCl and 1 mM $MgCl_2$, pH 7.0; Na_2HPO_4 and $MgCl_2$ from Roth). Cells were fixed for 5 minutes at room temperature. Using clean forceps, the membrane was dropped cells facing downward into 7.5 ml fixing solution, incubated for 10 minutes then washed two times 1 minute in Z-buffer. Histochemical staining for β-galactosidase activity was performed as previously reported (Dingermann et al 1989).

2.11 Cell synchronization

To obtain Ax2 cells in different phases of the cell cycle, cultures were artificially synchronized using the cold-shock protocol (Maeda 2011). Specifically cultures were diluted to $2x10^5$ cells ml^{-1} in HL5 and grown in shaken suspension for 4 to 5 generations (2 days) before synchronization. During this time period, the cultures were diluted in HL5 medium if necessary in order to keep them growing exponentially. Cultures between $0.5\text{-}1x10^6$ cells ml^{-1} were incubated for 16 hours at 9.5ºC in an incubator (Heraeus BK-600) with constant agitation (75 rpm). Given that the rotory shaker (Brunswick Scientific GmbH Model G2) generated heat, the incubator was set to 5.5 ºC. The actual temperature of the culture was monitored by placing a thermometer inside a flask filled with water (volume equivalent to the volume of the culture). The next morning, the cultures were rapidly warmed to 22ºC in a 40ºC water bath. Changes in culture temperature were monitored using an ethanol-washed thermometer. The quality of the synchronization was assessed by taking cell counts and size measurements in triplicate every thirty minutes with a Coulter counter. Also an aliquot of the synchronized culture was taken every hour for bromodeoxyuridine labelling to monitor passage through S phase.

For RNA-blot analysis, synchronously growing cells (approximately $1x10^7$) were harvested every hour, snap frozen in liquid nitrogen, and stored at -80 ºC until processing. For mRNA-sequencing about $5x10^7$ cells were harvested at 30 minute-intervals and fixed in 1 ml RNALater® (Ambion).

2.12 Mixing experiments

The standard operating procedure for fluorescently-labelling cells with fluorescein was the following: Cells ($4x10^6$) were thoroughly washed-free of growth medium and resuspended in KK2 buffer at a density of $4x10^6$ cells ml^{-1}. An equal volume of KK2 containing 20 µM of CellTracker™ Green 5-chloromethylfluorescein diacetate (CMFDA, Molecular Probes, Invitrogen; 20 x 50 µg; 10 mM stock in dimethylsulfoxide) was added and the suspensions incubated at room temperature for 30 minutes with constant agitation. Non-labelled cells ($2x10^7$) were washed in parallel, resuspended in 5 ml KK2, and mock stained by adding 5 ml of KK2 containing 0.2% dimethylsulfoxide.

For mixing experiments using the doxycycline-inducible strains, exponentially growing [tet]:*cdk1*(T14A):TAP cells and [tet]:*cdk1*:TAP cells in HL5 medium were induced with 20 µg ml^{-1} doxycycline for 24 hours prior to fluorescein labelling. A second culture of each strain was grown in HL5 without doxycycline and served as the source of uninduced cells. For induced expression during early development, [tet]:*cdk1*(T14A):TAP cells cultured in HL5 without doxycycline were labelled with fluorescein as described above then resuspended in phosphate buffer at $1x10^7$ cells ml^{-1}. In parallel, [tet]:*cdk1*(T14A):TAP cells were washed and mock labelled with 0.1% dimethylsulfoxide. Each of the cell suspensions (labelled and non-labelled) was divided

into two aliquots, and doxycycline (final concentration of 20 μg ml^{-1}) was added to one of the aliquots. The aliquots containing doxycycline were referred to as 'induced during development' whereas those without doxycycline were named 'uninduced'. Cell suspensions were incubated in the dark for four hours at room temperature with constant agitation.

The general procedure after fluorescein labelling was as follows: Cells were washed three times in ice-cold KK2, incubated for an additional 20 minutes to remove the excess dye then washed three times again. Both the fluorescein-labelled and non-labelled cells were resuspened in KK2 buffer at $2x10^7$ cells ml^{-1}. Labelled cells ($3x10^5$) were mixed with an excess of non-labelled cells ($2.7x10^6$) then 0.1 ml of the cell mixture was plated on 1% agarose (Bioshop) plates for slugs and 1% buffered agar for fruiting bodies (note that the plates were prepared the day of the experiment by pipetting 1 ml of melted agarose or agar into a 35 mm Petri dish (SARSTEDT)). Agarose has lower fluorescence than bacteriological agar and therefore allows for better imaging of the fluorescent slugs. The agarose plates with cells were sealed with parafilm to prevent them over-drying then incubated at 16 °C to prolong the slug stage. The plates for spores were stored in a moist chamber at 22 °C. Spores were harvested from fruiting bodies 2 days after plating the cells.

2.13 Microscopy

Multicellular structures stained for β-galactosidase activity were imaged at 63x magnification on a Nikon SMZ 1500 stereomicroscope and Leica DFC420 5 megapixel colour digital camera. To visualize fluorescently labelled microtubules, centrosomes, or PCNA, [tet]:*cdk1*(Y15F):TAP/*GFP*:*tubA*, [tet]:*cdk1*(Y15F):TAP/*CP224*:GFP, or

[tet]:*cdk1*(Y15F):TAP/RFP:*pcna* cells were settled onto circular coverslips (Roth, 15 mm diameter), incubated for 1 hour in LoFlo medium (Liu et al 2002) , rinsed twice in KK2 buffer then fixed in ice-cold methanol. The coverslips were air-dried then mounted onto a rectangular coverslip (Roth; 40 mm x 24 mm) in a drop of 50% glycerol containing 1 μg ml^{-1} 4′,6-diamidino-2-phenylindole DAPI (SIGMA; 1 mg ml^{-1} stock solution) . Cells were photographed using a Hamamatsu c8484 camera adapted to a Nikon Eclipse 2000 inverted microscope and 60x oil objective. Illumination was provided by an argon ion laser through UV and FITC optical filters. Slugs were photographed using the same microscope and camera but with a 10x objective. A portion of the agarose containing the slugs was excised using a clean scalpel. The gel slab was mounted onto a coverslip, cells facing downwards, in a drop of immersion oil. For the slug images included in this manuscript the anterior ends of the slugs are on the right unless otherwise stated.

To quantify cell-type preference, an aliquot of the mixed cells (approximately $1x10^5$) was diluted 15-fold in KK2 buffer containing 5 mM caffeine (SIGMA; 50 mM stock) to prevent the cells from aggregating. The diluted cell mixture (200 μl) was deposited onto chamber coverslips. Cells were allowed to settle then photographed sequentially in brightfield then fluorescence mode. For each sample, we took 10 frames, carefully moving the microscope stage after each image-acquisition to avoid photographing the same region twice. Images were batch converted into TIFF files using the Wasabi imaging software (Hamamatsu Phototonics version 1.5.0.2) then analysed using ImageJ version 1.44e (National Institutes of Health, Bethesda, MD) with a Cell Counter plugin (H.K. MacWilliams unpublished). The percentage of fluorescein-labelled cells was determined using a total of no less than 1000 particles in brightfield.

Spores were harvested from fruiting bodies, photographed, and counted as described above. Alternatively, percentage fluorescence was measured using FACS analysis.

2.14 FACS analysis

Cells (approximately $1x10^6$) or spores harvested from one agar plate were resuspended in 2 ml sheath fluid (Partec) then fed through a FACS instrument (Partec CyFlo® SL). Forward light scatter and fluorescence intensity were measured for no less than 30000 cells or 10000 spores (referred to as events) per sample. The data was visualized as scattergrams (Figure 12) using the FloMaxSoftware ®. Gating was used to select the populations of interest and to eliminate dead cells or debris by manually drawing (mouse-controlled) polygons around the fluorescent and non-fluorescent data points. The two subpopulations of cells or spores left after gating were used to calculate percentage fluorescence.

2.15 Immunoblotting

Immunological staining with a peroxidase-coupled antibody was used to confirm TAP-tagged fusion-protein expression. Briefly, $5x10^6$ cells were resuspended in 100 µl of sample buffer (50 mM Tris-Cl pH 6.8, 100 mM dithiothreitol, 2% SDS, 0.1% bromophenol blue, 10% glycerol; DTT and glycerol from Sigma, bromophenol blue from FLUKA) and boiled for 5 minutes. The proteins (3 µl or the equivalent of $1.5x10^5$ cells) were then separated on a 10% SDS-polyacrylamide gel and transferred onto a nitrocellulose membrane (Amersham Hybond™ ECL™) as described (Sambrook et al 1989). The membrane was stained with Ponceau S (Sigma; 0.1% (w/v) in 5% acetic acid) to assess loading and fractionation then blocked for 1 hour in 5% non-fat milk prepared in TBST (10 mM Tris- Cl, 130 mM NaCl, 0.5% Tween-20, pH 8.0).

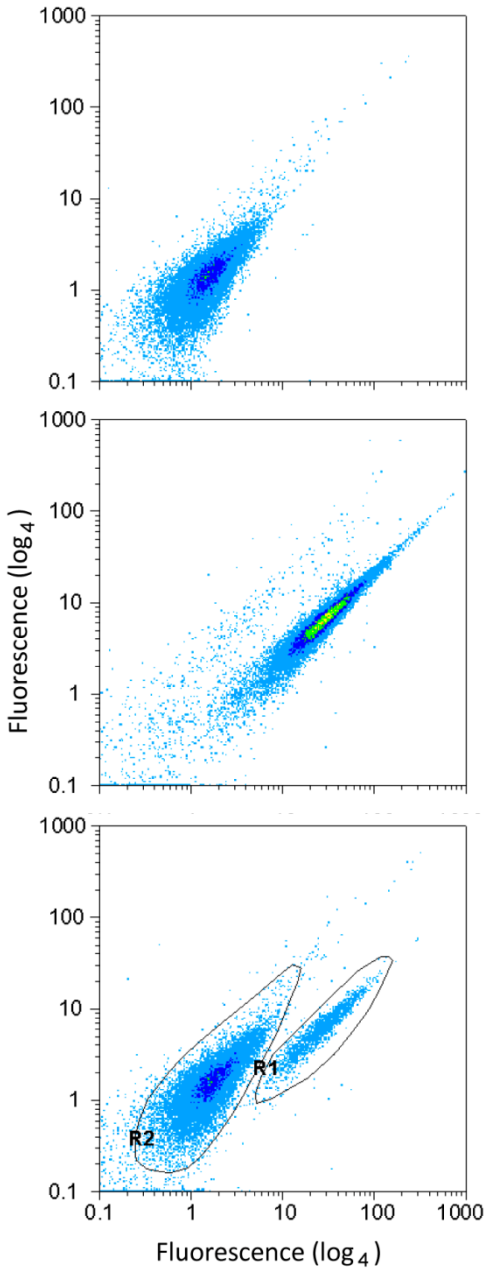

Figure 12. Example of the gating procedure using FACS

Ungated scattergrams of non-labelled cells (top panel) and fluorescent cells (middle panel). Each dot represents a cell. (Bottom panel) Gated scattergram of mixed, fluorescein labelled and non-labelled cells (ratio of 1:9). Polygon gates were manually drawn around the clouds of fluorescent (R1) and non-flurescent (R2) cells to determine the total number of cells in each region. Gating was performed with the Flomax software (Partec version 2.60). The x-axis is fluorescence intensity (scale $\log_4$). Note that even when no fluorescent dye is added, *Dictyostelium* cells have a low autofluorescence detectable by FACS. The y-axis is forward scatter (scale $\log_4$).

Peroxidase anti-peroxidase (Sigma Aldrich P1291) was used to detect the ProteinA moiety. The membrane was incubated with the antibody (diluted 1:6000 in 5% non-fat milk) for 1 hour at room temperature, washed three times with TBST then developed with Luminol following the protocol of the manufacturer (Amersham).

2.16 RNA-blot analysis

For RNA-blot analysis, total RNA was extracted from 1 X 10^8 cells at the appropriate cell-cycle phase or developmental stage using 1 ml TRIZOL (Invitrogen Life Technologies). Nucleic acids were quantified with a Cary 50 spectrophotometer (Varian) by recording the absorbance reading at 260 nm and/or a 2100 Bioanalyzer (Agilent). 20 µg of total RNA were resolved on 2.2 M formaldehyde gels as described (Sambrook et al 1989). Following electrophoresis, the nucleic acids were transferred by capillary action onto a Nytran membrane (Millipore) in 10x SSC (1.5 M NaCl, 0.15 M trisodium citrate, pH 7.0; sodium citrate from BioShop Canada Inc.), cross-linked by UV irradiation (UV Stratalinker 8000, Stratagene) and hybridized with a *cdk*1 radiolabelled probe synthesized by random priming using [α ^{32}P] dCTP (GE Healthcare).

2.17 Microarray and mRNA-sequencing

RNA was extracted for microarrays and mRNA-sequencing using BioRAD Aurum total RNA spin columns following the manufacturer's protocol (BioRad catalogue number 732-6820). To minimize column clogging, the cell lysates were drawn through a 23-gauge needle prior to loading. For microarray analysis, the samples were labelled, hybridized to arrays, and the data processed as described previously (Bloomfield et al 2008). The experiment included both biological and technical replicates. The mRNA-Seq protocol of the Illumina/Solexa platform was used for whole transcriptome sequencing at

the DNA Core Facility of the University of Missouri in Columbia and at the McGill University and Génome Québec Innovation Centre in Montréal. Reads of 42 bp (wild type/mutant comparison) or 36 bp (cell-cycle experiment) were obtained. To validate our findings, biological replicates of growing and developing *rblA*- and Ax2 cells were also sequenced. Three samples from the cell-cycle synchronization experiment (0, 1, and 3 hours after release from cell-cycle arrest) were sequenced at least twice and served as technical replicates.

2.17.1 mRNA-sequencing read mapping

mRNA-Seq reads were mapped to transcriptional units using software written specifically for this project (Harry MacWilliams and Asa MacWilliams, unpublished). The mapping software was written in Java and used a straightforward hash-based approach. The software incorporates two features that are not yet widely used in RNA-Seq read mapping: (1) it eliminated all targets from the mapping process that are identical to other potential targets in all but one base. This obviated mismapping due to single-base sequencing errors. (2) Groups of near-identical genes were recognized automatically and organized into “collectives”. Reads that could be mapped to the collective but not to an individual gene were assigned to the “collective gene”. All reads that could be assigned uniquely to a gene within the collective continued to be so.

66% of the reads could be matched to “robustly unique” sequences in single genes or collective genes. 7% matched to sequences that had been marked as non-mappable. 27% either were not matchable at all using exact matching or matched to sequences that were duplicated within a single gene. The mRNA-Seq data has been deposited in GeneExpression Omnibus (Edgar et al 2002) and is available through GEO series

accession number GSE30368 (http://www.ncbi.nlm.nih.gov/geo/query/acc.cgi?acc=GSE30368).

2.17.2 Selection of RblA-repressed genes for analysis

For all genes, we first calculated the normalized hits in each experiment by dividing the total number of mappable reads for a particular transcript by the total number of mappable reads in the experiment (RPKM) (Mortazavi et al 2008).

$$\text{RPKM} = \frac{(1000000)(\text{total number of mappable reads for a particular gene})}{(\text{total number of mappable reads in the experiment})(\text{length of the transcript})}$$

Mutant-specific regulation factors were defined as normalized hits in the *rblA* disruptant divided by the normalized hits to the wild type; these were calculated separately for growing and developing cells.

$$\text{Mutant-specific regulation factor} = \frac{\left(\frac{\text{total number of mappable reads for a particular gene}}{\text{total number of mappable reads in the experiment}}\right)_{rblA\text{- mutant}}}{\left(\frac{\text{total number of mappable reads for a particular gene}}{\text{total number of mappable reads in the experiment}}\right)_{\text{Ax2 parental}}}$$

Development-specific regulation factors were defined as the total number of mappable reads for the developmental samples divided by the total mappable reads for the growth-phase samples.

$$\text{Development-specific regulation factor} = \frac{\left(\frac{\text{total number of mappable reads for a particular gene}}{\text{total number of mappable reads in the experiment}}\right)_{\text{Development}}}{\left(\frac{\text{total number of mappable reads for a particular gene}}{\text{total number of mappable reads in the experiment}}\right)_{\text{Growth}}}$$

Transcripts or collectives with linear induction factors of 2.0 or more were selected for closer examination. For each of these, a statistical test using edgeR (Robinson et al 2010) was performed. Genes with adjusted p-values of <0.05 were considered to be RblA-regulated.

2.18 Quantitative RT-PCR

Two S-phase genes found to be upregulated in the *rblA* disruptant and two genes that showed no difference in expression between the mutant and parental strain were selected for real-time PCR analysis. Primers were designed using the Primer Express Software (Applied Biosystems) and cross-checked with the Finnzymes Multiple Primer Analyzer program. cDNA libraries were generated from 100 nanograms of the same developmental RNA employed in the mRNA-Seq experiments using a RevertAid H Minus First Strand cDNA Synthesis Kit (Fermentas). qPCR reactions were done in triplicate on biological duplicates using SYBR Green PCR mix (Applied Biosystems) and 0.3 μM of each oligonucleotide. Efficiencies were determined using a pool of the mutant and wild-type cDNAs on five 5-log dilutions. Dissociation curves showed the absence of non-specific products (not shown).

3. RESULTS

3.1 *cdk1* expression in growing and in developing cells

To analyse the role of the cyclin-dependent protein kinase Cdk1 in the cell cycle and differentiation, we first examined the expression of *cdk1* in synchronously growing cells using Northern blot hybridization. Cells were cold synchronized and samples were taken at hourly intervals for RNA isolation after the cells were released from the cell-cycle block (time-zero). The resulting RNA blot was probed with *cdk1* (Figure 13A). In parallel, we cultured an aliquot of the cold-synchronized cells in the presence of the thymidine analogue, bromodeoxyuridine, to monitor cell-cycle progression through S phase. The number of bromodeoxyuridine-positive cells peaked 4 hours after release from the cell-cycle block. The duration of the *Dictyostelium* cell cycle is approximately 8 hours with a 5-minute M phase and a 20-minute S phase (Muramoto and Chubb 2008, Weijer et al 1984). The levels of *cdk1* l transcript fluctuated during the cell cycle, reaching a maximum two hours after the cells had resumed growth. Since there is no G1 phase (Muramoto and Chubb 2008, Weijer et al 1984), this places *cdk1* expression during the cell cycle in late G2 shortly before mitosis.

We also examined the expression of *cdk1* during development using Northern blot hybridization by extracting RNA from cells at different developmental stages. Consistent with the results of others (Michaelis and Weeks 1993, Parikh et al 2010), *cdk1* levels dropped as the cells entered development but rose again as they proceeded from the tight aggregate to the slug stage (Figure 13B). This fits with the observation that although cells withdraw from the cell cycle at the onset of differentiation, subpopulations continue to proliferate during mid-development (Bonner 1952, Durston and Vork 1978, Muramoto

and Chubb 2008, Weijer et al 1984, Zada-Hames and Ashworth 1978, Zimmerman and Weijer 1993).

To determine if the *cdk1* transcript accumulated in both prestalk and prespore cells or if it was cell-type specific, we complemented our RNA blot analyses with reporter-gene studies. We cloned the promoter region of *cdk1* upstream of a gene coding for an unstable β-galactosidase (Gaudet et al 2001) and introduced the vector into AX2 cells to make [cdk1]:UBI:lacZ . The cells were fixed at different developmental stages then assayed for β-galactosidase activity. We found that β-galactosidase activity (and thus *cdk*1 accumulation) was confined to the centre of tight aggregates at 8 hours of development, the lowermost cells of tipped mounds at 12 hours of development, the rear of the slugs at 14 hours of development, and the sori of culminants during terminal differentiation (Figure 14A**)**. We therefore concluded from this experiment that *cdk1* accumulates mainly in cells of the spore pathway during development.

The cell-cycle cyclin Cyclin B, encoded by the *cycB* gene, is predicted to interact with Cdk1 (Luo et al 1994) . Much like *cdk1*, *cycB* mRNA accumulates during mid-development (Luo et al 1995). We asked whether *cycB* expression was also specific to prespore cells. We used the promoter region of *cycB* to drive the same unstable beta-galactosidase in the reporter strain [cycB]:UBI:lacZ. As seen in the whole-mount preparations, the staining pattern of these cells was similar to that of [cdk1]:ubi:lacZ cells (Figure 14B). Namely, β-galactosidase activity in [cycB]:ubi:lacZ cells was located in the sorus of the late culminant. The staining intensities were also comparable between the two strains.

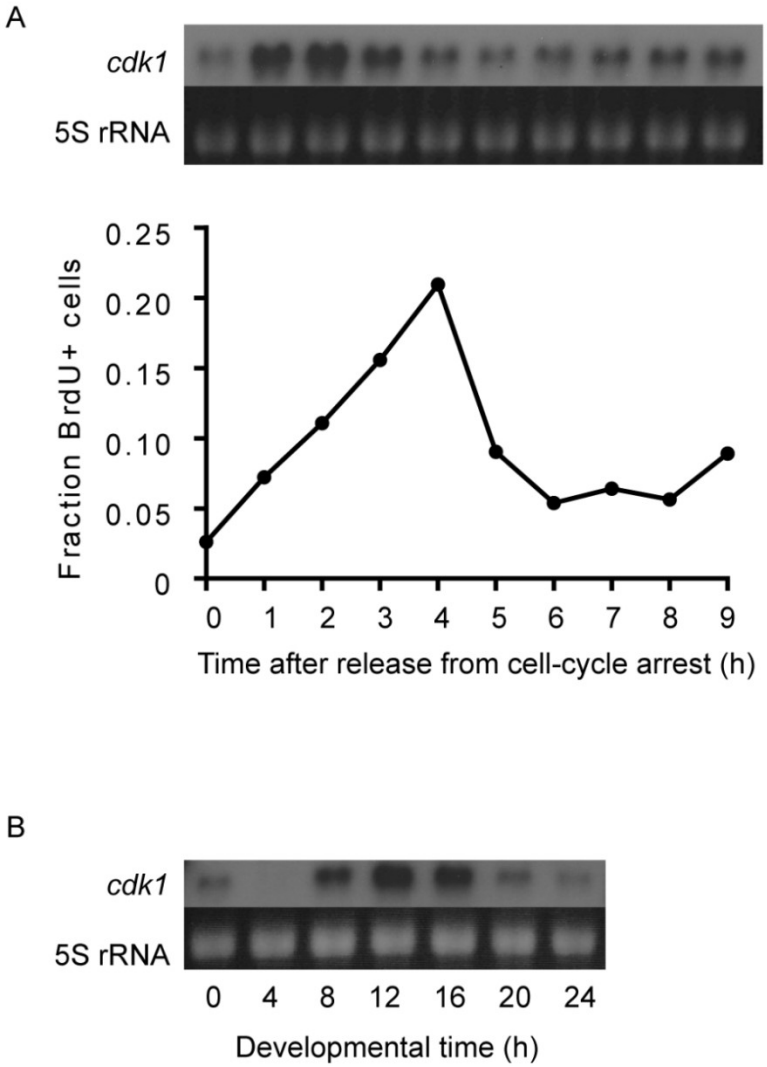

Figure 13. *cdk1* accumulation in growing and developing cells

(A) In the upper panel, RNA blot showing *cdk1* accumulation in cells synchronized in the cell cycle. RNA samples were collected at hourly intervals following release from the cell-cycle block (time zero), probed using radiolabelled *cdk1*, and visualized using autoradiography. 5S ribosomal RNA bands stained with ethidium bromide included as a loading control. In the lower panel a fraction of the synchronized cells were pulse-labelled every hour with bromodeoxyuridine to monitor passage through S phase. The time (hours; x-axis) and the fraction of bromodeoxyuridine cells (y-axis) are indicated. (B) RNA blot showing *cdk1* accumulation in developing cells. Developmental times are indicated. 5S rRNA stained with ethidium bromide presented as a loading control.

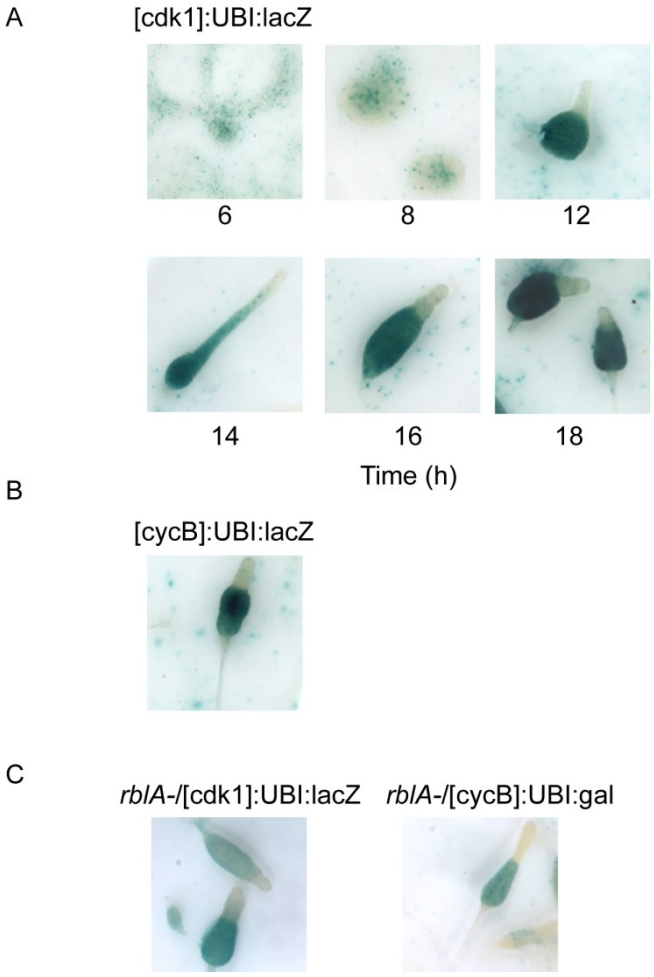

Figure 14. *cdk1* and *cycB* accumulate in cells of the spore pathway

(A) The reporter construct [cdk1]:UBI:lacZ containing the *cdk1* promoter region and ubiquitin-tagged lacZ was introduced into Ax2 cells. These were starved then stained for β-galactosidase activity (blue). Developmental times are indicated. (B) The cyclinB reporter construct [cycB]:UBI:lacZ was expressed in Ax2 cells. Photograph of cells stained for β-galactosidase activity (blue) at the late culminant stage. (C) The same reporter constructs were introduced independently into *rblA* deficient cells to make *rblA*-/[cdk1]:UBI:lacZ and *rblA*-/[cycB]:UBI:lacZ. Stable transformants were fixed at the late culminant stage and stained for β -galactosidase activity. For the *rblA*-/[cdk1]:UBI:lacZ cells shown here the X-gal substrate was diluted ten-fold.

In human cells, the Myb-MuvB DREAM complex, containing a Retinoblastoma-like protein, controls the transcription of *cdk1* and *cycB* during S phase (Muller 2011). The *Dictyostelium* genome encodes homologues of the DREAM complex (see Table 1). To test whether RblA is implicated in the regulation of *cdk1* and *cycB* we transformed a *rblA*-deficient strain (MacWilliams et al 2006) with the cdk1/UBI-lacZ or the cycB/UBI-lacZ reporter construct then stained developing cells for β-galactosidase activity. As seen in Figure 14C the expression pattern of *cdk1* and *cycB* was unaltered in the *rblA* null background and mostly found in differentiating spores. β-galactosidase activity, however, was much stronger in *rblA*-/[cdk1]:UBI:lacZ cells. X-gal staining spread to all areas of the fixed specimen within seconds after adding the regular amount of substrate. For this reason, we diluted the substrate tenfold.

3.2 Rapid and reversible expression of *cdk1* using the doxycycline-inducible vector system

Having established that *cdk1* is a cell-cycle dependent gene we went on to look at the role of Cdk1 in the *Dictyostelium* cell cycle. Yeast and mammalian cells with the Cdk1T14AY15F substitutions enter mitosis prematurely (Krek et al 1992, Krek and Nigg1991). Thus these mutants reveal a role for Cdk1 in regulating G2/M-phase transition. To determine if Cdk1 phosphorylation at T14 and Y15 restrains mitosis in *Dictyostelium*, we made *cdk1* alleles that lack these phosphorylation sites. Given that the Y15F mutation is lethal (Gould and Nurse1989) we used a modified version of the doxycycline-inducible vector system (H.K. MacWilliams, unpublished) to conditionally express TAP-tagged versions of the genes in a wild-type background. We transformed the constructs independently into Ax2 cells then confirmed fusion-protein expression by

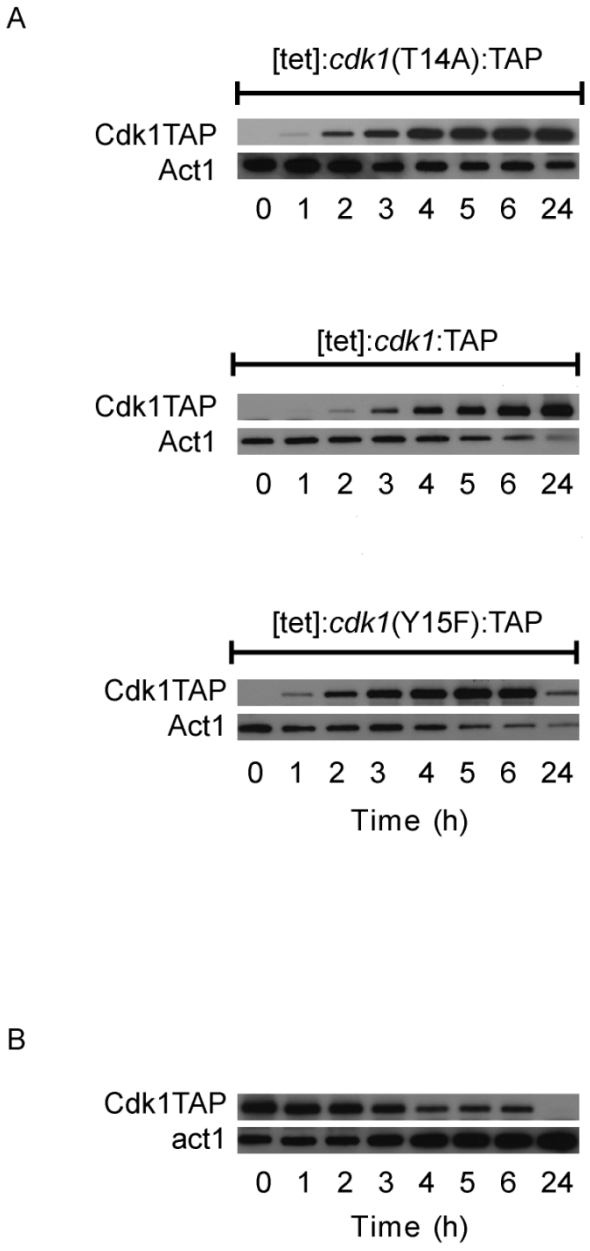

Figure 15. Doxycycline-inducible expression of *cdk*1 in growing cells

(A) Exponentially-growing cells carrying the tetON vector system were induced with 20 µg ml^{-1} of doxycycline (time zero). Whole-cell extracts were prepared at the indicated times for immunoblotting using an antibody directed against the TAP tag. Immunoblots from [tet]:*cdk1*(T14A):TAP (top panel), [tet]:*cdk1*:TAP (middle panel), and [tet]:*cdk1*(Y15F):TAP (lower panel) time series shown here. As a loading control, the blots were also probed with an antibody recognizing actin1. (B) [tet]:*cdk1*(T14A):TAP cells induced with doxycycline for 24 hours were washed (time zero) and resuspended in growth medium without doxycycline. Cells were harvested at the indicated time and whole-cell extracts were analysed by immunoblot with TAP or actin1 antibodies.

immunoblot analysis with an antibody directed against the TAP tag. We observed low basal activity in [tet]:*cdk1*(T14A):TAP cells cultured without doxycycline (Figure15A, top panel, time point zero). Doxycycline was added to the culture at time zero and samples were removed at selected time points for immunoblotting. As seen in Figure 15A (top panel), Cdk1(T14A)TAP was detectable in the crude cell extracts within 1 hours after the addition of doxycycline and levels of the fusion protein continued to rise for the duration of the experiment. The induction kinetics were similar for [tet]:*cdk1*:TAP cells which overexpress a wild-type version of *cdk1* (Figure 15A, middle panel) and [tet]:*cdk1*(Y15F):TAP cells (Figure 15A, lower panel) although the tyrosine mutant showed low transgene expression at the 24h probably due to cell death.

To determine if the doxycycline-inducible system was reversible, we took [tet]:*cdk1*(T14A):TAP cells that had been grown in medium with 20 µg ml^{-1} of doxycycline for 24 hours, washed them, and resuspended them in growth medium without doxycycline. We then took samples at hourly intervals for immunoblot analysis with a TAP antibody. Over time, we observed a gradual decrease in the amount Cdk1T14ATAP. The fusion protein was undetectable in cell lysates 22 hours after removal of the inducer (Figure 15B). The doxycycline inducible gene expression system was, therefore, deemed suitable for our experiments since it provided reversible expression of *cdk1* cDNA.

3.3 Effect of *cdk1*T14A on cell size

Fission yeast expressing *cdk1*T14A have a 'wee' phenotype (Den Haese et al 1995, Krek et al 1992) meaning that they are smaller than wild-type control cells. To determine whether the 'wee' phenotype was mirrored in *Dictyostelium* carrying this

mutation, we measured the size of [tet]:*cdk1*(T14A):TAP cells at regular intervals after the addition of 20 μg ml^{-1} of doxycycline. As seen in Figure 16, *cdk1*T14A expression caused a gradual decrease in cell size suggesting that the mutation allowed the cells to bypass a size checkpoint and dividing prematurely. We noted that the cells began to shrink two hours after the addition of doxycycline and so the timing of this event correlated with the accumulation of Cdk1T14A seen in our immunoblots (Figure 15A). We followed the size of induced [tet]:*cdk1*(T14A):TAP cells over several days and found that it decreased at first but reached a minimum value within 24 hours after the addition of doxycycline (Figure 16A left panel). At this time, cells expressing *cdk1*T14A were approximately 15% smaller than control cultures in the uninduced state (Table 5). This observation points to another control event in the cell cycle which prevents the cells from becoming indefinitely small. Moreover we found that the cells returned to the normal size when the doxycycline was washed off implying that the 'wee' phenotype is reversible (Figure 16B).

3.4 Effect of *cdk1*T14A on cell division

In addition to providing size distributions, the automated Coulter counter measures the number cells in a fixed volume. The method is much faster than counting cells the conventional way using a hæmacytometer. It allowed us to handle multiple cultures at the same time. In one experiment, we monitored the growth of four cultures: (1) Induced [tet]:*cdk1*(T14A):TAP, (2) uninduced [tet]:*cdk1*(T14A):TAP, (3) induced [tet]:*cdk1*:TAP, and (4) uninduced [tet]:*cdk1*:TAP by taking cell counts every 30 minutes with a Coulter counter. We visualized the data by graphing the cell density as a function of time. As seen in Figure 17A (left panel), [tet]:*cdk1*(T14A):TAP cells cultured with

Table 5. Average cell size of *Dictyostelium* strains used in this study

***Dictyostelium* strain**	**Glucose**	**Doxycycline**	**Average cell size (µm)**
[tet]:*cdk1*(wt):TAP	+	-	10.44 ± 0.07
[tet]:*cdk1*(wt):TAP	+	+	10.32 ± 0.09
[tet]:*cdk1*(T14A):TAP	+	-	10.40 ± 0.08
[tet]:*cdk1*(T14A):TAP	+	+	9.53 ± 0.08
[tet]:*cdk1*(T14A):TAP	-	-	10.24 ± 0.33
[tet]:*cdk1*(T14A):TAP	-	+	9.59 ± 0.23
Ax2	+		10.32 ± 0.12
Ax2 $^{-}$	-		10.09 ± 0.09
rblA disruptant	+		9.96 ± 0.17
rblA disruptant	-		10.05 ± 0.10
rblA -/[tet]:*cdk1*(T14A):TAP	+	-	9.63 ± 0.13
rblA -/[tet]:*cdk1*(T14A):TAP	+	+	8.58 ± 0.31

Strains cultured with doxycycline (20 µg ml^{-1} final concentration) were induced for at least 24 hours prior to size determination using a Coulter counter. Cells cultured without glucose were maintained at densities below $5x10^5$ cells ml^{-1}. The size values were taken from two independent [tet]:*cdk1*(wt):TAP clones, three independent [tet]:*cdk1*(T14A):TAP clones, and two independent *rblA* -/[tet]:*cdk1*(T14A):TAP clones. Sizes are averages from at least three different experiments per clone.

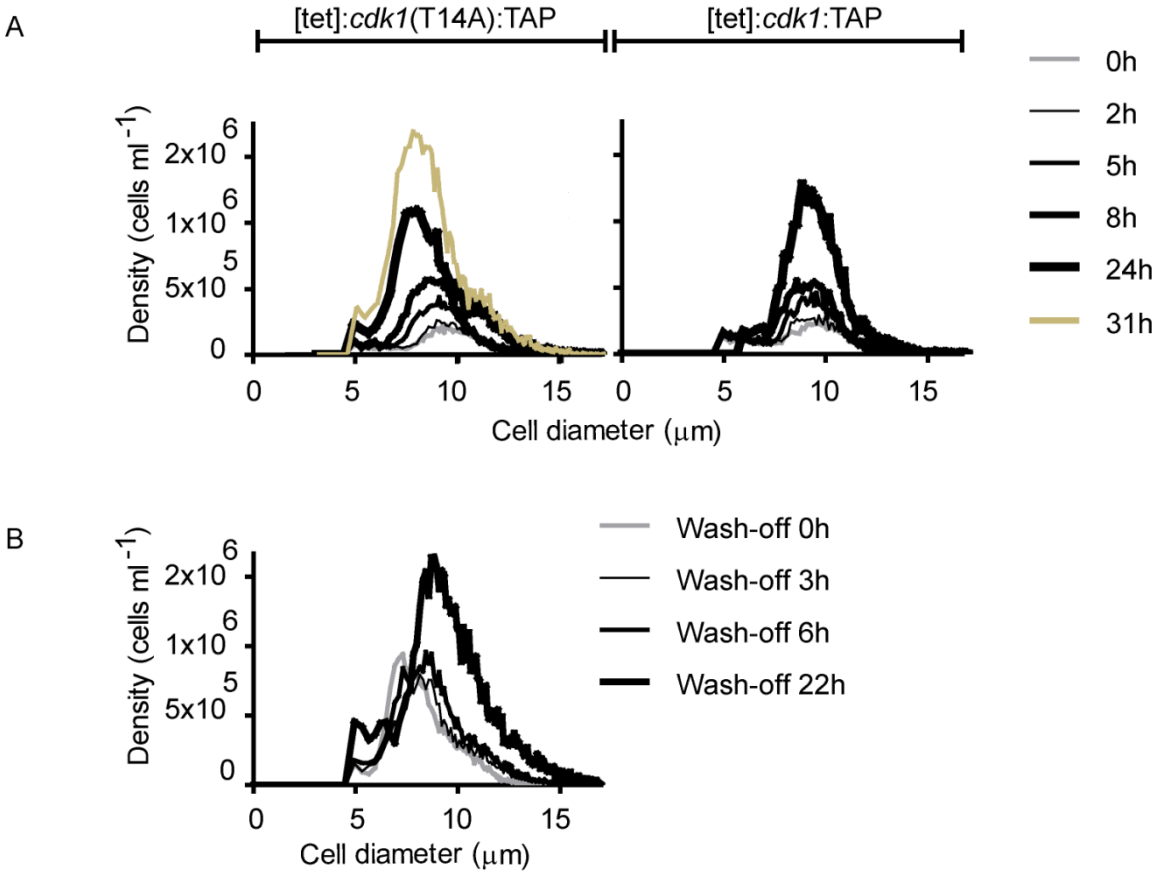

Figure 16. Cells expressing *cdk1*T14A decrease in size

(A) Cell-size measurements after the addition of doxycycline. Doxycycline was added to growing [tet]:*cdk1*(T14A):TAP cells at time zero and cell size was measured at the indicated times using a Coulter counter. Size measurements for [tet]:*cdk1*:TAP cells, which express a TAP tagged version of wild-type *cdk1*, included on the right for comparison. (B) Cell-size measurements after the removal of doxycycline. [tet]:*cdk1*(T14A):TAP cells induced for 24 hours were washed at time zero, resuspended in growth medium without doxycycline, and cell-size distributions determined at the times shown using a Coulter counter. Cell size (μM; x-axis) and density (cells ml^{-1}; y-axis) are indicated.

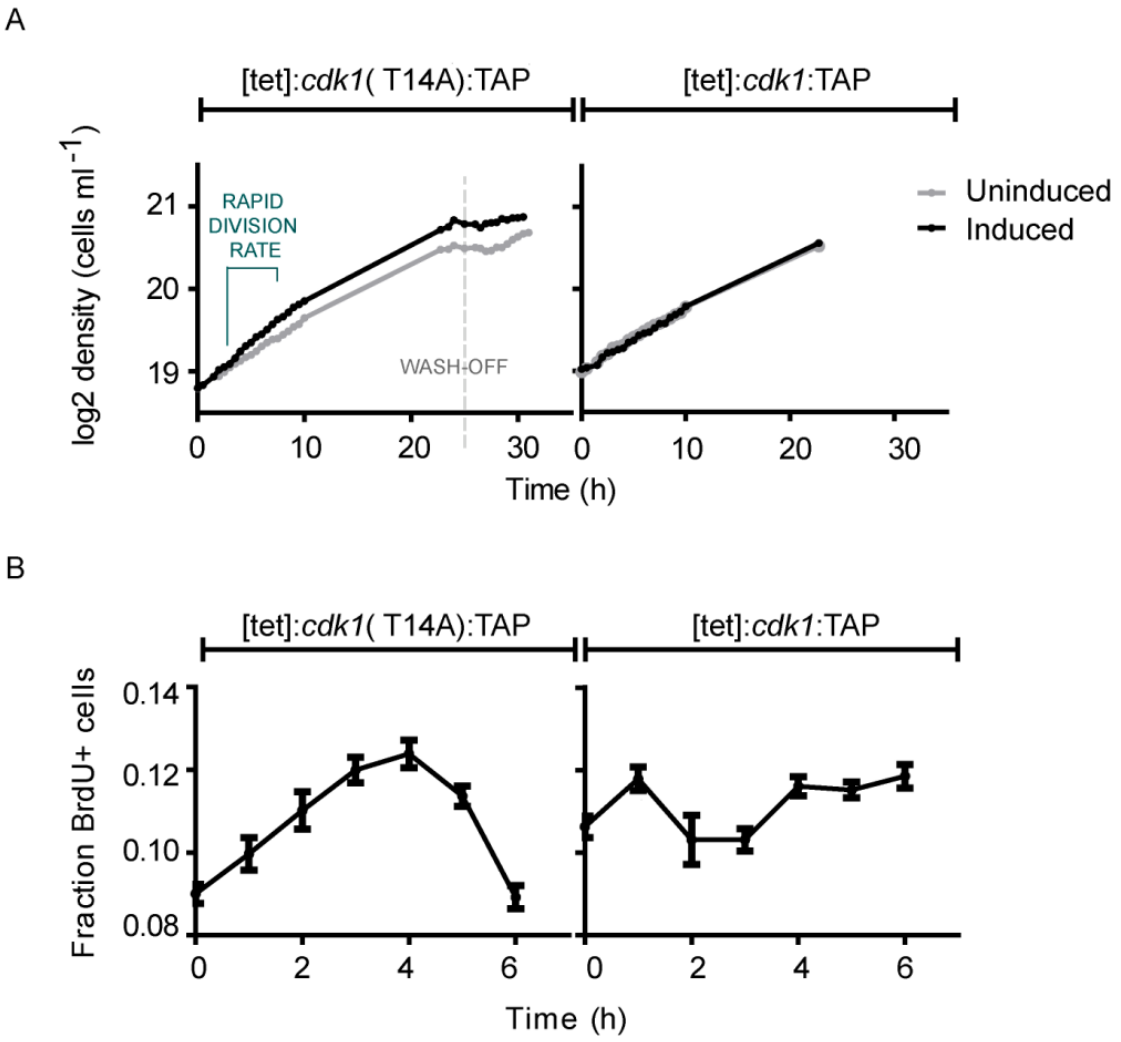

Figure 17. *cdk1*T14A expression causes cells to divide faster and prolongs S phase.

(A) Doxycycline was added to the [tet]:*cdk1*(T14A):TAP (left) and [tet]:*cdk1*:TAP (right) cultures at time zero then cell counts were taken every 30 minutes using a Coulter counter. After 24 hours in doxycycline, the [tet]:*cdk1*(T14A):TAP cells were washed (grey-dotted line) and resuspended in growth medium without doxycycline. Cell density was monitored for the next 6 hours. Black points denote induced cells while grey points are for parallel, uninduced cultures. Results representative of experiments performed in triplicate. (B) [tet]:*cdk1*(T14A):TAP cells (left) and [tet]:*cdk1*:TAP cells (right) were induced with doxycycline at time zero and samples were taken at hourly intervals for pulse labelling with bromodeoxyuridine. Data represented graphically after scoring cells for bromodeoxyuridine-stained nuclei. Time (hours; x-axis) and the fraction of bromodeoxyuridine positive cells (y-axis) are indicated. Data shown as mean ± s.d.m.

doxycycline showed a temporary increase in the rate of cell division seen as a shift upwards in the growth curve. We noted, however, that although the growth curves of the induced and uninduced cells diverged from each other initially they ran in parallel after about 8 hours. We hypothesized that induced [tet]:*cdk1*(T14):TAP cells were able to regain a normal growth rate through the lengthening of other cell-cycle phases. To measure the time that it took for cells to traverse S phase of the cell cycle, an aliquot of the cells was pulse labelled with bromodeoxyuridine every hour after the addition of doxycycline. The cells were fixed and stained for bromodeoxyuridine incorporation using immunohistochemistry. Those that were positive for bromodeoxyuridine were considered to be in S phase. As seen in Figure 17B the fraction of bromodeoxyuridine-positive [tet]:*cdk1*(T14A):TAP cells increased gradually from about 9% in the uninduced state to up to 12% 4 hours after the addition of doxycycline implying that these cells had a slightly longer S phase. The effect was only provisional since the fraction of bromodeoxyuridine-positive cells returned to normal approximately 6 hours.

Twenty-four hours after the start of the induction time course, the cells were thoroughly washed with buffer (Figure 17A; grey-dotted line) then resuspended in growth medium without doxycycline. Afterwards, cell-density changes over time were monitored using a Coulter coulter. We noted that the growth curve dropped to re-encounter its original course after the removal of doxycycline. We concluded from this set of experiments that the *cdk1*T14A phenotype is reversible.

3.5 Cells expressing *cdk1*Y15F and *cdk1*T14AY15F stop dividing

Next we looked at the effect of the Y15F and T14AY15F mutations on *Dictyostelium* cell growth. The [tet]:*cdk1*(Y15F):TAP and [tet]:*cdk1*(T14AY15F):TAP

strains were cultured with or without doxycycline and cell counts were taken at regular intervals over a 10-hour period using a Coulter counter. Within 2 hours after the addition of doxycycline, the induced [tet]:*cdk1*(Y15F):TAP and [tet]:*cdk1*(T14AY15F):TAP cells showed a transient increase in their division rates, viewed as a slight shift upwards in the growth curves (Figure 18). After approximately 8 hours, however, both of the induced cultures grew much more slowly than the uninduced cells. The following day, the cells were washed to remove the doxycycline and counted every 30 minutes for the next 6 hours. We found that during this time period the slow-growth phenotype could not be reversed. In cultures that had been exposed to doxycycline, the cell density continued to increase over time after washing but at a much slower rate than the control cells. Moreover cells expressing *cdk1*Y15F or *cdk1*T14AY15F had a rounded appearance and detached from the substratum when cultured in dishes (results not shown). These characteristics are associated with cell undergoing mitosis (McDonald and Durston 1984).

3.6 Cells expressing *cdk1*Y15F and *cdk*1T14AY15F arrest in mitosis

Consistent with the phenotype observed in mammalian cells (Krek and Nigg 1991) nuclear-DAPI staining of fixed [tet]:*cdk1*(Y15F):TAP cells that had been cultured in presence of doxycycline for 24 hours revealed that the cells had highly condensed chromatin (Figure 19A**)**. We look at the accumulation of mitotic figures over time by culturing [tet]:*cdk1*(Y15F):TAP and [tet]:*cdk1*(T14AY15F):TAP cells separately in multi-well plates. Doxycycline

(20 μg ml^{-1}) was added to each well with the exception of the first which serve as the uninduced control. Then the contents of one well were fixed at 2 or 4 hour-intervals,

Table 6. Phenotypes of Cdk1 phosphorylation mutants

	Phenotype
[tet]:*cdk1*(T14A):TAP	Amoebae are smaller than the wild type, stalk-cell bias
[tet]:*cdk1*(Y15F):TAP	Lethal, blocked in mitosis
[tet]:*cdk1*(T14AY15F):TAP	Lethal; blocked in mitosis
[tet]:*cdk1*:TAP	wild type

Doxycycline-inducible versions of the genes were expressed in Ax2 (wild type) cells.

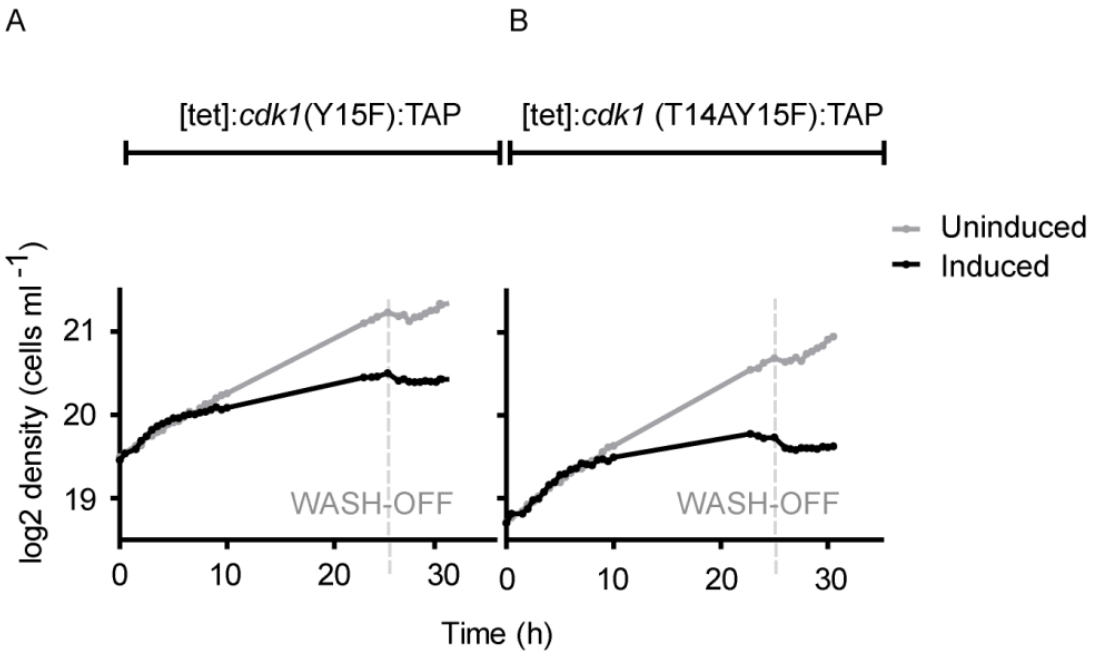

Figure 18. Cells expressing *cdk1*Y15F or *cdk1*T14AY15F grow slowly

Doxycycline was added to the cultures (time zero) and cell counts were taken after that every 30 minutes using a Coulter counter. Time series shown here with the time (hours; x-axis) and density (log_2 cells ml^{-1}; y-axis) indicated. Black points denote induced cells while grey points are for parallel, uninduced cultures. After 24 hours in doxycycline the cells were washed (grey-dotted line) and resuspended in growth medium without the inducer. Cell density was monitored for another 6 hours. Growth curve for (A) [tet]:*cdk1*(Y15F):TAP cells and (B) [tet]:*cdk1*(T14AY15F):TAP cells.

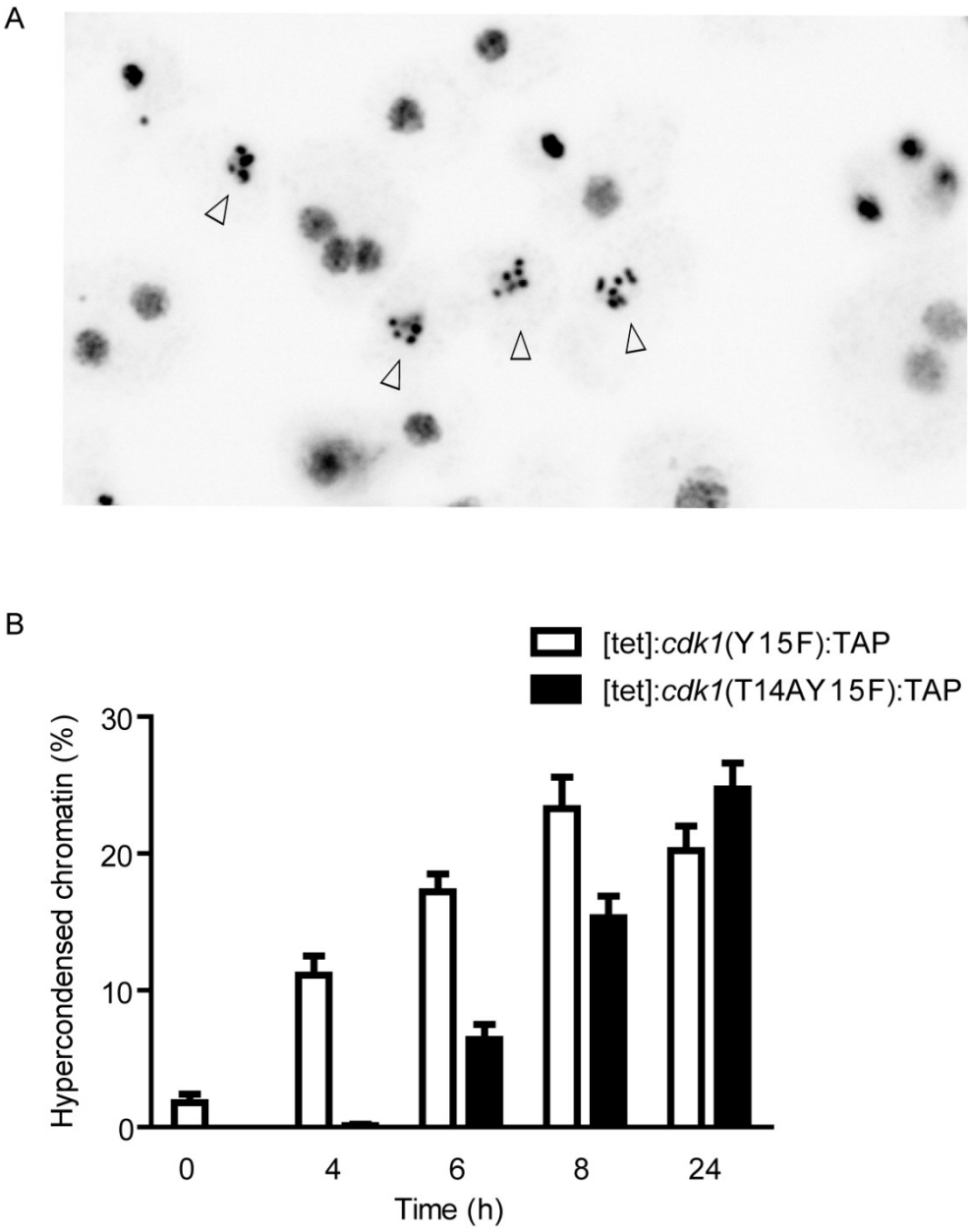

Figure 19. Cells expressing *cdk*1Y15F have highly condensed chromatin

(A) DAPI staining of nuclear DNA in [tet]:*cdk1*(Y15F):TAP cells induced for 24 hours. Examples of cells with highly condensed chromatin are indicated with *arrowheads*. (B) Doxycycline was added to cells at time zero. Cells were fixed at times shown, stained with DAPI, and scored for hypercondensed chromatin. Data presented graphically as the time (hours; x-axis) compared to the percentage of [tet]:*cdk1*(Y15F) :TAP cells (white bars) and [tet]:*cdk1*(T14AY15F):TAP cells (black bars) with hypercondensed chromatin (y-axis). Values determined using no less than 1000 cells per time point.

stained with DAPI, and scored for hypercondensed chromatin. We found that more and more mitotic figures accumulated over time (Figure 19B) suggesting a delay in mitosis although a number of cells remained in interphase even after 24 hours of induction, as judged by the state of their genomic DNA.

To better characterize the Cdk1Y15F phenotype, we looked at other central mitotic events including microtubule organization and spindle assembly. In *Dictyostelium*, microtubule depolymerisation and centrosome duplication occur in prophase; the two centrosomes separate at the prophase/prometaphase boundary (Ueda et al 1997). We looked at the spindle apparatus of induced [tet]:*cdk1*(Y15F):TAP cells by transforming them with vectors that encode GFP fusions of alpha tubulin (Koonce et al 1999) or the centrosomal protein CP224 (Graf et al 2000). Stable transformants were induced for 24 hours with doxycycline, cells were fixed in methanol, nuclear DNA was stained with DAPI, and the cells were visualized using a fluorescence microscope. Fixed and stained uninduced cells served as the control. As shown in Figure 20, uninduced [tet]:*cdk1*(Y15F):TAP cells marked with GFP:*tubA* had decondensed chromatin and an organized microtubule array during interphase. Uninduced mitotic cells had condensed chromatin and unorganized microtubules. Induced [tet]:*cdk1*(Y15F):TAP cells had highly condensed chromatin but an organized, interphase microtubule array. In Figure 21 uninduced [tet]:*cdk1*(Y15F):TAP cells with green fluorescent centrosomes had decondensed chromatin and a single centrosome during interphase. Normal mitotic cells had condensed chromatin and two centrosomes positioned at opposite poles of the cell. Induced [tet]:*cdk1*(Y15F):TAP cells had highly condensed chromatin but non-duplicated or non-separated centrosomes. All together these results indicate that cells expressing

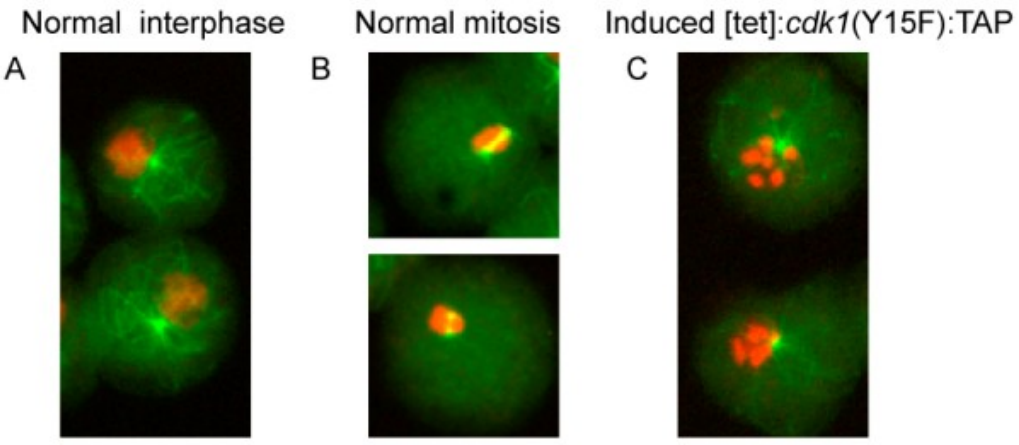

Figure 20. Cells expressing *cdk*1Y15F have highly condensed chromatin but microtubules with an interphase array

[tet]:*cdk1*Y15F:TAP cells were transformed with a vector carrying GFP-alpha tubulin to label the microtubules (green). Stable transformants were fixed in methanol, the nuclear DNA was stained with DAPI (red), and cells were visualized using a fluorescence microscope. Merged fluorescent images are shown here. A) Uninduced cells in interphase, (B) uninduced cells in mitosis, and (C) cells induced for 24 hours with 20 μg ml^{-1} doxycycline.

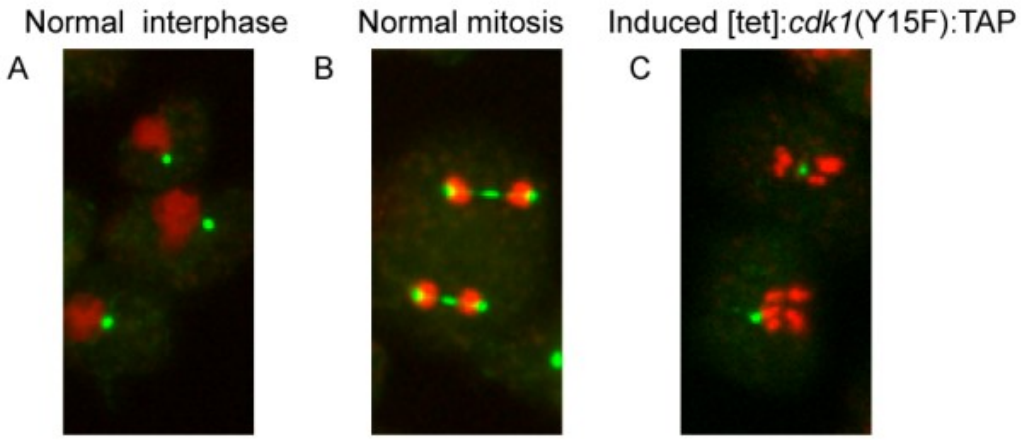

Figure 21. Cells expressing *cdk*1Y15F have defects in centrosome duplication and/or segregation

Fluorescent image of [tet]:*cdk1*(Y15F):TAP cells carrying *CP224*-Gfp. The centrosomes are labelled in green and nuclear DAPI staining is shown in red. (A) Uninduced cells in interphase, (B) uninduced cells in mitosis, and (C) cells induced for 24 hours with 20 μg ml^{-1} doxycycline.

*cdk1*Y15F had lost the ability to coordinate spindle assembly with chromatin remodelling.

Devoid of a G1 phase, the *Dictyostelium* cell cycle is reduced to a G2/mitosis/S phase cadence with cells frequently initiating DNA synthesis prior to completing cytokinesis (Muramoto and Chubb 2008, Weijer et al 1984)**.** To determine whether induced [tet]:*cdk1*(Y15F):TAP cells were able to enter S phase following mitosis, we transformed the strain with fluorescently labelled proliferating cell nuclear antigen (Rfp-PCNA) (Muramoto and Chubb 2008). PCNA is a replication factor that diffuses from the nucleus into the cytoplasm during S phase. As seen in Figure 22A, the Rfp-PCNA fluorescence was low and predominantly nuclear during interphase. In S-phase cells, the signal was stronger and distributed throughout the cytoplasm (Figure 22B). In cells expressing *cdk1*Y15F (with hypercondensed chromatin) we found that PCNA distribution was both nuclear and cytoplasmic, and although the fluorescence signal in the cytoplasm was unusually strong, the pattern was not like the one seen in S-phase cells (Figure 22C). We concluded that mitotic delay via Cdk1 phosphorylation at Y15 is a non-redundant pathway in *Dictyostelium*. Substituting this tyrosine for a structurally similar but non-phosphorylatable phenylalanine causes the cells to remain blocked in prophase.

3.7 Cells expressing *cdk1*T14A differentiate preferentially into stalk cells

Having established a role for *cdk1* in the *Dictyostelium* cell cycle, we addressed the issue of the cell cycle and differentiation by turning our attention again to the Cdk1T14A mutant. Previous studies have shown that cells that have just divided preferentially become stalk cells when starved while older cells favour the

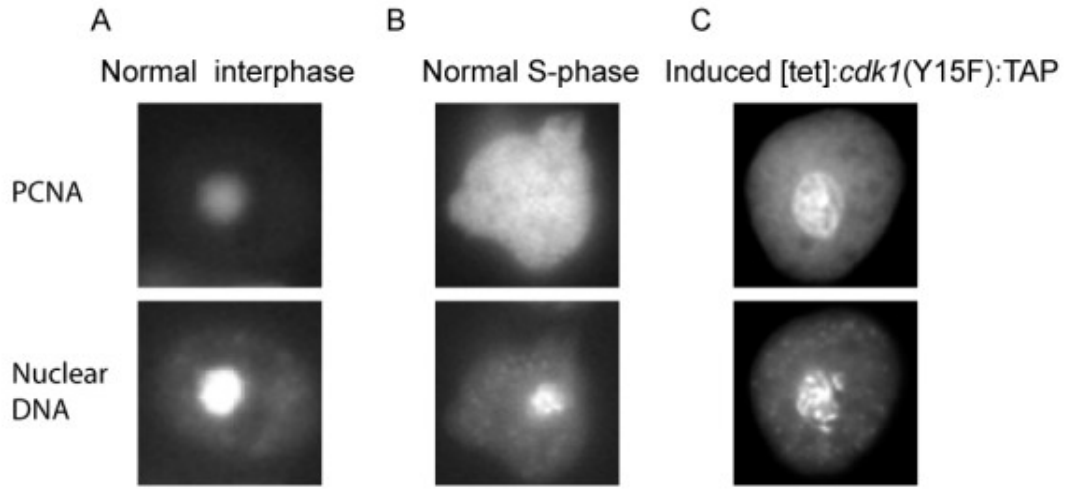

Figure 22. Cells expressing *cdk*1Y15F have cytoplasmic and nuclear PCNA levels

Fluorescent image of [tet]:*cdk1*(Y15F):TAP cells carrying RFP-*pcna*. Black-and-white images of fluorescent PCNA distribution (top panel) and nuclear-DAPI staining (lower panel). (A) Uninduced cells in interphase, (B) uninduced cells in S phase, and (C) cells induced for 24 hours with 20 µg ml^{-1} doxycycline.

spore pathway (Araki et al 1994, Araki and Maeda 1998, Gomer and Firtel 1987, MacWilliams et al 2001, MacWilliams et al 2006, Maeda 2011, McDonald and Durston 1984, Ohmori and Maeda 1987, Weeks and Weijer 1994, Weijer et al 1984, Wood et al 1996, Zimmerman and Weijer 1993). Based on these observations we anticipated that the Cdk1T14A mutant, capable of dividing prematurely, would adopt the stalk-cell fate over the spore fate. To test this hypothesis we used 'mixing experiments' (MacWilliams and Bonner 1979, Thompson and Kay 2000). In such experiments, a small population of cells is flagged usually with a fluorescent dye or a protein such as GFP (Figure 23). The fluorescent cells are then mixed with a large excess of non-labelled cells that are of different genetic constitution. When such cell mixtures develop, they form a chimeric organism. At the slug stage, fluorescent cells that have a stalk bias will sort to the anterior end while those that spore bias will sort out to the rear. Fluorescently-labelled cells that have no particular differentiation preference will distribute randomly throughout the slug.

We performed mixing experiments on [tet]:*cdk1*(T14A):TAP cells. Typical results are shown in Figure 24. When fluorescent [tet]:*cdk1*(T14A):TAP cells in the induced state were combined with an excess of non-labelled cells in the uninduced state, the labelled cells expressing *cdk1*T14A sorted out to the anterior, prestalk region of the slug (Figure 24A). We also tested for cell-type bias using the reverse combination. Uninduced labelled cells were mixed into induced [tet]:*cdk1*(T14A):TAP cells (Figure 24B) . The non-fluorescent cells expressing *cdk1*T14A concentrated in the anterior, prestalk region of the slugs. When we mixed cells overexpressing a wild-type version of *cdk1* in the same combinations as those described above, no cell-type bias was observed (Figure 24C and D).

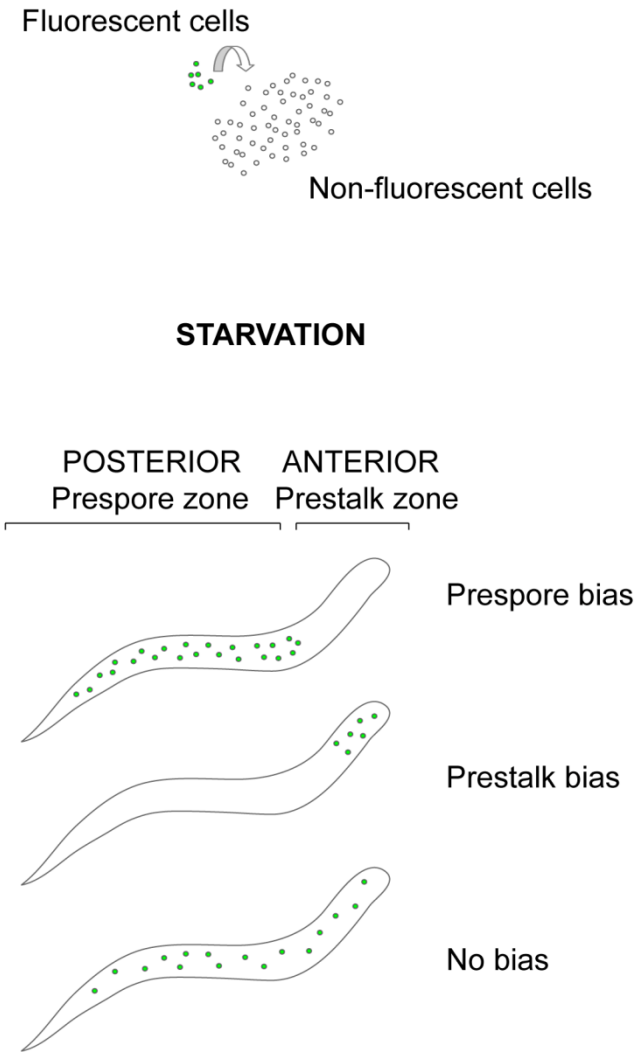

Figure 23. Schematic representation of cell-type biases observed in mixing experiments

In mixing experiments, a few fluorescently labelled cells (shown in green) are mixed into a large amount of non-labelled cells. Differentiation preference is assigned based on the fluorescence distribution in chimeric slugs. Fluorescent cells that have a spore bias sort out to the rear of slugs. Fluorescent cells that have a stalk bias sort to the anterior end of the slugs. Fluorescently-labelled cells with no differentiation preference distribute randomly throughout the slug.

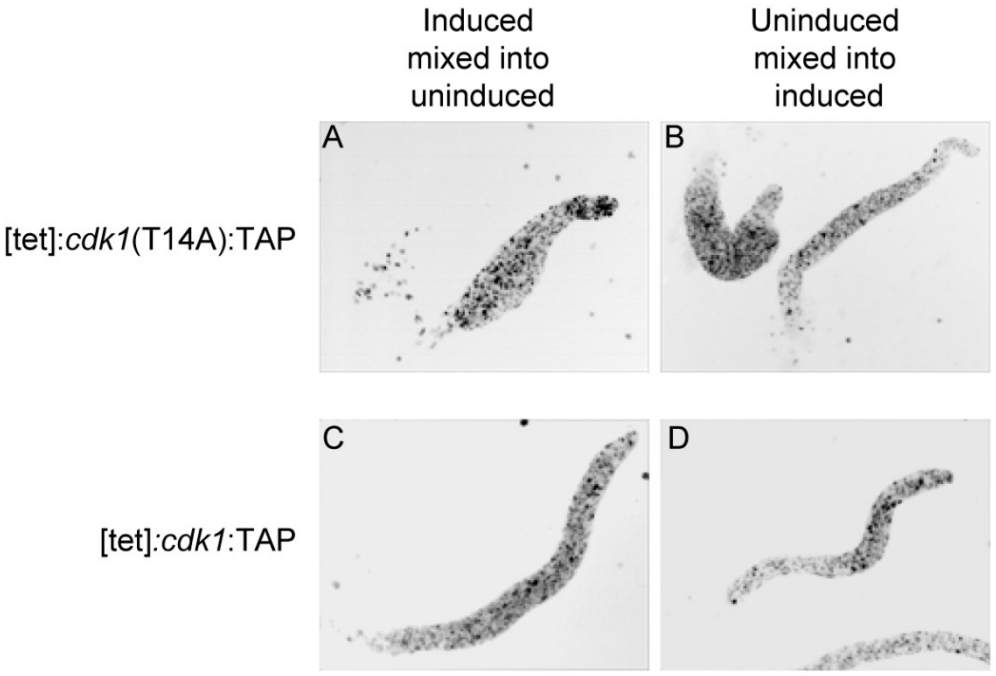

Figure 24. Cells expressing *cdk1*T14A sort to the prestalk region of slugs

Shown here are fluorescent images of chimeric slugs. These are inverted black-and-white images and so the fluorescent cells appear as black dots. (A) Cells expressing *cdk1*T14A were labelled with a fluorescent dye and mixed with an excess of non-labelled uninduced cells. (B) Fluorescent uninduced [tet]:*cdk1*(T14A):TAP cells were mixed with cells induced to express *cdk1*T14A. (C) Fluorescent [tet]:*cdk1*:TAP cells which express a TAP tagged version of wild-type *cdk1* were mixed with uninduced non-labelled cells. (D) Uninduced fluorescently-labelled [tet]:*cdk1*:TAP cells mixed with induced non-labelled [tet]:*cdk1*:TAP cells. Images are representative of experiments performed in triplicate.

With mixing experiments, one can also quantify fate preference by allowing the cell mixture to complete development. The fraction of labelled cells in the original mixtures is then compared to the fraction of labelled spores recovered from mature fruiting bodies (Thompson and Kay 2000a). Typical quantitative results from mixing experiments using the inducible [tet]:*cdk1*(T14A):TAP strain are shown in Figure 25. For the sample at the very left of the graph, cells expressing cdk1T14A were fluorescently labelled then mixed with an excess of uninduced [tet]:*cdk1*(T14A):TAP cells. In the starting cell mixture there were about 15% fluorescent cells. After development, we recovered only about 5% fluorescent spores from the fruiting bodies. This means that cells expressing *cdk1*T14A mostly formed stalk cells. For the opposite combination-uninduced and fluorescently labelled [tet]:*cdk1*(T14A):TAP cells were mixed with an excess of cells expressing *cdk1*T14A. There were about 15% labelled cells in the starting mixture but we recovered almost 25% fluorescent spores after development. Thus cells expressing *cdk1T14A* preferentially developed into stalk cells. When we mixed cells transformed with a doxycycline-inducible wild-type version of *cdk1* in the induced and uninduced states, we observed no cell-type bias. It has been proposed that the size of a *Dictyostelium* cell influences its developmental fate (Araki and Maeda 1998, Muramoto and Chubb 2008). Since growing cells overexpressing *cdk1*T14A were smaller than the uninduced control cells, it seemed possible that their stalk preference was due to their reduced cell size.

Next, we asked whether the expression of *cdk1*T14A during the growth phase was a precondition for the stalk-cell preference or whether expressing the gene after the cells had entered development would also make them stalky. We repeated the mixing

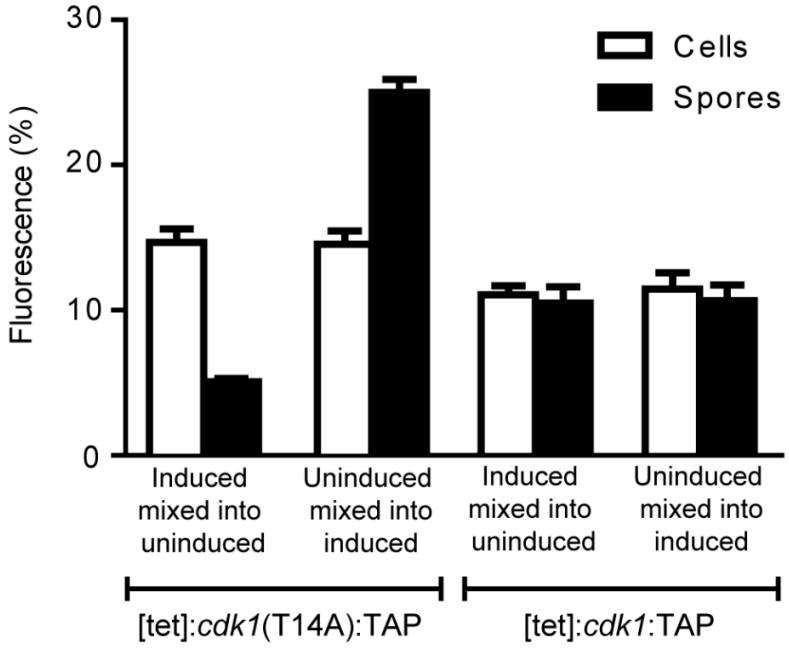

Figure 25. Cells expressing *cdk1*T14A preferentially become stalk cells

[tet]:*cdk1*(T14A):TAP cells and [tet]:*cdk1*:TAP cells, which overexpress wild-type *cdk1* cDNA when induced, were cultured in growth medium with or without doxycycline. An aliquot of the cells was fluorescently labelled, mixed with an excess of unlabelled cells in a ratio of 1:9 then developed. The mixtures were the following (from left to right): induced fluorescent [tet]:*cdk1*(T14A):TAP mixed with an excess of uninduced non-labelled [tet]:*cdk1*(T14A):TAP; uninduced fluorescently-labelled [tet]:*cdk1*(T14A):TAP mixed with and excess of induced non-labelled [tet]:*cdk1*(T14A):TAP; induced fluorescent [tet]:*cdk1*:TAP mixed with an excess of uninduced non-labelled [tet]:*cdk1*:TAP; uninduced fluorescently-labelled [tet]:*cdk1*:TAP cells mixed with an excess of induced non-labelled [tet]:*cdk1*:TAP. White bars represent the percentage of fluorescent cells in the starting cell mixtures and black bars represent the percentage of fluorescent spores recovered from mature fruiting bodies. Error bars represent sampling distribution of the mean above and below the point. Results are representative of three independent experiments.

experiments but this time, we starved the cells before adding the doxycycline inducer. In this experiment, [tet]:*cdk1*(T14A):TAP cells were grown in HL5 medium without the doxycycline. An aliquot of the cells was labelled with fluorescein, washed extensively to remove the excess dye then resuspended in phosphate buffer with or without doxycycline. Another aliquot of the cells was washed in parallel and resuspended in buffer, divided into two parts, and doxycycline was added to one of the cell suspensions; these served as a source of non-labelled cells. The cells in buffer were maintained under constant agitation for 4 hours prior to mixing them. Under these conditions *Dictyostelium* cells can progress normally through the few hours of development (Gaudet et al 2008). Immunoblots on lysates from cells induced during early development showed the accumulation of Cdk1T14A (Figure 26A). Using a Coulter counter we measured the size of these cells and found that [tet]:*cdk1*(T14A):TAP cells induced during development were identical in size to the uninduced control (Figure 26B). Then we scored for differentiation preference by mixing fluorescent cells with an excess of non-labelled cells. An aliquot of the cell mixture was analysed by FACS in order to determine accurately the percentage of fluorescently-labelled cells. The rest of the cells were spread onto non-nutrient plates to complete development. Some cells were photographed at the slug stage while others were allowed to culminate. Spores were then harvested from mature fruiting bodies and their fluorescence intensities measured by FACS. The FACS data from the cells and the spores was then viewed graphically. We found that cells induced to express *cdk1*T14A during early development did not have a cell-type preference. As seen in Figure 27A, induced fluorescent [tet]:*cdk1*(T14A):TAP cells distributed randomly throughout the slugs when combined with uninduced non-

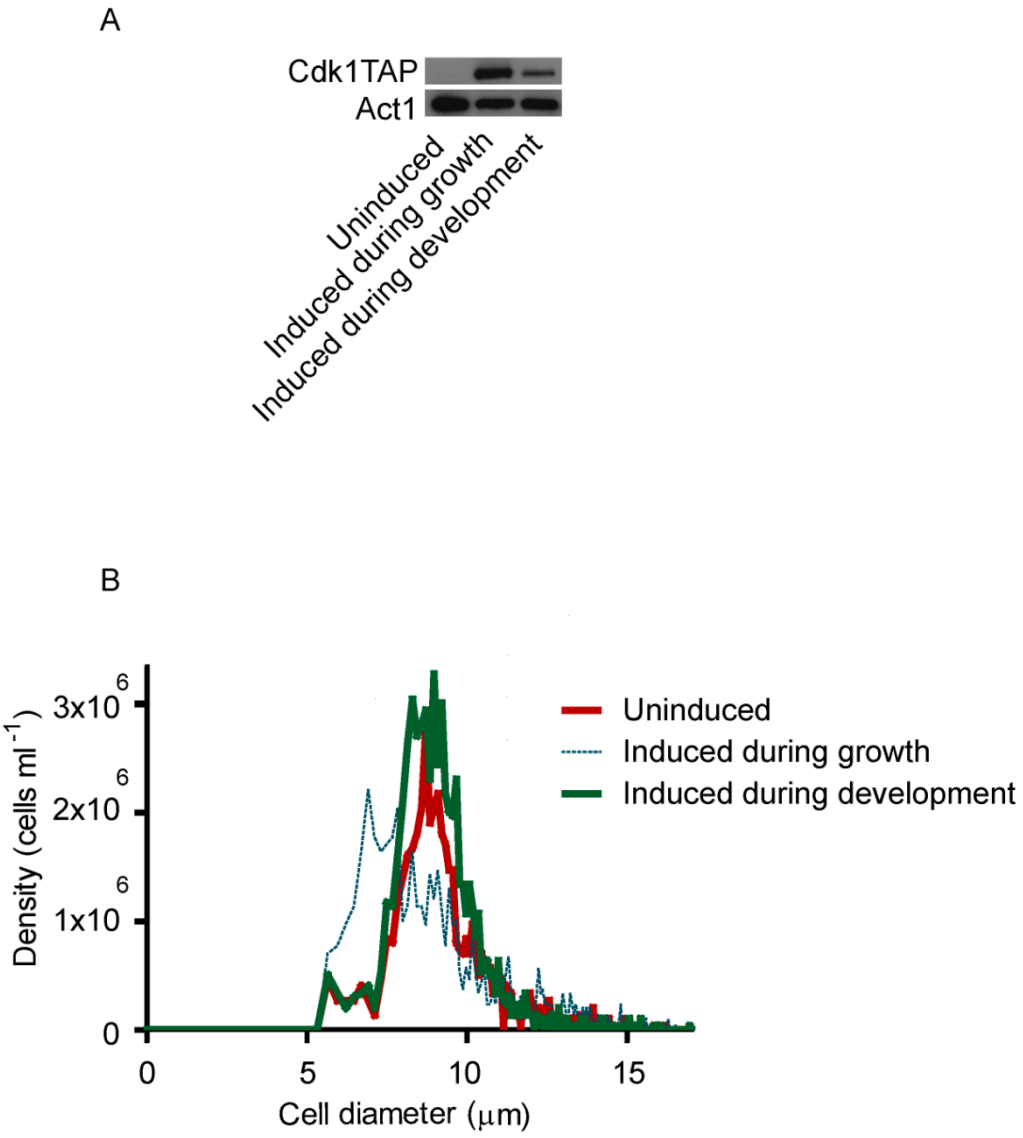

Figure 26. *cdk1*T14A accumulates in developing cells but cell size does not change

[tet]:*cdk1*(T14A):TAP cells growing in rich HL5 medium induced for 24 hours with 20 µg ml^{-1} doxycycline (induced during growth) or washed and resuspended in non-nutrient KK2 buffer without doxycycline (uninduced) or with 20µg ml^{-1} doxycycline (induced during development). (A) Lysates from [tet]:*cdk1*(T14A):TAP cells in the uninduced state, induced during growth, or induced during early development (4 hours in buffer) were analysed by immunoblotting with an antibody directed against TAP. Blots were also probed with Actin1 (Act1) as a loading control. (B) Cell-size distributions. Sizing was obtained using a Coulter counter. The red curve is for uninduced cells, the blue-dotted curve is for cells induced with doxycycline for 24 hours during the growth stage, and the green curve is for cells induced with doxycycline for the first 4 hours of development. Cell diameter (µm; x-axis) and cell density (cells ml^{-1}; y-axis) are indicated.

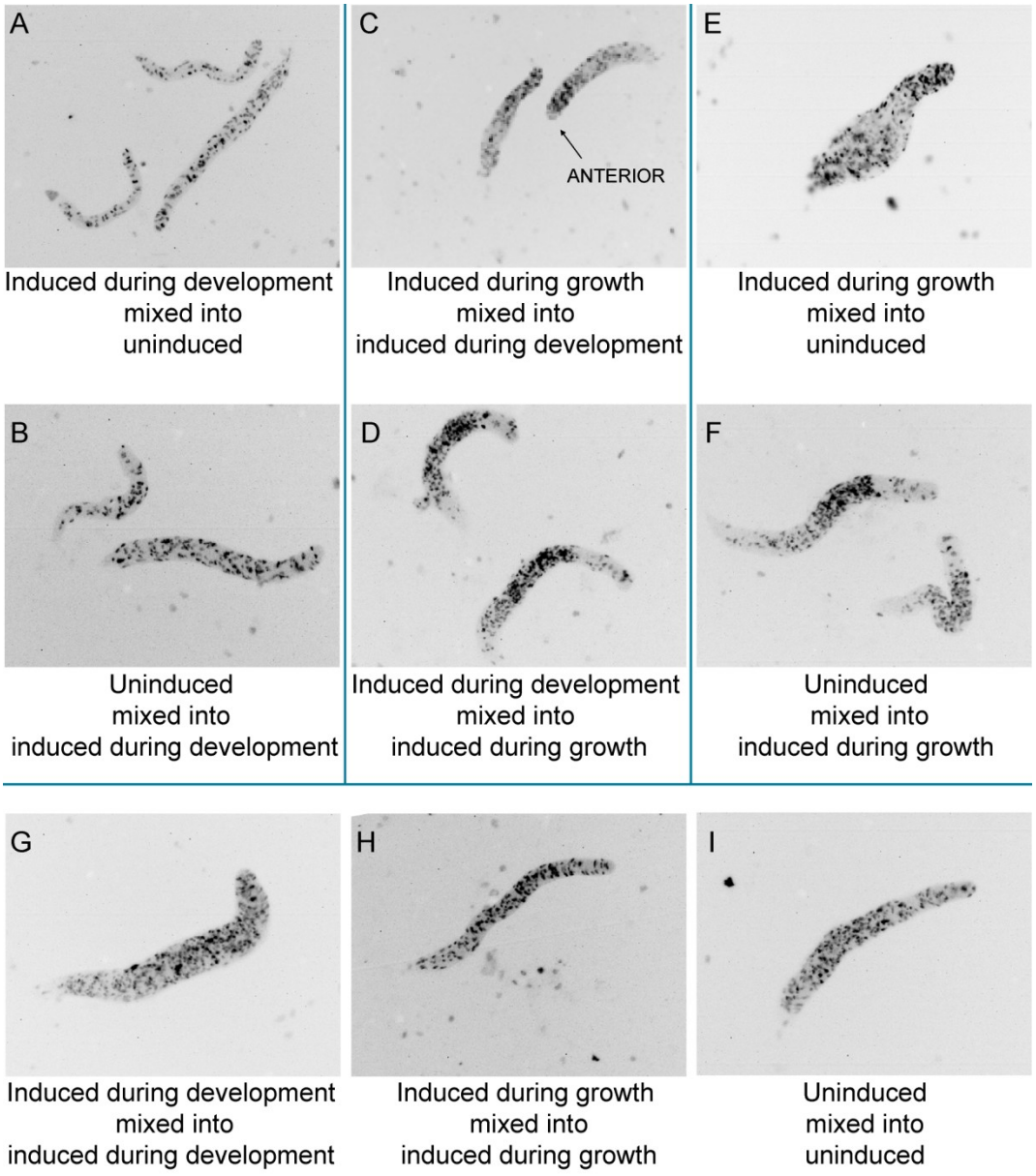

Figure 27. Expression of *cdk1*T14A during early development does not cause a cell-type bias (slug images)

[tet]:*cdk1*(T14A):TAP cells were grown in HL5 medium with doxycycline for 24 hours (induced during growth) or washed, resuspended in buffer, and maintained in shaken suspension for 4 hours in the presence (induced during development) or absence (uninduced) of doxycycline. Cells were fluorescently labelled as usual and 10% fluorescent cells were mixed with 90% non-fluorescent cells in the combinations indicated. Shown here are cell mixtures photographed at the slug stage. These are inverted black-and-white images and so the fluorescent cells appear as black dots. Results are representative of three independent experiments.

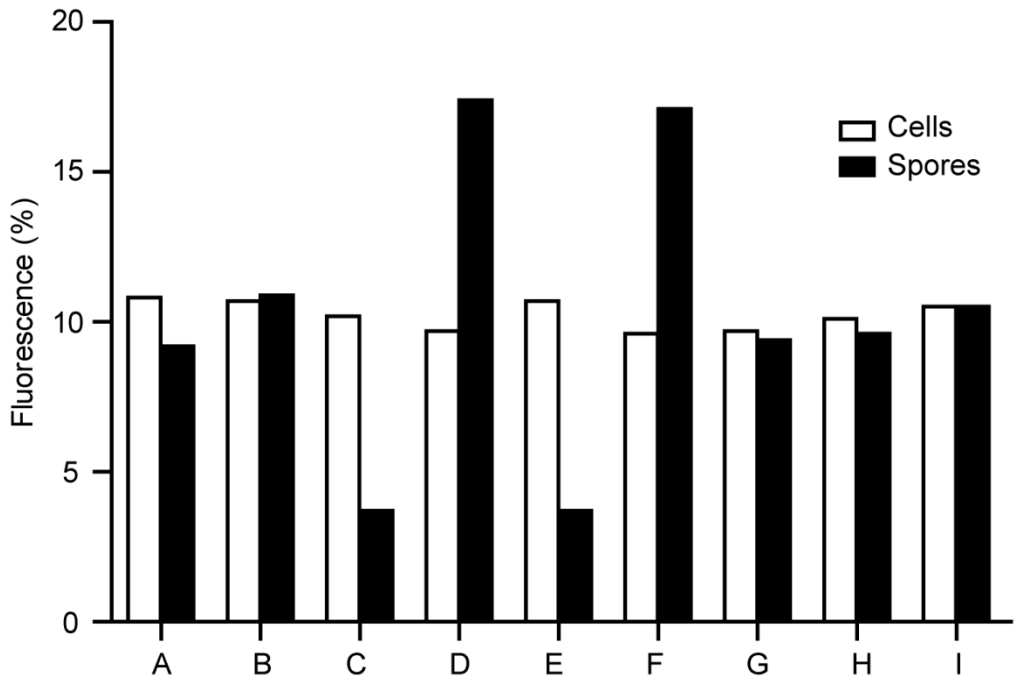

Figure 28. Expression of *cdk1*T14A during early development does not cause a cell-type bias (quantitative data)

[tet]:*cdk1*(T14A):TAP cells were resuspended in non-nutrient KK2 buffer and maintained in shaken suspension for 4 hours with doxycycline (induced during development) or without (uninduced) doxycycline. [tet]:*cdk1*(T14A):TAP cells cultured in rich HL5 medium with doxycycline for 24 hours (induced during growth) served as a control. Some of the cells were fluorescently labelled and 10% fluorescent cells were mixed with 90% non-fluorescent cells in the following combinations: (A) Cells induced during early development mixed into uninduced cells, (B) uninduced cells mixed into cells induced during early development. The remaining cell mixtures were controls: (C) Cells induced during growth mixed into cells induced during early development, (D) cells induced during early development mixed into cells induced during growth, (E) cells induced during growth mixed into uninduced cells, (F) uninduced cells mixed into cells induced during growth, (G) cells induced during early development mixed with cells induced during early development, (H) cells induced during growth mixed into cells induced during growth, (I) uninduced cells mixed into uninduced cells.

fluorescent [tet]:*cdk1*(T14A):TAP cells. The reverse mixture consisting of uninduced fluorescent [tet]:*cdk1*(T14A):TAP cells mixed into induced non-fluorescent [tet]:*cdk1*(T14A):TAP cells produced the same result (Figure 27B). We included control samples in which [tet]:*cdk1*(T14A):TAP cells induced during the growth phase were combined with non-labelled [tet]:*cdk1*(T14A):TAP cells induced during early development (Figure 27C and D) or combined with uninduced cells (Figure 27E and F). Consistent with the results described in Section 3.4, [tet]:*cdk1*(T14A):TAP cells induced during growth showed a strong stalk-cell bias even when mixed into [tet]:*cdk1*(T14A):TAP cells induced during early development. Additional control mixtures containing fluorescein labelled and non-labelled cells of the same genetic background showed no sorting in the slugs (Figure 27G, H, and I). The quantitative data from this experiment also showed the absence of a developmental phenotype. As seen in the graph in Figure 28A and B, the percentage of fluorescent spores (black bars) recovered from fruiting bodies was about the same as the percentage of fluorescent cells (white bars) in mixtures containing developmentally induced or uninduced [tet]:*cdk1*(T14A):TAP cells. We concluded from this experiment that *cdk1*T14A must be expressed in growing cells before the transition to multicellularity in order to affect cell-type bias. Expressing *cdk1*T14A after the onset of development has no influence on cell fate. This observation reinforces the idea that events taking place during the growth phase set the stage for later developmental processes in *Dictyostelium* (Thompson and Kay 2000a).

3.8 Cells expressing *cdk1*T14A are sensitive to glucose in the growth medium

Developmental pathway choice is influenced by the composition of the broth in which the cells are cultured. Ax2 cells grown in HL5 medium without glucose tend to be stalky while those cultured in complete medium favour the spore pathway (Leach et al 1973, Thompson and Kay 2000a). Since induced [tet]:*cdk1*(T14A):TAP cells divided prematurely we explored the possibility that this site was involved in sensing and relaying nutritional cues. We reasoned that if the addition of a phosphate group at T14 served as an indicator of poor nutrition (i.e. the need to grow in size before dividing), then converting the phosphorylatable threonine to a non-phosphorylatable alanine would eliminate glucose-based cell-type preferences. We cultured induced [tet]:*cdk1*(T14A):TAP cells in HL5 medium with glucose (G+) or without (G-) then performed mixing experiments. Both the slug images and quantitative data showed that cells expressing *cdk1*T14A remained sensitive to glucose levels in the growth medium (Figure 29). Induced [tet]:*cdk1*(T14A)TAP cells grown without glucose leaned towards the stalk fate as seen by the abundance of labelled, glucose-deprived cells in the collar region and anterior-like area of the slug and the lower percentage of labelled spores recovered from mature fruiting bodies. As a positive control we included Ax2 cells grown with or without glucose in the experiment and found that their sorting pattern in developing slugs was very similar to the [tet]:*cdk1*(T14A):TAP cells. It has been reported that glucose-deprived cells are smaller than usual (Muramoto and Chubb 2008). In our experiments we closely monitored cell size and noted that it remained constant whether or not glucose was added to the medium (Table 5). We found this intriguing since it implied that initial developmental decisions are not necessary linked to cell size.

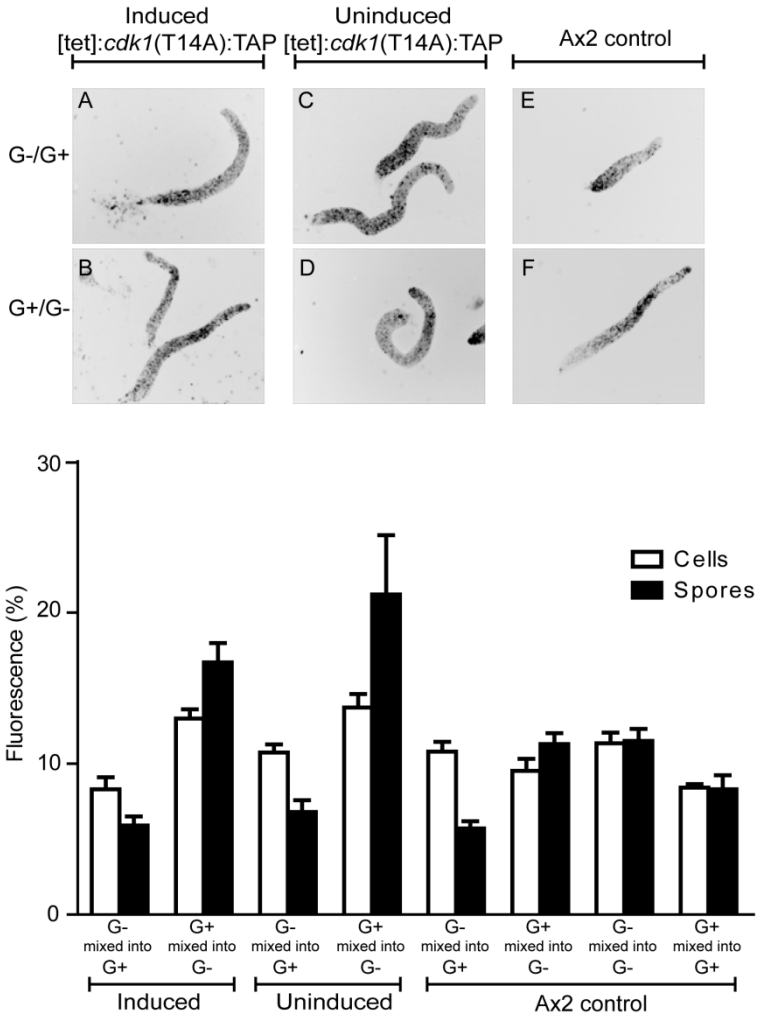

Figure 29. Cells expressing *cdk1*T14A remain sensitive to glucose in the growth medium

The distribution of cells cultured with glucose (G+) or without glucose (G-) in chimeric slugs (top panel). 10% fluorescently-labelled cells were mixed with 90% non-labelled cells in the following combinations: (A) Induced [tet]:*cdk1*(T14A):TAP G- cells mixed into an excess of induced [tet]:*cdk1*(T14A):TAP G+ cells, (B) induced [tet]:*cdk1*(T14A):TAP G+ cells mixed into an excess of induced [tet]:*cdk1*(T14A):TAP G- cells, (C) uninduced [tet]:*cdk1*(T14A):TAP G- cells mixed into an excess of uninduced [tet]:*cdk1*(T14A):TAP G+ cells, (D) uninduced [tet]:*cdk1*(T14A):TAP G+ cells mixed into an excess of uninduced [tet]:*cdk1*(T14A):TAP G- cells, (E) Ax2 G- cells mixed into an excess of Ax2 G+ cells, (F) Ax2 G+ cells mixed into an excess of Ax2 G- cells. Inverted black-and-white; fluorescent cells appear as black dots. The bottom panel is the quantitative data for this experiment. The fraction of fluorescent cells in the starting mixture (white bars) compared to the fraction of fluorescent spores (black bars) in the fruiting bodies that these cells formed. The cell mixtures (x-axis), the percentage fluorescence (y-axis), and the strains are indicated. Results are representative of experiments done in triplicate.

3.9 *RblA*-deficient cells expressing *cdk1*T14A show no cell-type bias

Cells of a *rblA*-disruption mutant resemble those overexpressing *cdk1*T14A in that they, too, are smaller than usual and stalky (MacWilliams et al 2006). The stalk-cell preference is seen in mixing experiments very similar to the ones described (MacWilliams et al 2006). We asked whether overexpression of *cdk1*T14A in *rblA*– deficient cells would cause an even stronger stalk-cell bias. To this end we transformed the *rblA* disruptant with the doxycycline-inducible tet/*cdk1*(T14A)-TAP vector to make the *rblA*-/[tet]:*cdk1*(T14A):TAP strain. We cultured the strain in the presence or absence of doxycycline then performed immunoblot analyses on crude-cell extracts to confirm inducible expression (Figure 30A). We also measured the size of the cells in the induced and uninduced states and found that *rblA* cells expressing *cdk1*T14A were smaller than the *rblA*- mutant alone and the uninduced control (Figure 30B). We then looked at cell-type bias by performing mixing experiments. In Figure31 boxed in red, cells of the *rblA* disruption mutant were mixed with the AX2 parental strain. As reported (MacWilliams et al 2006), the *rblA*- mutant displayed a strong a prestalk bias. When *rblA*-deficient cells were fluorescently labelled and mixed into an excess of Ax2 wild-type cells, very few fluorescent spores were recovered from the fruiting bodies. This means that *rblA*-deficient cells mostly differentiated into stalk cells. As for the *rblA*/[tet]*cdk1*(T14A):TAP compound mutant, although the induced cells showed a small-size phenotype, they did not show a cell-type preference. Rather, we recovered approximately the same percentage of fluorescent spores when cells in the induced and uninduced states were mixed together and developed (Figure 31). Here a stalk bias would have been expected for the induced *rblA*-/[tet]*cdk1*(T14A):TAP cells. To begin to understand why these cells no longer favoured the stalk pathway we decided to better characterize the *Dictyostelium rblA*-

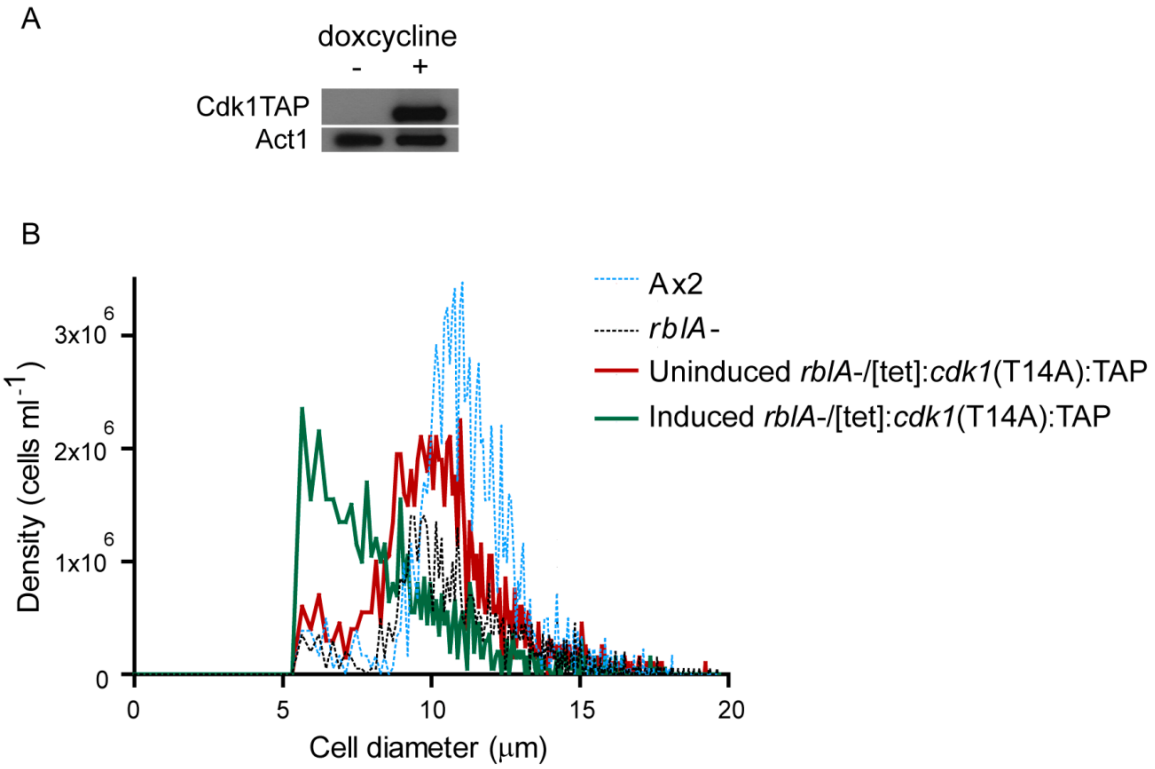

Figure 30. *RblA*-deficient cells expressing *cdk1*T14A decrease in size

rblA-/[tet]:cdk1(T14A):TAP cells were cultured with 20 µg ml^{-1} doxycycline or without for 24 hours. Samples were collected and (A) immunoblotted using an antibody recognizing Cdk1(T14A)TAP fusion protein. The same blot was probed with an Actin1 antibody as a loading control. (B) Cell-size distributions (µM; x-axis) of the original Ax2 strain (blue-dotted curve) used to generate the *rblA*- mutant, the *rblA*- strain (black-dotted curve), uninduced *rblA*-/[tet]:*cdk1*(T14A):TAP cells (red curve), and induced *rblA*-/[tet]:*cdk1*(T14A):TAP cells (green curve) compared to cell density (cells ml^{-1}; y-axis).

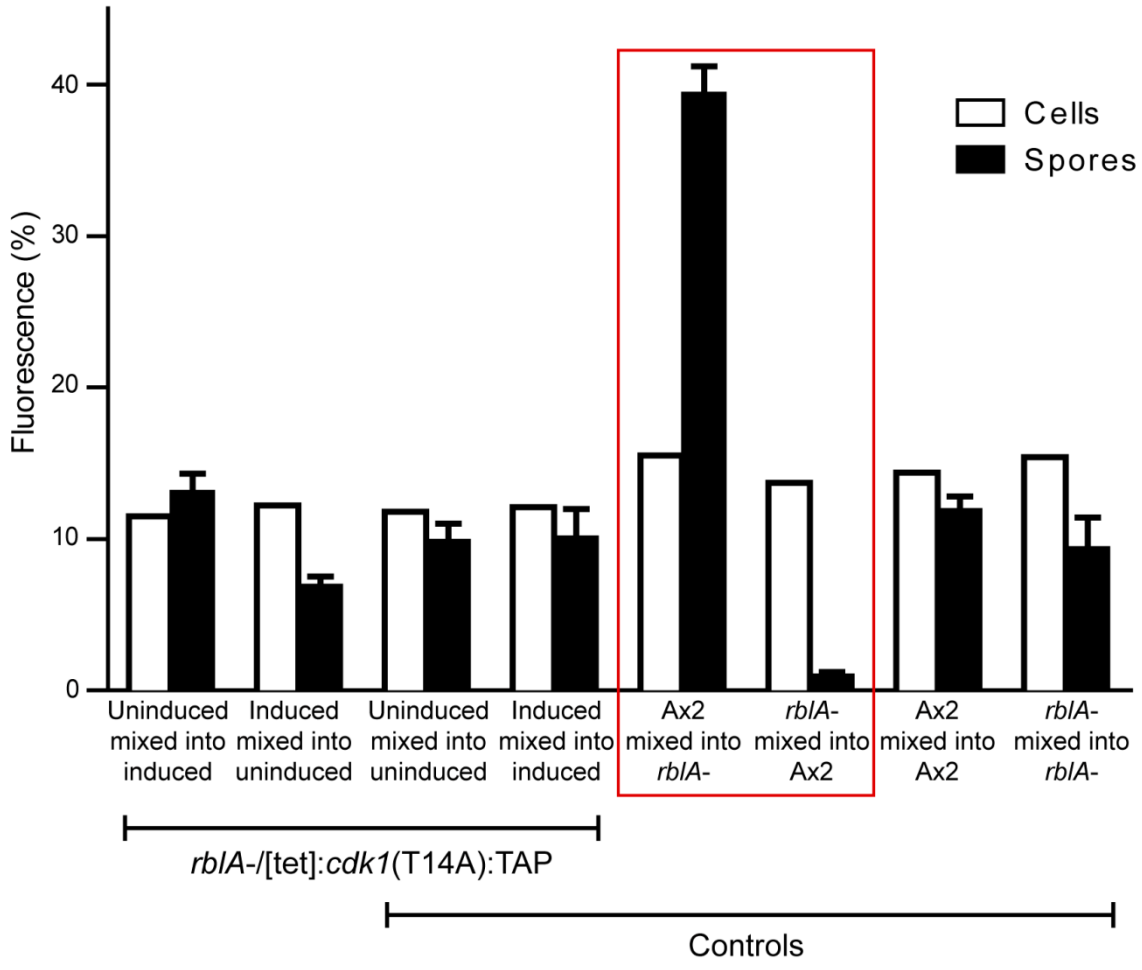

Figure 31. *RblA*-deficient cells expressing *cdk1*T14A have no cell-type bias

Fluorescently-labelled *rblA*-/[tet]*cdk1*(T14A):TAP cells were mixed with an excess of non-labelled cells in the following combinations (from left to right): uninduced mixed into induced cells, induced mixed into uninduced cells, uninduced mixed into uninduced cells, induced mixed into induced cells. The additional controls were also included: fluorescent Ax2 cells mixed into an excess of non-labelled *rblA*- cells (Ax2 mixed into *rblA*-), fluorescent *rblA*- cells mixed into an excess of non-labelled Ax2 cells (*rblA*- mixed into Ax2), fluorescent Ax2 cells mixed into an excess of non-labelled Ax2 cells (Ax2 mixed into Ax2), fluorescent *rblA*- cells mixed into an excess of non-labelled *rblA*- cells (*rblA*- mixed into *rblA*-). The percentage of fluorescent cells (white bars) was determined before the onset of development. The percentage of fluorescent spores (black bars) was determined after 48 hours of development. Results typical of experiments performed in duplicate using two independent clones.

deficient strain by performing mRNA-sequencing (mRNA-Seq) analyses.

3.10 Differentially-regulated genes in the *rblA* disruptant

We prepared mRNA samples from growing and developing cells of a *rblA* disruptant (MacWilliams et al 2006) and the Ax2 parental strain in two independent experiments, then analysed the samples using both microarrays (Bloomfield et al 2008) and mRNA-Seq.. The number of genes showing significant differences in expression was higher in the mRNA-Seq data set than in the microarray (367 versus 251 transcripts with p-value < 0.05). Many of the transcripts whose differential expression was judged significant in the microarray were also strongly regulated in the mRNA-Seq data set (Figure 32). Regulation levels were similar for the most abundant transcripts. Low abundance transcripts behaved heterogeneously. Expression changes were higher on the average in the mRNA-Seq data set but we also saw some genes, judged significant in the microarray, which showed little or no regulation in the mRNA-Seq data. These genes included several whose transcripts were not detectable by sequencing. Such events are presumably microarray false-positives resulting from cross-hybridization and deficiencies in array construction. We also performed qRT-PCR to support this cross-platform validation on selected genes (Table 7).

We tried several ways of visualizing the mRNA-Seq data set as a whole. The most informative seemed to be a plot, gene by gene, of the developmental regulation factor versus the regulation factor in the *rblA* disruptant (Figure 33). This allowed us to identify three groups of differentially-regulated genes. One group (red dots) was upregulated in

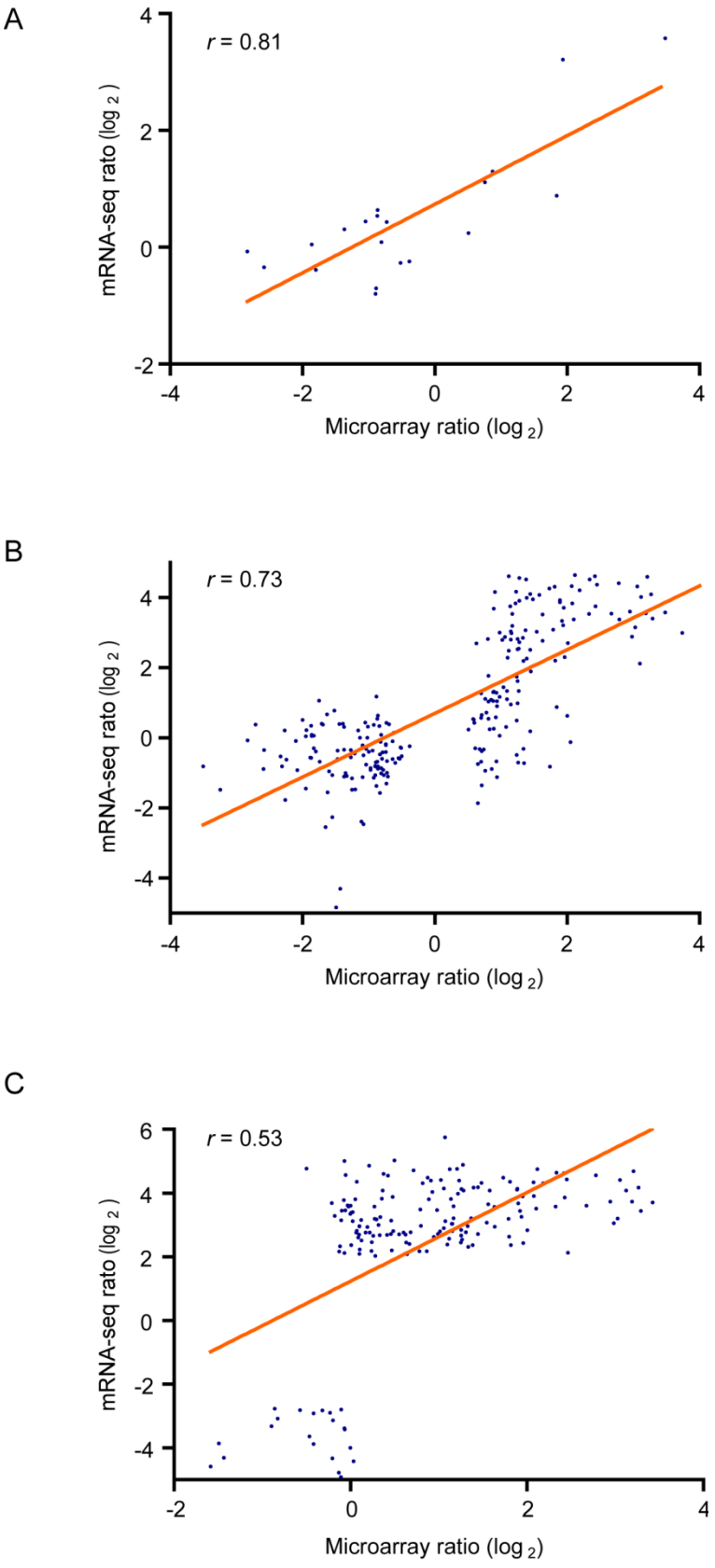

Figure 32. Fundamental agreement between microarray and mRNA-Seq data

Compared are the data for developing cells, where the microarray signals were clearest. Normalized fold-change ratios (*rblA* disruptant mutant/AX2 parental strain) were compared and visualized as scatterplots. The abundance of a particular transcript measured by microarray (x-axis) compared to the abundance of the same transcript measured by mRNA-Seq (y-axis). Compared are the data for developing cells, where the microarray signals were clearest. The linear regression line is in orange and Pearson's correlation coefficient (*r*) is included in the upper, left-hand corner of each graph. (A) Comparison of the 20 most abundant transcripts. (B) Comparison of 247 transcripts considered to be strongly differentially expressed between samples in the microarray analysis. (C) Correlation of 175 genes scored as significant ($p<0.05$) in the mRNA-Seq data with the corresponding microarray measurements.

the *rblA* disruptant compared to the wild type and was, therefore, considered to be transcriptionally repressed by RblA in normal cells. Another group (blue dots) consisted of genes that were upregulated during development but downregulated in the *rblA* mutant. These genes were presumed to be normally induced during development by RblA. The third group (green dots) included genes upregulated during development independently of RblA. These have been extensively studied in *Dictyostelium* and are not discussed here.

3.11 Genes repressed by RblA are involved in cell-cycle control

We found that many of the genes repressed by RblA code for proteins with known or inferred roles in the cell cycle including general cell-cycle controllers along with S-phase and M-phase mediators. A partial list of the RblA-repressed genes is provided in Table 8. A complete list is available in supplementary Table S1. It is a Microsoft Excel spreadsheet with macros designed to assist the user in graphing gene expression profiles. RblA-repressed genes encoding proteins involved in the overall control of the cell cycle include *cdk1,* as well as its inhibitor *wee1*, and five out of the ten identifiable subunits of the anaphase promoting complex. Putative members of the DREAM complex such as *rbbD* (an orthologue of the mammalian retinoblastoma binding protein RBBP4), *lin9*, *lin54,* and *dp* were also negatively regulated by RblA in our data set**.**

Putative S-phase genes negatively regulated by RblA included those encoding the several members of the origin recognition complex (orc), Cdc6*,* and all six subunits of the mini-chromosome maintenance (mcm) helicase. Transcript levels of genes associated with the biosynthesis of deoxyribonucleotides, such as the large and small subunits of ribonucleotide reductase were also higher in *rblA*-deficient cells.

Table 7. Quantitative real-time PCR (qRT-PCR) validation on developmental RNA

		mRNA-Seq	Microarray		qPCR		
Gene name	**Gene ID**	**Average normalized fold change**	**Ratio**	**Fold change**	**Fold change[2] Biol.1**	**Fold change Biol.2**	**Average normalized fold change**
arfgap	DDB0233654	1.34	NA[1]	-	1.00	1.00	1.00
mcm7	DDB0232349	22.31	1,73	3.32	10.80	3.09	6.95
patA	DDB0214945	0.73	0,31	1.23	0.59	0.69	0.69
rfc4	DDB0232233	26.81	2.12	4.35	10.45	3.42	6.94

[1]Gene not present on the array.
[2]Normalized-fold change calculated according to the Pfaffl equation using the *arfgap* gene to normalize (Pfaffl 2001).

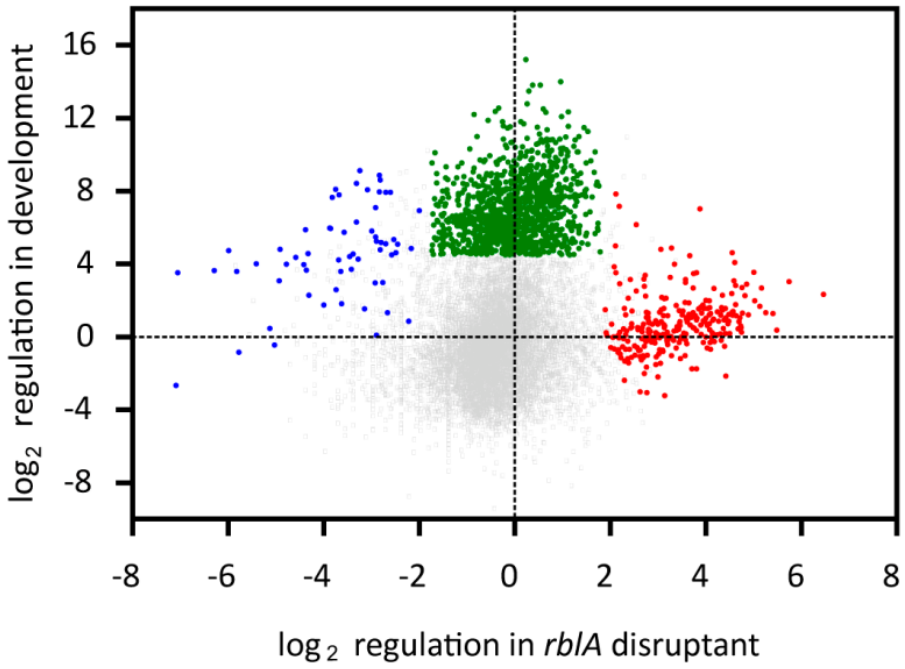

Figure 33. Groups of RblA-regulated genes

Scatter plot of RblA-specific regulation during development (x-axis; scale is log2) compared to developmental regulation (y-axis; scale is log2).Each point represents a gene. The red dots are genes repressed by RblA in both growth and development. The green dots are genes induced during development but not significantly regulated by RblA. The blue dots are genes whose activation depends wholly or partly on RblA.

Table 8. Major groups of RblA-repressed gene

Cell cycle controllers	
Protein-level regulators	*cdk1*, *cks1*, *nek2*, Aurora (*aurK*), *wee* kinase, 5 anaphase promoting complex subunits, *pich*
Transcriptional modulators	*rblA*, DP (*tfdp2*), *lin9*, *lin54*, *myb0*, SMYD3, *ada2*, L-antigen/PCC1, Ki-67, C/EBP
S-phase actors or regulators	
Origin recognition complex	*orcs*
Other initiation factors	*cdc6*, *cdc45*, 3 *gins*, *ctf4*
DNA helicase subunits and interactors	*mcm2-7*, Timeless, *wrnip1*
DNA polymerase subunits	all recognizable subunits of pol alpha, delta, and epsilon
Nucleotide biosynthesis genes	*rnrA&B*, dCMP deaminase
Sliding clamp and clamp loaders	*pcna*, *rfc*, *ctf8*, *dcc1*, ELG1
Other replication fork factors	flap endonuclease (*repG*), DNA ligase I (*lig1*), DNA topoisomerase II (*top2*)
Cohesins and interactors	*smc1,3,5&6*, STAG, Nipped-B, *rad21*, *pds5*, *eco1*
Histone mRNA processing factors	*eriA*, COBRA1
Chromatin disassembly/assembly factors	*ssrp1*, *asf1*, HAT1, HAT2/RbAp46 (*rbbD*), CAF1a&b, 2 SAPs
DNA mismatch repair	*msh2&3&6*, *myh*, *apnA*
Post replication repair	*rad18*
Double strand break repair (HR)	RepA (*rfa1*), *rad51*, *rad52*
Double strand break repair (NHEJ)	*xrcc4*, *lig4*, putative aprataxin, 53BP1
Intrastrand crosslink repair	*mtmr15*
9-1-1 complex and interactors	*rad9*, *hus1*, Rad53/CHK2 (*fhkA*)
Mitotic actors or regulators	
Centrosomal components and interactors	*spc97&98*, CP75, CP91, *mps1*
Centromere and kinetochore	*spc25*, *ndc80*, *nuf2*, Cenp68, Haspin, SPC105
Condensins and interactors	*smc2&4*, *ncapD2*, *D3*, *Ga, Gb*, *G2*, *H*, and *H2*
Spindle components	*tubC*, *tubC* folding cofactor (*tbcD*), *eb1*, *clasp*, mitotic kinesins (*kif*s)
Spindle checkpoint	*bub1* and *3*, Mad2, *cdc20*, *ube2c*, Separase (*espl1*)

components	
Cytokinesis regulators	INCENP (*icpA*), 2 dynamin-related proteins (*dlp*)
Transposable elements	
Skipper	9 Skipper POL and GAG genes, plus 3 diverged GAG
Tdd-5	one of two *Dictyostelium* Tdd-5 sequences
Conserved proteins associated with proliferation or cancer	
Shaker-related voltage gated potassium channel correlated with proliferation in vertebrate Schwann cells (Hallows and Tempel 1998).	
Ube2s, ubiquitylates VHL and thus indirectly upregulates HIFalpha and tumour angiogenesis in vertebrates (Jung et al 2006).	
Other widely conserved proteins	
Putative orthologue of Monad (*wdr92*) which potentiates apoptosis in response to TNF-alpha (Saeki et al 2006).	
Putative orthologue of SIVA, an E2F-induced proapoptotic protein in vertebrates (Fortin et al 2004).	
Vacuolar import and degradation protein Vid27.	
CARKD, universally conserved protein of unknown function.	

These genes were at least twofold overexpressed ($p<0.05$) in the *rblA* disruptant. Details and links to the individual genes are in supplementary Table S1. In the interest of clarity where the gene name was unclear or cumbersome the name of the corresponding protein was given.

Mitotic genes repressed by RblA included most of the *Dictyostelium* type I and II condensins and some whose products are important in spindle assembly or spindle mechanics. Notably, the seven overexpressed kinesins corresponded exactly to those thought to be involved in mitotic processes (Kollmar and Glockner 2003, Nag et al 2008); none of the kinesins with putative functions in vesicle transport were regulated by RblA. RblA-repressed genes with probable roles in cytokinesis included the inner centromere protein INCENP, and two genes coding for dynamin-like proteins (Miyagishima et al 2008).

Genes associated with DNA repair and rearrangement are repressed by RblA including components of the DNA mismatch repair system. Genes whose products are involved in rescuing stalled replication forks by homologous recombination are also upregulated in the *rblA* disruptant, including the PCNA-targeting E3 ubiquitin ligase RAD18 and the recombination enzymes RAD51 and RAD52. There is however dichotomy in the role of RblA on the non-homologous end joining (NHEJ) pathway. The genes encoding members of the "X4L4" complex are RblA-repressed while several others (*dnapkcs*, *ku70*, *ku80*, *polB*, and *wrn*) are not regulated by RblA.

In addition, we found that RblA repressed several highly-conserved genes whose functions in the cell cycle are not well understood. These included *shaker*, *ube2, and elaC* which are correlated with normal or abnormal proliferation when expressed (Hallows and Tempel 1998, Jung et al 2006, Tavtigian et al 2001) and two (SIVA and Monad) that are considered to be apoptotic genes in metazoans (Fortin et al 2004, Saeki et al 2006). *Dictyostelium* may serve as a useful model to clarify the roles of these genes in the cell cycle.

3.12 Expression of RblA-repressed genes in the cell cycle

To determine whether RblA-repressed genes were expressed periodically during the cell cycle, wild-type cells were synchronized using the temperature block-and-release method (Maeda 1986). Afterwards, cells were harvested at 1-hour intervals over a 12 hour period for RNA isolation and for pulse labelling with bromodeoxyuridine. Cell numbers were also measured every 30 minutes using a Coulter counter. As seen in Figure 34, the cells divided rapidly over a 3-hour period after release from the cell-cycle block (time zero). At 3 hours, we observed a bromodeoxyuridine-incorporation peak in the synchronously-growing cells. The number of cells in S phase was about three times higher at this time point than in asynchronous growth. Thus the synchronization was in agreement with previously published data (Araki et al 1994). Analysis of mRNA abundance in the synchronized cells revealed that most RblA-repressed genes were cell-cycle regulated. Their transcript levels accumulated during the cell cycle about one hour after the release from the cell-cycle block and two hours before the peak of bromodeoxyuridine incorporation. In *Dictyostelium* mitosis is immediately followed by S phase; a cell takes about 40 minutes to complete the two processes (Muramoto and Chubb 2008, Weijer et al 1984). Hence RblA-repressed genes accumulated during the cell cycle in late G2. We found that the *rblA* transcript behaved like the genes that it repressed, increasing shortly before S phase. This suggests that RblA is also regulated at the protein level in growing cells. In animal and plant cells, active Cyclin D-Cdk complexes regulate early phosphorylation of Retinoblastoma at the G1/S transition

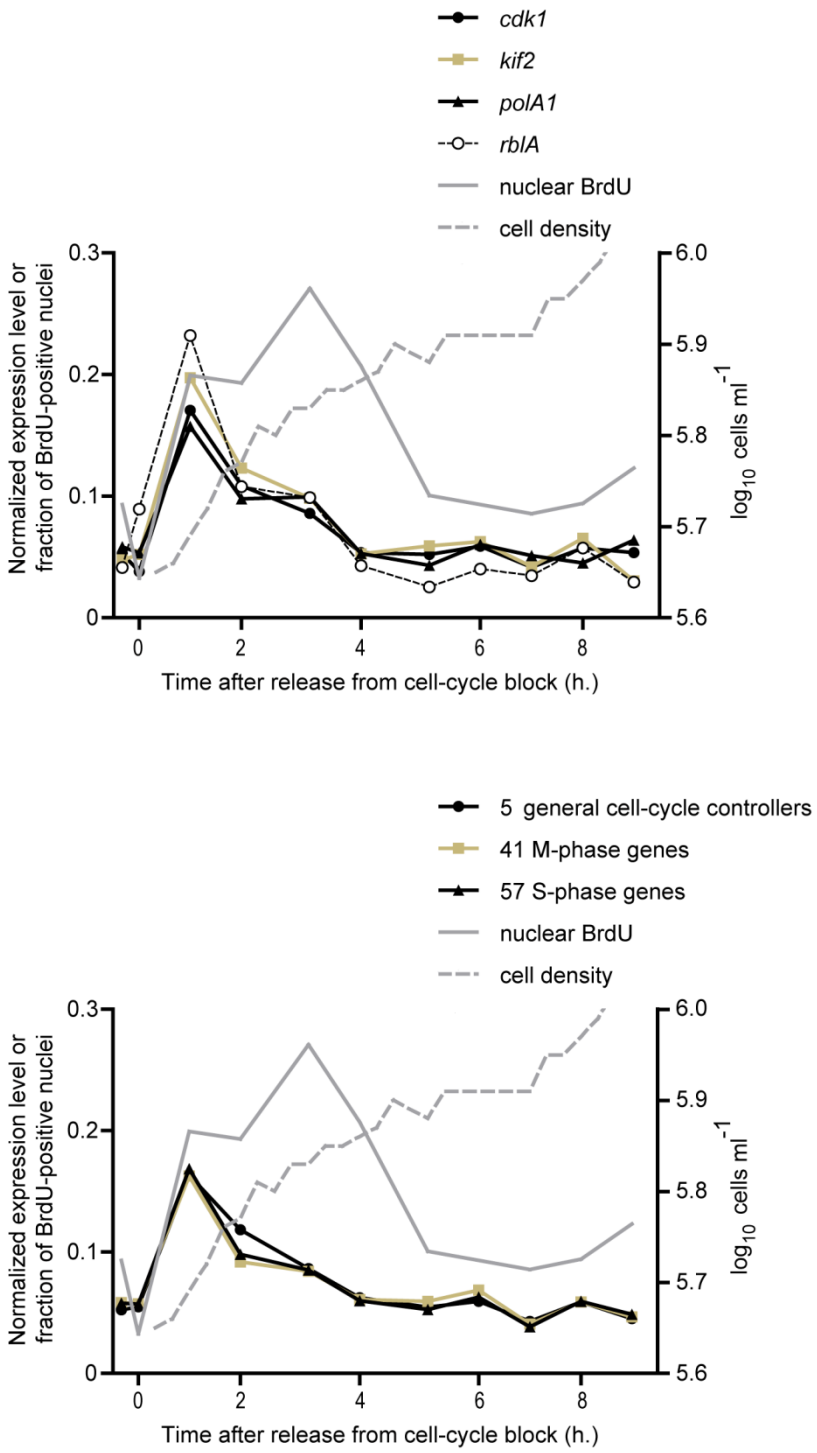

Figure 34. S-phase and mitotic genes are expressed in late G2

Cells were synchronized using cold arrest and released from the block at time zero. RNA samples were collected at hourly intervals over a 12-hour period for mRNA-sequencing. Cells were counted every 30 minutes (grey-dotted line) and pulse-labelled every hour with bromodeoxyuridine to monitor passage through S phase (grey line). The expression pattern of (A) the selected genes *cdk1*, *kif2*, *polA1*, and *rblA* and (B) gene groups during the cell cycle. Expression levels for cell-cycle genes with RblA-repression factors of 2.0 or greater ($p<0.05$) averaged here. Note that because of the incomplete synchronization, modulation of greater than threefold is not expected even if a gene is expressed exclusively at the G2/M transition.

(de Jager et al 2009, Lundberg and Weinberg 1998). Cyclin D may play a parallel role in *Dictyostelium.* We noted that the *cycD* transcript increased 7.5-fold within an hour after the cells were released from the cold block ($p < 0.0033$) thus preceding by one hour the expression peak of RblA-repressed genes.

We also identified genes that were transcriptionally regulated during the cell cycle but not by RblA. The list included *cdc25* which encodes the Cdk1T14 and Y15 dual phosphatase and the three cell-cycle cyclins (*cycA*, *cycB*, and *cycD*) which code for proteins predicted to activate Cdk1 (see www.Dicytbase.org/gene/DDB_G0283617 and DDB_G0279085 and DDB_G0275493 and DDB_G0277439).

3.13 Expression of cell-cycle dependent genes during development

Cell-cycle activity during *Dictyostelium* multicellular development has been reported (Bonner 1952, Durston and Vork 1978, Muramoto and Chubb 2008, Weijer et al 1984, Zada-Hames and Ashworth 1978, Zimmerman and Weijer 1993). We examined the developmental expression of *Dictyostelium* cell-cycle dependent genes using previously published mRNA-Seq data (Parikh et al 2010). In this study, starving cells were harvested for RNA isolation and mRNA-sequencing at 4 hour-intervals over a 24 hour period until terminal differentiation. To ensure strict comparability between datasets the raw reads were obtained (courtesy of G. Shaulsky and A. Parikh) and reanalysed using our analysis protocol. We found that the transcripts of most cell-cycle genes accumulated in mid-development as the cells progressed from the tipped-aggregate to the slug stage (Figure 35). Like the cell-cycle experiment, the transcriptional profile of *rblA* was comparable to those of the genes that it repressed with a maximum expression peak between 8 to16 hours of development. This is in accordance with a previous study

(MacWilliams et al 2006) and it suggests that RblA is inactive at the protein level in most cells during this period. We also noted that the *cycD* transcript accumulated shortly but significantly ($p < 10^{-44}$, by chi-squared comparison of profiles) before the RblA-repressed genes, suggesting a role for Cyclin D in RblA inactivation in developing cells.

3.14 Genes induced by RblA during development

In metazoans, Rb interacts with other activators of terminal-differentiation genes to facilitate differentiation and stabilize the differentiated state (Khidr and Chen 2006, Korenjak et al 2004). We identified a group of genes that was upregulated in development but downregulated in the *rblA* disruptant. Many of the genes activated by RblA during development belong to a family of prestalk-specific genes similar to sigN. SigN is a transcriptional target of the serum-response related factor, SrfA (Escalante et al 2004). In contrast to the RblA-repressed genes, most of the RblA-activated genes are novel with no recognizable homologues outside the cellular slime moulds. This is not surprizing since they code for proteins that regulate the genesis of slime mould specific structures or natural products.

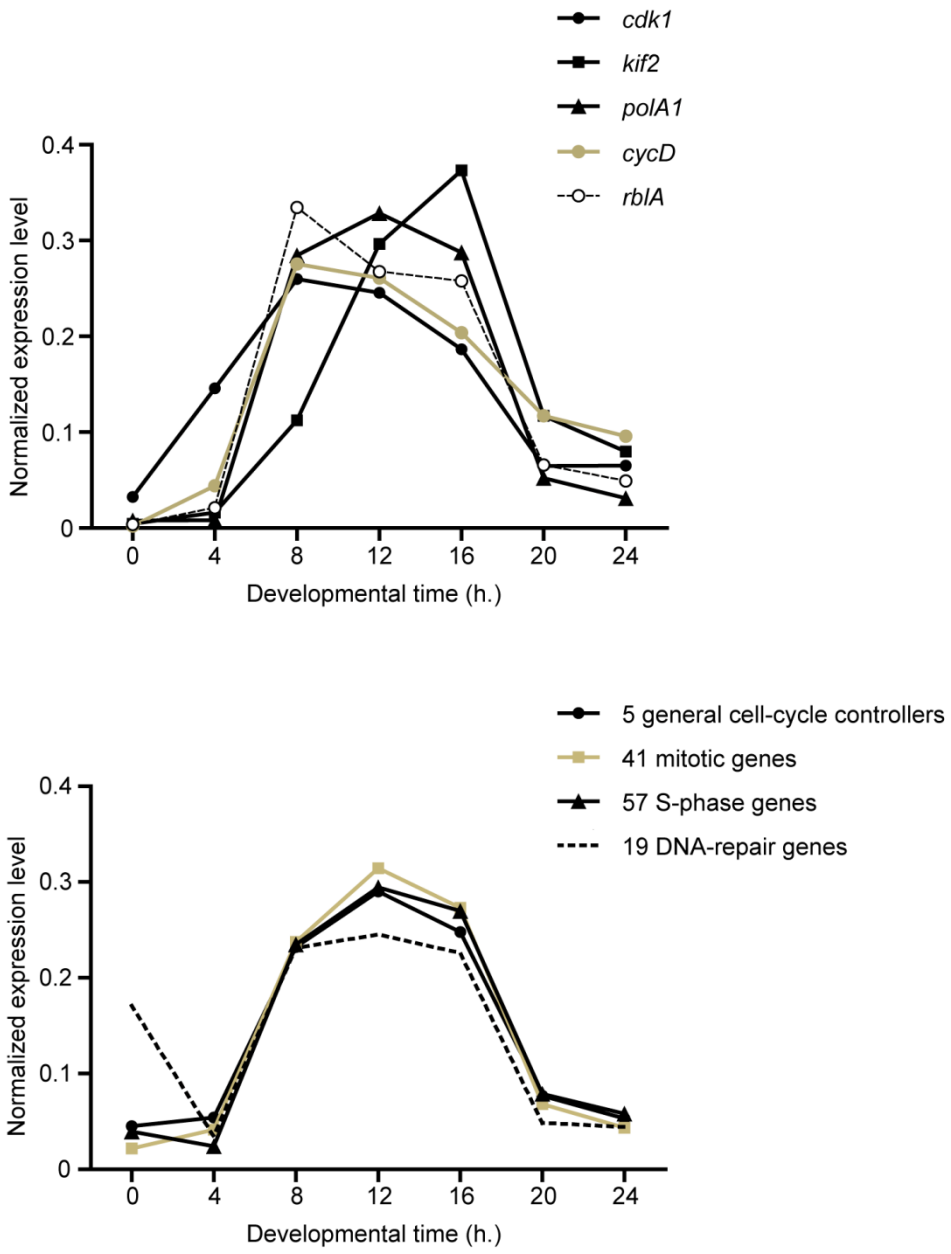

Figure 36. Cell-cycle genes are induced in mid development

Raw data from Parikh *et al* reanalysed (Parikh et al 2010). The time (in hours; x-axis) and mRNA abundance normalized to give a value of 1 (y-axis) are shown. (A) Developmental regulation of the selected cell cycle genes *cdk1*, *kif2*, *polA1*, *cycA*, *cycD*, and *rblA*. (B) Averaged transcriptional profiles of gene groups including 5 general cell cycle controllers, 41 mitotic genes. 57 S-phase genes, and 22 DNA repair genes. Raw data from Parikh *et al* reanalysed (Parikh et al 2010). The developmental time in hours (x-axis) and normalized mRNA levels (y-axis) are shown.

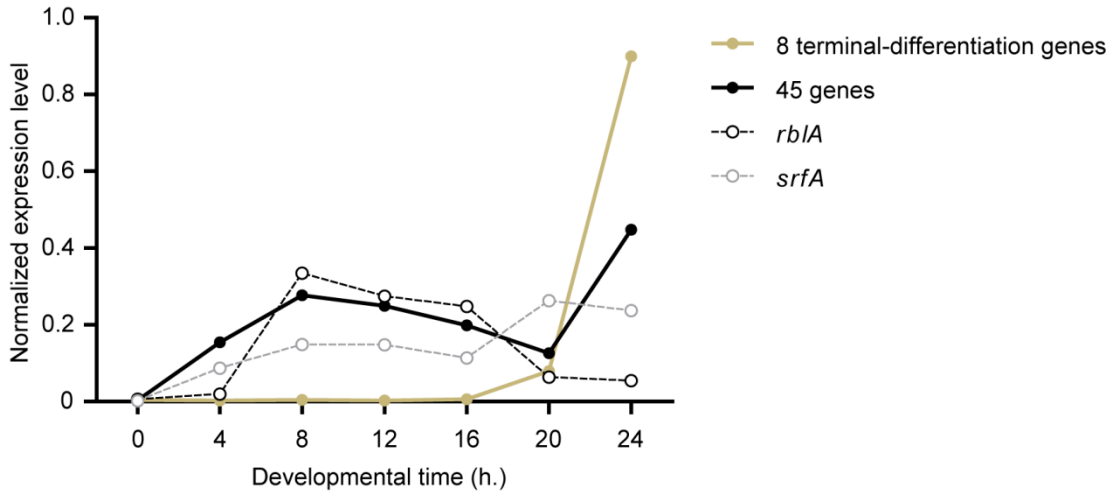

Figure 37. Developmental regulation of RblA-activated genes

Cells were developed for the amount of time indicated and analysed using mRNA-sequencing. The averaged-developmental profiles of 8 terminal-differentiation genes and 45 genes regulated during development by RblA, as well as the profiles for *rblA*, and *srfA*. Raw data from Parikh *et al* reanalysed (Parikh et al 2010). The developmental time in hours (x-axis) and normalized mRNA levels (y-axis) are shown. Expression profiles were normalized to give a total value of 1.

4. DISCUSSION

We have investigated the role of the cell cycle in *Dictyostelium* differentiation by manipulating the activity of the cyclin-dependent protein kinase Cdk1 and the homologue of Retinoblastoma, RblA. Through genetic manipulations that render Cdk1 constitutively active and transcriptional profiling of a *rblA*-deficient strain, we have provided additional knowledge on the *Dictyostelium* cell cycle.

4.1 Checkpoints in the *Dictyostelium* cell cycle

We found that *Dictyostelium* has a size-maintenance checkpoint shortly before mitosis. The threshold size required to pass this checkpoint appears to be set at a diameter of 10.3 μm ± 0.05. In *Dictyostelium,* cell size and mitotic entry are at least in part coordinated through Cdk1 phosphorylation on threonine 14. Replacing the residue with an alanine resulted in a dominant, gain-of-function mutation that allowed the cells to divide prematurely. Until now a role for Cdk1T14 in size control has only been shown in fission yeast (Den Haese et al 1995). This may reflect the cell cycle of *S. pombe* in which the G1 phase of wild-type cells is usually brief making the G2/M-phase transition the dominant regulatory point (Murray and Hunt 1993). In most other systems, cells must reach a critical size in order to enter S phase (Pardee 1989). This size checkpoint, also known as the Restriction point, is in late G1 and controlled by Retinoblastoma and Cdks bound to G1 cyclins (Blagosklonny and Pardee 2002) . In the *Dictyostelium* cell cycle, where a G1 phase is absent (Muramoto and Chubb 2008, Weijer et al 1984) we found that most genes needed for DNA synthesis were induced shortly before mitosis, at the same time as mitotic genes. This transcriptional event is regulated for the most part by RblA.

It has been shown that RblA-deficient cells are smaller than wild-type cells (MacWilliams et al 2006). So are cells that express *cdk1*T14A. A possible interpretation for this observation is that there are at least two mechanisms controlling cell size in the *Dictyostelium* cell cycle. One is regulated by RblA and the other by Cdk1. Accordingly we found that cell size was smallest in induced cells of the *rblA*-/[tet]:*cdk1*(T14A):TAP double mutant strain. Thus, conforming to the G2/M-phase/S-phase profile of *Dictyostelium* cells, it appears that a S-phase like transition in late G2 controls cell size along with the transcription of S-phase and mitotic genes.

The expression of *cdk1*T14A in wild-type Ax2 caused the cells to jump from a normal to a rapid growth rate and get progressively smaller up to, at most, 24 hours. There was, however, a second event in the cell cycle which prevented the cells from becoming indefinitely small. The transient increase in the number of bromodeoxyuridine-positive cells following induction suggested a delay in S phase. The number of cells undergoing DNA synthesis peaked at 4 hours with levels returning to normal by 6 hours. Still, lengthening of the S phase was not the only way in which the cells compensated for entering mitosis prematurely since they continued to decrease in size well beyond 6 hours after the addition of doxycycline. Together with specific phosphorylation and dephosphorylation events, the Cdk1 circuitry also relies on the periodic accumulation of cyclins for activation (Morgan 1995). In the case of the Cdk1T14A mutant, it is likely that rapid division was not maintained because Cdk1 activity was still dependent on the presence of Cyclin B whose mRNA levels fluctuate during the cell cycle (see Luo et al 1995, Norbury et al 1991, and this study).

We also identified a mitotic, spindle-assembly checkpoint in the *Dictyostelium* cell cycle which coordinates chromosome condensation with spindle formation. As in other model organisms, Cdk1-mediated checkpoint arrest required the addition of a phosphate group on tyrosine 15. Substituting this amino acid residue with a non-phosphorylatable phenylalanine locked the Cdk1 protein in an active state allowing the cells to trigger mitosis early. The phenotype was irreversible.

4.2 Developmental programming and the cell cycle

At the multicellular stage of development a *Dictyostelium* cell has a memory of the time when it was still a single cell. Cells that were in late G2 when the developmental program was launched are most often assigned to the spore pathway whereas amoebae that were in M, S or the early G2 phase are more likely to give rise to stalk cells (Araki et al 1994, Araki and Maeda 1998, Gomer and Firtel 1987, MacWilliams et al 2001, McDonald and Durston 1984, Ohmori and Maeda 1987, Weeks and Weijer 1994, Weijer et al 1984, Wood et al 1996, Zimmerman and Weijer 1993). We addressed the issue of cell-cycle phasing and differentiation using the [tet]:*cdk1*(T14A):TAP strain. In the absence of a cell-size control point in late G2, cells expressing *cdk1*T14A generated prestalk cells more readily than spores. When the same gene was expressed in a *rblA* null background, the cells showed a dramatic decrease in size but no cell-type preference in our mixing experiments. These results imply that initial cell-type choice in *Dictyostelium* has little to do with the size of a cell. We do not have a clear explanation yet as to why the stalk-cell preference was lost in the *rblA*-/[tet]:*cdk1*(T14A):TAP double mutant. Our mRNA-sequencing results showed that RblA-deficient cells overexpress *cdk1*. Even if higher levels of endogenous *cdk1* could negate the effects of induced *cdk1*T14A

expression in the *rblA* mutant (presumably by titrating out components of the cell-cycle machinery), untransformed *rblA*- cells should have a strong stalk-cell bias (MacWilliams et al 2006 and this study).

We also re-examined the effect of medium composition on cell fate. Studies have shown that glucose-starved cells have a prestalk bias and are, apparently, smaller than glucose-fed cells (Muramoto and Chubb 2008). Hence cells would appear to modify their threshold size for mitosis in response to nutrient availability. While culturing cells with or without glucose, we noted that G- cells were approximately the same size at G+ cells. In a previous work Thompson and Kay showed clear localization of G- cells to the anterior, prestalk zone of slugs (Thompson and Kay 2000a). We confirmed the stalk cell preference of cells cultured without glucose although the intermediate cell-type seemed to vary. In our hands, cells cultured without glucose appeared to form only a subset of the prestalk cells. These inconsistencies could be due the age of the cultures. We found that G- cells reach stationary phase at $2x10^6$ cells ml^{-1}, a density at which G+ cells were still exponentially dividing. In our mixing experiments we used G+ and G- cultures that were in the exponential phases of their respective growth curves. Despite the invariability in size, G- cells still ultimately became stalk cells in these experiments implying, again in this instance, that a stalk-forming bias is not attributed to cell size.

Returning to the topic of cell subtypes, the quantitative data from two of our mixing experiments indicated a stalk preference for cell expressing *cdk1*T14A and cells cultured in the absence of glucose. The slug images, however, shows two very different sorting patterns. Cdk1T14A cells were concentrated in the anterior, prestalk region whereas glucose-starved cells sorted to the collar region and rear of the slugs, suggesting

that in the latter case, stalk cells were derived from pstO cells and anterior–like cells (Jermyn and Williams 1991). These differences in intermediate stalk cell-types may reflect the presence of two separate mechanisms that influence early development in *Dictyostelium*, one that allows the cells to respond to intracellular signals coming from the cell cycle and the other responsive to environmental cues such as nutrient availability (Thompson and Kay 2000a). In this vein, cells expressing *cdk1*T14A remained sensitive to the amount of glucose in the growth medium. Hence, the nutrient sensing pathway in *Dictyostelium* functions independently of Cdk1T14 phosphorylation and probably involves a different signalling factor.

4.3 Corroborative evidence of cell-cycle activity during *Dictyostelium* development

Although initially interrupted, cell cycling is thought to resume at the slug stage (Bonner 1952, Durston and Vork 1978, Muramoto and Chubb 2008, Weijer et al 1984, Zada-Hames and Ashworth 1978, Zimmerman and Weijer 1993). We found that the cell-cycle genes were activated during mid-development strongly suggesting cell-cycle activity during this period. Interestingly the upregulation levels during development were higher than in the growth-phase experiment. It may be that separate promoter elements become active during development to enable strong, coordinated re-expression of genes following the growth arrest that occurs upon starvation. The phenotype of the *rblA* mutant at the level of mRNA was striking; the mild overall phenotype of *rblA* nulls observed during growth (MacWilliams et al 2006) and the fact that there were high levels of the *rblA* transcript when the gene product was expected to be inactive support the idea that post-transcriptional mechanisms play a major role in cell-cycle control in *Dictyostelium* as in other organisms.

4.4 Applying our findings to existing models

Maeda has proposed a model in which time links cell division to development (Maeda 2005, Maeda 2011). Cells leave the cycle at a developmental checkpoint in mid-late G2 to become stalk cells or spores. Those found closest to the checkpoint are the first to differentiate. If the aggregate is left undisturbed these cells become the spores. Despite the absence of nutrients mitotic, S-phase, and early G2 cells continue to cycle until they also reach the differentiation block; this population of cells contributes to the stalk. The checkpoint is reminiscent of Start, passage through which commits the cells to completing the cell cycle even if growth conditions are not ideal. Such a model could explain the stalk bias of cells cultured without glucose which have much longer generation times (i.e. G2) than glucose fed cells (Muramota and Chubb 2007). When combined with G+ cells and starved, G- cells presumably required more time to exit the cell cycle. They would be restricted to the stalk pathway as a result of initiating differentiation last. In cells overexpressing *cdk1*T14A we saw no lengthening of the cell cycle other than a temporary increase in the duration of S phase. This cannot account for their stalk cell preference, however, because the cells were sorted after an overnight induction when the interdivision times of the induced and uninduced [tet]:*cdk1*(T14A):TAP cultures were identical. Thus there is no indication that the Cdk1T14A mutant was sorting on the basis of cell size or cell-cycle length.

Focusing our attention again on the expression peak of cell-cycle genes during late G2, the timing of this event overlapped with the differentiation checkpoint described by Maeda and others (Maeda 2005, Maeda 2011, Weeks and Weijer 1994). In light of this, it might be tempting to think that the transition into development is regulated by RblA. During periods of stress, such as the absence of nutrients, RblA would trigger

differentiation by fostering cell-cycle arrest. Under more favourable growth conditions, Cdk1 would phosphorylate and inactive RblA, thereby decreasing the amount of gene repression allowing the cells to continue cycling. This model would explain the behaviour of the ratio mutant, *rtoA,* which is blind to the cell-cycle phase when starved and differentiates randomly into stalk cells or spores (Wood et al 1996). These cells presumably have defects in components of the cell cycle. It would also account for the low fraction of spores recovered from *Dictyostelium* treated with nocadozole, an agent that arrests the cells in mitosis (Araki and Maeda 1998). Applying this model to our observations, however, one would expect cells with an active RblA (or inactive Cdk1) to enter development first and be more spore-like. While it is true that *rblA*-deficient cells are stalky, they develop more rapidly than wild-type cells (MacWilliams et al 2006). It seems more likely, then, that RblA and Cdk1 exert their effects on early development by affording the cells with different degrees of DIF1 sensitivity (Thompson and Kay 2000a). Indeed, *rblA*-deficient cell are about three times more responsive to DIF-1 than wild-type cells (MacWilliams et al 2006).

Based partly on our findings we propose a model in which the Retinoblastoma homologue RblA (with E2F and DP) represses important S-phase and G2/M-phase genes at the transcriptional level. RblA-independent regulators, such as the cell-cycle cyclins, act with Cdk1 to phosphorylate and inactivate RblA, allowing cells to advance through the cell-cycle. At the time of starvation cells with an active Cdk1 (or inactive RblA) are most likely to become stalk cells because of their heighten sensitivity to the stalk morphogen DIF-1 (Figure 37).

4.5 Future directions

In the future it would be important to measure DIF1 response in induced [tet]:*cdk1*(T14A):TAP cells. One could do this by transforming the cells with the [ecmO]:lacZ reporter construct in which the promoter region of the prestalk specific extracellular matrix O (ecmO) gene is used to drive the expression of beta-galactosidase (MacWilliams et al 2006). Then induced and uninduced [tet]:*cdk1*(T14A)TAP/[ecmO]:lacZ cells would be exposed to increasing amounts of DIF1 (0 to 100 nM) and beta-galactosidase activity measured as a function of DIF-1 concentration. Since DIF-1 is a stalk morphogen (Thompson and Kay 2000b) and Ax2 cells expressing *cdk1*T14A are stalky, a hypersensitive to DIF-1 (viewed as an increase in betagalactosidase activity compared to the control cells) is expected for induced [tet]:*cdk1*(T14A)TAP/[ecmO]:lacZ cells.

While this study established that Cdk1 and RblA regulate entry into mitosis and S phase much remains to be learned about the *Dictyostelium* cell cycle. For instance, when do each of the cyclins associated with Cdk1? *CyclinD* appeared to accumulate first at the level of RNA. Does the active Cyclin D-Cdk1 complex initiate the phosphorylation of RblA? Future studies should focus on identifying the individual components of the Cdk1 complex during the cell cycle and during development. This should be possible using the TAP tag for pull-down assays on synchronously growing and developing cells.

Another open question concerns the RblA-independent genes such as *cdc25* and the cyclins. What induces their expression? We think that they are induced by external signals such as glucose in the growth medium. If so, then a logical approach would be to perform transcriptome analyses on cells cultured with and without glucose.

Finally, how do Cdk1 and RblA regulate DIF sensitivity? What are the downstream factors involved? Here again mRNA sequencing could serve as a valuable tool. By analysing the transcriptome of [tet]:*cdk1*(T14A):TAP cells in the induced and uninduced states, then comparing the spectrum of genes regulated by Cdk1 with those repressed by RblA, we may identify these regulators. Experiments along these lines are underway.

4.5 Concluding remarks

Although yeast cells still serve as the paradigm for cell-cycle studies, key regulators such as Retinoblastoma are missing from these systems. *Dictyostelium* offers an interesting alternative. We found that *Dictyostelium* uses homologues of the mammalian cell-cycle regulators Retinoblastoma and Cdk1 to drive its cell cycle. The functions of these proteins are highly conserved. RblA regulates the cell cycle at the level of transcription by repressing S-phase and M-phase genes whereas Cdk1 functions post-translationally to bring about cell-cycle progression and mitosis. Unlike higher cells in which multiple pocket proteins and Cdks have evolved, *Dictyostelium* carries one member of each group offering a simple system with which to study the cell cycle, particularly in the context of developing cells.

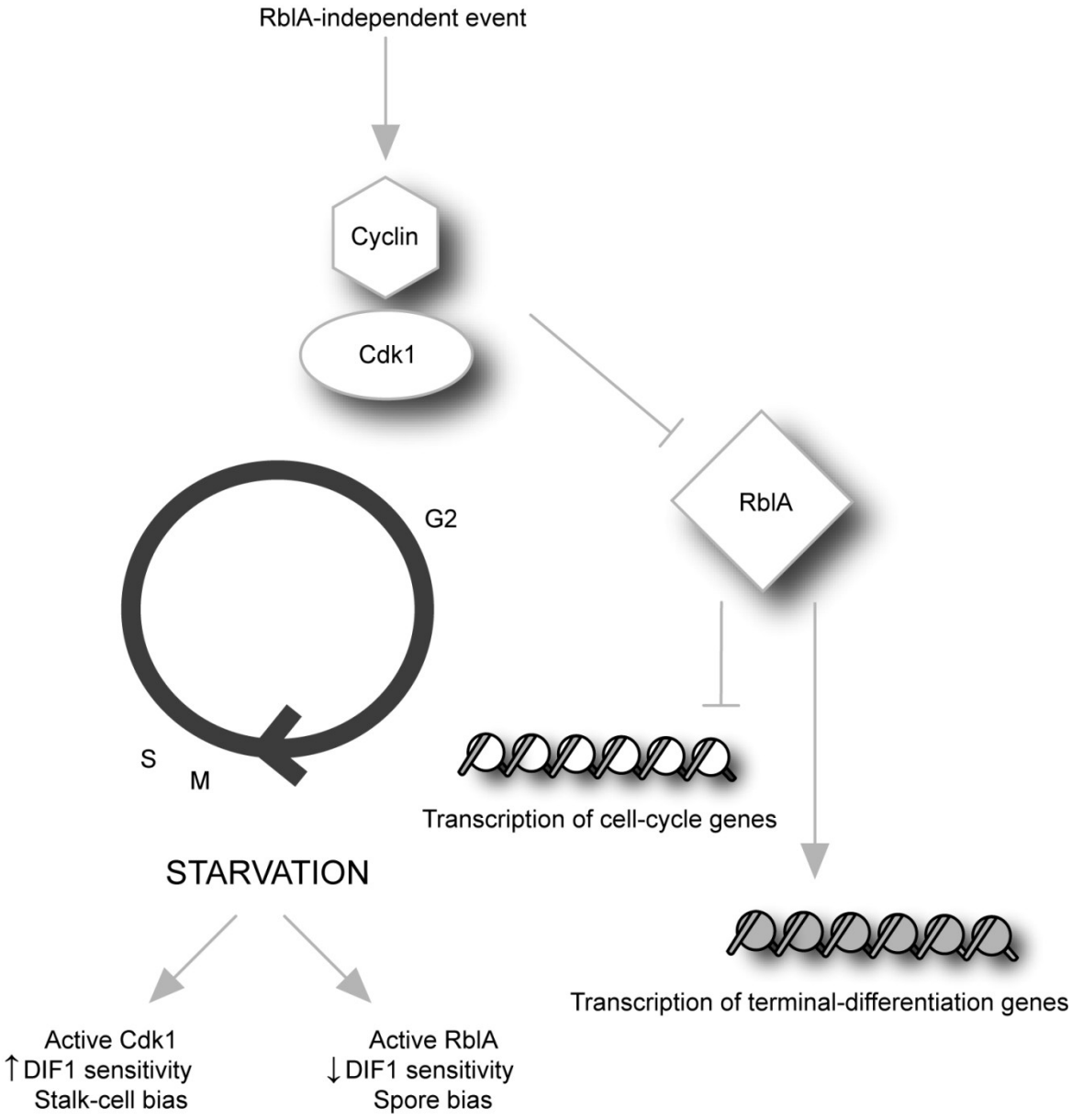

Figure 38. Schematic model of how the cell cycle regulates cell-type specification during *Dictyostelium* development

We propose a model in which the Retinoblastoma homologue RblA (with E2F and DP) represses important S-phase and M-phase genes at the transcriptional level. RblA-independent regulators, such as the cell-cycle cyclins, act with Cdk1 to phosphorylate and inactivate RblA. At the time of starvation cells with an active Cdk1 are most likely to become stalk cells because of their heighten sensitivity to the stalk-cell morphogen DIF-1.

5. REFERENCES

Abe F, Maeda Y (1994). Precise expression of the cAMP receptor gene, CAR1, during transition from growth to differentiation in Dictyostelium discoideum. *FEBS Lett* **342:** 239-241.

Araki T, Nakao H, Takeuchi I, Maeda Y (1994). Cell-cycle-dependent sorting in the development of Dictyostelium cells. *Dev Biol* **162:** 221-228.

Araki T, Maeda Y (1998). Mutual relation between the cell-cycle progression and prespore differentiation in Dictyostelium development. *Zoolog Sci* **15:** 77-84.

Atherton-Fessler S, Liu F, Gabrielli B, Lee MS, Peng CY, Piwnica-Worms H (1994). Cell cycle regulation of the p34cdc2 inhibitory kinases. *Mol Biol Cell* **5:** 989-1001.

Bandara LR, Buck VM, Zamanian M, Johnston LH, La Thangue NB (1993). Functional synergy between DP-1 and E2F-1 in the cell cycle-regulating transcription factor DRTF1/E2F. *Embo J* **12:** 4317-4324.

Barriere C, Santamaria D, Cerqueira A, Galan J, Martin A, Ortega S *et al* (2007). Mice thrive without Cdk4 and Cdk2. *Mol Oncol* **1:** 72-83.

Batsche E, Moschopoulos P, Desroches J, Bilodeau S, Drouin J (2005). Retinoblastoma and the related pocket protein p107 act as coactivators of NeuroD1 to enhance gene transcription. *J Biol Chem* **280:** 16088-16095.

Blagosklonny MV, Pardee AB (2002). The restriction point of the cell cycle. *Cell Cycle* **1:** 103-110.

Bloomfield G, Tanaka Y, Skelton J, Ivens A, Kay RR (2008). Widespread duplications in the genomes of laboratory stocks of Dictyostelium discoideum. *Genome Biol* **9:** R75.

Bonner JT (2009). *The social amoebae : the biology of cellular slime molds*. Princeton University Press: Princeton.

Bonner JTaF, E.B (1952). Mitotic activity in relation to differentiation in the slime mold Dictyostelium discoideum. *Journal of Experimental Zoology***:** 561-572.

Botz J, Zerfass-Thome K, Spitkovsky D, Delius H, Vogt B, Eilers M *et al* (1996). Cell cycle regulation of the murine cyclin E gene depends on an E2F binding site in the promoter. *Mol Cell Biol* **16:** 3401-3409.

Chen HH, Wang YC, Fann MJ (2006). Identification and characterization of the CDK12/cyclin L1 complex involved in alternative splicing regulation. *Mol Cell Biol* **26:** 2736-2745.

Chen HH, Wong YH, Geneviere AM, Fann MJ (2007). CDK13/CDC2L5 interacts with L-type cyclins and regulates alternative splicing. *Biochem Biophys Res Commun* **354:** 735-740.

Chen PL, Riley DJ, Chen Y, Lee WH (1996). Retinoblastoma protein positively regulates terminal adipocyte differentiation through direct interaction with C/EBPs. *Genes Dev* **10:** 2794-2804.

Ciechanover A (1994). The ubiquitin-mediated proteolytic pathway: mechanisms of action and cellular physiology. *Biol Chem Hoppe Seyler* **375:** 565-581.

Ciechanover A, Orian A, Schwartz AL (2000). The ubiquitin-mediated proteolytic pathway: mode of action and clinical implications. *J Cell Biochem Suppl* **34:** 40-51.

Ciemerych MA, Sicinski P (2005). Cell cycle in mouse development. *Oncogene* **24:** 2877-2898.

Cobrinik D (2005). Pocket proteins and cell cycle control. *Oncogene* **24:** 2796-2809.

Cole KA, Harmon AW, Harp JB, Patel YM (2004). Rb regulates C/EBPbeta-DNA-binding activity during 3T3-L1 adipogenesis. *Am J Physiol Cell Physiol* **286:** C349-354.

De Bondt HL, Rosenblatt J, Jancarik J, Jones HD, Morgan DO, Kim SH (1993). Crystal structure of cyclin-dependent kinase 2. *Nature* **363:** 595-602.

de Jager SM, Scofield S, Huntley RP, Robinson AS, den Boer BG, Murray JA (2009). Dissecting regulatory pathways of G1/S control in Arabidopsis: common and distinct targets of CYCD3;1, E2Fa and E2Fc. *Plant Mol Biol* **71:** 345-365.

Den Haese GJ, Walworth N, Carr AM, Gould KL (1995). The Wee1 protein kinase regulates T14 phosphorylation of fission yeast Cdc2. *Mol Biol Cell* **6:** 371-385.

Deshpande A, Sicinski P, Hinds PW (2005). Cyclins and cdks in development and cancer: a perspective. *Oncogene* **24:** 2909-2915.

Dimova DK, Dyson NJ (2005). The E2F transcriptional network: old acquaintances with new faces. *Oncogene* **24:** 2810-2826.

Dingermann T, Reindl N, Werner H, Hildebrandt M, Nellen W, Harwood A *et al* (1989). Optimization and in situ detection of Escherichia coli beta-galactosidase gene expression in Dictyostelium discoideum. *Gene* **85:** 353-362.

Doree M, Hunt T (2002). From Cdc2 to Cdk1: when did the cell cycle kinase join its cyclin partner? *J Cell Sci* **115:** 2461-2464.

Durston AJ, Vork F (1978). The spatial pattern of DNA synthesis in Dictyostelium discoideum slugs. *Exp Cell Res* **115:** 454-457.

Edgar R, Domrachev M, Lash AE (2002). Gene Expression Omnibus: NCBI gene expression and hybridization array data repository. *Nucleic Acids Res* **30:** 207-210.

Escalante R, Vicente JJ (2000). Dictyostelium discoideum: a model system for differentiation and patterning. *Int J Dev Biol* **44:** 819-835.

Escalante R, Iranfar N, Sastre L, Loomis WF (2004). Identification of genes dependent on the MADS box transcription factor SrfA in Dictyostelium discoideum development. *Eukaryot Cell* **3:** 564-566.

Euteneuer U, Graf R, Kube-Granderath E, Schliwa M (1998). Dictyostelium gamma-tubulin: molecular characterization and ultrastructural localization. *J Cell Sci* **111 (Pt 3):** 405-412.

Ewen ME (2000). Where the cell cycle and histones meet. *Genes Dev* **14:** 2265-2270.

Fey P, Kowal AS, Gaudet P, Pilcher KE, Chisholm RL (2007). Protocols for growth and development of Dictyostelium discoideum. *Nat Protoc* **2:** 1307-1316.

Fisher RP, Morgan DO (1994). A novel cyclin associates with MO15/CDK7 to form the CDK-activating kinase. *Cell* **78:** 713-724.

Fisher RP, Jin P, Chamberlin HM, Morgan DO (1995). Alternative mechanisms of CAK assembly require an assembly factor or an activating kinase. *Cell* **83:** 47-57.

Fleig UN, Gould KL (1991). Regulation of cdc2 activity in Schizosaccharomyces pombe: the role of phosphorylation. *Semin Cell Biol* **2:** 195-204.

Fletcher L, Cheng Y, Muschel RJ (2002). Abolishment of the Tyr-15 inhibitory phosphorylation site on cdc2 reduces the radiation-induced G(2) delay, revealing a potential checkpoint in early mitosis. *Cancer Res* **62:** 241-250.

Fortin A, MacLaurin JG, Arbour N, Cregan SP, Kushwaha N, Callaghan SM *et al* (2004). The proapoptotic gene SIVA is a direct transcriptional target for the tumor suppressors p53 and E2F1. *J Biol Chem* **279:** 28706-28714.

Galderisi U, Jori FP, Giordano A (2003). Cell cycle regulation and neural differentiation. *Oncogene* **22:** 5208-5219.

Gao X, Yo P, Keith A, Ragan TJ, Harris TK (2003). Thermodynamically balanced inside-out (TBIO) PCR-based gene synthesis: a novel method of primer design for high-fidelity assembly of longer gene sequences. *Nucleic Acids Res* **31:** e143.

Gaudet P, MacWilliams H, Tsang A (2001). Inducible expression of exogenous genes in Dictyostelium discoideum using the ribonucleotide reductase promoter. *Nucleic Acids Res* **29:** E5.

Gaudet P, Fey P, Chisholm R (2008). Multicellular development of dictyostelium. *CSH Protoc* **2008:** pdb prot5100.

Geng Y, Eaton EN, Picon M, Roberts JM, Lundberg AS, Gifford A *et al* (1996). Regulation of cyclin E transcription by E2Fs and retinoblastoma protein. *Oncogene* **12:** 1173-1180.

Gilbert SF (1997). *Developmental biology*, 5th edn. Sinauer Associates: Sunderland, Mass.

Gilbert SF (2006). *Developmental biology*, 8th edn. Sinauer Associates, Inc. Publishers: Sunderland, Mass.

Glotzer M, Murray AW, Kirschner MW (1991). Cyclin is degraded by the ubiquitin pathway. *Nature* **349:** 132-138.

Goldberg JM, Manning G, Liu A, Fey P, Pilcher KE, Xu Y *et al* (2006). The dictyostelium kinome--analysis of the protein kinases from a simple model organism. *PLoS Genet* **2:** e38.

Gomer RH, Firtel RA (1987). Cell-autonomous determination of cell-type choice in Dictyostelium development by cell-cycle phase. *Science* **237:** 758-762.

Gould KL, Nurse P (1989). Tyrosine phosphorylation of the fission yeast cdc2+ protein kinase regulates entry into mitosis. *Nature* **342:** 39-45.

Graf R, Daunderer C, Schliwa M (2000). Dictyostelium DdCP224 is a microtubule-associated protein and a permanent centrosomal resident involved in centrosome duplication. *J Cell Sci* **113 (Pt 10):** 1747-1758.

Gu W, Schneider JW, Condorelli G, Kaushal S, Mahdavi V, Nadal-Ginard B (1993). Interaction of myogenic factors and the retinoblastoma protein mediates muscle cell commitment and differentiation. *Cell* **72:** 309-324.

Gutierrez C (2005). Coupling cell proliferation and development in plants. *Nat Cell Biol* **7:** 535-541.

Hallows JL, Tempel BL (1998). Expression of Kv1.1, a Shaker-like potassium channel, is temporally regulated in embryonic neurons and glia. *J Neurosci* **18:** 5682-5691.

Hanahan D, Weinberg RA (2000). The hallmarks of cancer. *Cell* **100:** 57-70.

Harborth J, Elbashir SM, Bechert K, Tuschl T, Weber K (2001). Identification of essential genes in cultured mammalian cells using small interfering RNAs. *J Cell Sci* **114:** 4557-4565.

Harbour JW, Luo RX, Dei Santi A, Postigo AA, Dean DC (1999). Cdk phosphorylation triggers sequential intramolecular interactions that progressively block Rb functions as cells move through G1. *Cell* **98:** 859-869.

Hartwell LH, Weinert TA (1989). Checkpoints: controls that ensure the order of cell cycle events. *Science* **246:** 629-634.

Hartwell LH, Kastan MB (1994). Cell cycle control and cancer. *Science* **266:** 1821-1828.

Helin K, Wu CL, Fattaey AR, Lees JA, Dynlacht BD, Ngwu C *et al* (1993). Heterodimerization of the transcription factors E2F-1 and DP-1 leads to cooperative trans-activation. *Genes Dev* **7:** 1850-1861.

Hellmich MR, Pant HC, Wada E, Battey JF (1992). Neuronal cdc2-like kinase: a cdc2-related protein kinase with predominantly neuronal expression. *Proc Natl Acad Sci U S A* **89:** 10867-10871.

Hemerly A, Engler Jde A, Bergounioux C, Van Montagu M, Engler G, Inze D *et al* (1995). Dominant negative mutants of the Cdc2 kinase uncouple cell division from iterative plant development. *Embo J* **14:** 3925-3936.

Ho SN, Hunt HD, Horton RM, Pullen JK, Pease LR (1989). Site-directed mutagenesis by overlap extension using the polymerase chain reaction. *Gene* **77:** 51-59.

Hochegger H, Takeda S, Hunt T (2008). Cyclin-dependent kinases and cell-cycle transitions: does one fit all? *Nat Rev Mol Cell Biol* **9:** 910-916.

Hoffmann I, Clarke PR, Marcote MJ, Karsenti E, Draetta G (1993). Phosphorylation and activation of human cdc25-C by cdc2--cyclin B and its involvement in the self-amplification of MPF at mitosis. *Embo J* **12:** 53-63.

Holt LJ, Krutchinsky AN, Morgan DO (2008). Positive feedback sharpens the anaphase switch. *Nature* **454:** 353-357.

Hoover DM, Lubkowski J (2002). DNAWorks: an automated method for designing oligonucleotides for PCR-based gene synthesis. *Nucleic Acids Res* **30:** e43.

Huang HJ, Takagawa D, Weeks G, Pears C (1997). Cells at the center of Dictyostelium aggregates become spores. *Dev Biol* **192:** 564-571.

Iavarone A, King ER, Dai XM, Leone G, Stanley ER, Lasorella A (2004). Retinoblastoma promotes definitive erythropoiesis by repressing Id2 in fetal liver macrophages. *Nature* **432:** 1040-1045.

Jermyn KA, Williams JG (1991). An analysis of culmination in Dictyostelium using prestalk and stalk-specific cell autonomous markers. *Development* **111:** 779-787.

Ji P, Jiang H, Rekhtman K, Bloom J, Ichetovkin M, Pagano M *et al* (2004). An Rb-Skp2-p27 pathway mediates acute cell cycle inhibition by Rb and is retained in a partial-penetrance Rb mutant. *Mol Cell* **16:** 47-58.

Jiang Z, Zacksenhaus E, Gallie BL, Phillips RA (1997). The retinoblastoma gene family is differentially expressed during embryogenesis. *Oncogene* **14:** 1789-1797.

Jung CR, Hwang KS, Yoo J, Cho WK, Kim JM, Kim WH *et al* (2006). E2-EPF UCP targets pVHL for degradation and associates with tumor growth and metastasis. *Nat Med* **12:** 809-816.

Kaldis P (1999). The cdk-activating kinase (CAK): from yeast to mammals. *Cell Mol Life Sci* **55:** 284-296.

Kay RR, Jermyn KA (1983). A possible morphogen controlling differentiation in Dictyostelium. *Nature* **303:** 242-244.

Khidr L, Chen PL (2006). RB, the conductor that orchestrates life, death and differentiation. *Oncogene* **25:** 5210-5219.

Kimata Y, Baxter JE, Fry AM, Yamano H (2008). A role for the Fizzy/Cdc20 family of proteins in activation of the APC/C distinct from substrate recruitment. *Mol Cell* **32:** 576-583.

Knecht D, Pang KM (1995). Electroporation of Dictyostelium discoideum. *Methods Mol Biol* **47:** 321-330.

Kollmar M, Glockner G (2003). Identification and phylogenetic analysis of Dictyostelium discoideum kinesin proteins. *BMC Genomics* **4:** 47.

Koonce MP, Kohler J, Neujahr R, Schwartz JM, Tikhonenko I, Gerisch G (1999). Dynein motor regulation stabilizes interphase microtubule arrays and determines centrosome position. *Embo J* **18:** 6786-6792.

Korenjak M, Taylor-Harding B, Binne UK, Satterlee JS, Stevaux O, Aasland R *et al* (2004). Native E2F/RBF complexes contain Myb-interacting proteins and repress transcription of developmentally controlled E2F target genes. *Cell* **119:** 181-193.

Krek W, Nigg EA (1991). Mutations of p34cdc2 phosphorylation sites induce premature mitotic events in HeLa cells: evidence for a double block to p34cdc2 kinase activation in vertebrates. *Embo J* **10:** 3331-3341.

Krek W, Marks J, Schmitz N, Nigg EA, Simanis V (1992). Vertebrate p34cdc2 phosphorylation site mutants: effects upon cell cycle progression in the fission yeast Schizosaccharomyces pombe. *J Cell Sci* **102 (Pt 1):** 43-53.

Krek W, Livingston DM, Shirodkar S (1993). Binding to DNA and the retinoblastoma gene product promoted by complex formation of different E2F family members. *Science* **262:** 1557-1560.

Kumagai A, Dunphy WG (1991). The cdc25 protein controls tyrosine dephosphorylation of the cdc2 protein in a cell-free system. *Cell* **64:** 903-914.

Lammer C, Wagerer S, Saffrich R, Mertens D, Ansorge W, Hoffmann I (1998). The cdc25B phosphatase is essential for the G2/M phase transition in human cells. *J Cell Sci* **111 (Pt 16):** 2445-2453.

Leach CK, Ashworth JM, Garrod DR (1973). Cell sorting out during the differentiation of mixtures of metabolically distinct populations of Dictyostelium discoideum. *J Embryol Exp Morphol* **29:** 647-661.

Li H, Chen Q, Kaller M, Nellen W, Graf R, De Lozanne A (2008). Dictyostelium Aurora kinase has properties of both Aurora A and Aurora B kinases. *Eukaryot Cell* **7:** 894-905.

Liu F, Stanton JJ, Wu Z, Piwnica-Worms H (1997). The human Myt1 kinase preferentially phosphorylates Cdc2 on threonine 14 and localizes to the endoplasmic reticulum and Golgi complex. *Mol Cell Biol* **17:** 571-583.

Liu F, Rothblum-Oviatt C, Ryan CE, Piwnica-Worms H (1999). Overproduction of human Myt1 kinase induces a G2 cell cycle delay by interfering with the intracellular trafficking of Cdc2-cyclin B1 complexes. *Mol Cell Biol* **19:** 5113-5123.

Liu T, Mirschberger C, Chooback L, Arana Q, Dal Sacco Z, MacWilliams H *et al* (2002). Altered expression of the 100 kDa subunit of the Dictyostelium vacuolar proton pump impairs enzyme assembly, endocytic function and cytosolic pH regulation. *J Cell Sci* **115:** 1907-1918.

Lodish HF (2000). *Molecular cell biology*, 4th edn. W.H. Freeman: New York.

Loomis WF (1996). Genetic networks that regulate development in Dictyostelium cells. *Microbiol Rev* **60:** 135-150.

Lundberg AS, Weinberg RA (1998). Functional inactivation of the retinoblastoma protein requires sequential modification by at least two distinct cyclin-cdk complexes. *Mol Cell Biol* **18:** 753-761.

Lundgren K, Walworth N, Booher R, Dembski M, Kirschner M, Beach D (1991). mik1 and wee1 cooperate in the inhibitory tyrosine phosphorylation of cdc2. *Cell* **64:** 1111-1122.

Luo Q, Michaelis C, Weeks G (1994). Overexpression of a truncated cyclin B gene arrests Dictyostelium cell division during mitosis. *J Cell Sci* **107 (Pt 11):** 3105-3114.

Luo Q, Michaelis C, Weeks G (1995). Cyclin B and Cdc2 expression and Cd2 kinase activity during Dictyostelium differentiation. *DNA Cell Biol* **14:** 901-908.

Ma Q, Kintner C, Anderson DJ (1996). Identification of neurogenin, a vertebrate neuronal determination gene. *Cell* **87:** 43-52.

MacWilliams H, Gaudet P, Deichsel H, Bonfils C, Tsang A (2001). Biphasic expression of rnrB in Dictyostelium discoideum suggests a direct relationship between cell cycle control and cell differentiation. *Differentiation* **67:** 12-24.

MacWilliams H, Doquang K, Pedrola R, Dollman G, Grassi D, Peis T *et al* (2006). A retinoblastoma ortholog controls stalk/spore preference in Dictyostelium. *Development* **133:** 1287-1297.

MacWilliams HK, Bonner JT (1979). The prestalk-prespore pattern in cellular slime molds. *Differentiation* **14:** 1-22.

Maeda Y, Maeda M (1974). Heterogeneity of the cell population of the cellular slime mold Dictyostelium discoideum before aggregation, and its relation to the subsequent locations of the cells. *Exp Cell Res* **84:** 88-94.

Maeda Y (1986). A new method of inducing synchronous growth of Dictyostelium discoideum cells using temperature shifts. *J Gen Microbiol* 1189-1196.

Maeda Y (2005). Regulation of growth and differentiation in Dictyostelium. *Int Rev Cytol* **244:** 287-332.

Maeda Y (2011). Cell-cycle checkpoint for transition from cell division to differentiation. *Dev Growth Differ* **53:** 463-481.

Malumbres M, Barbacid M (2005). Mammalian cyclin-dependent kinases. *Trends Biochem Sci* **30:** 630-641.

Malumbres M, Barbacid M (2009). Cell cycle, CDKs and cancer: a changing paradigm. *Nat Rev Cancer* **9:** 153-166.

Marschalek R, Hofmann J, Schumann G, Gosseringer R, Dingermann T (1992). Structure of DRE, a retrotransposable element which integrates with position specificity upstream of Dictyostelium discoideum tRNA genes. *Mol Cell Biol* **12:** 229-239.

Mayanagi T, Maeda Y, Hirose S, Arakane T, Araki T, Amagai A (2004). Cloning, sequencing, and expression of the genomic DNA encoding the protein phosphatase cdc25 in Dictyostelium discoideum. *Dev Genes Evol* **214:** 510-514.

McDonald SA, Durston AJ (1984). The cell cycle and sorting behaviour in Dictyostelium discoideum. *J Cell Sci* **66:** 195-204.

McGowan CH, Russell P (1993). Human Wee1 kinase inhibits cell division by phosphorylating p34cdc2 exclusively on Tyr15. *Embo J* **12:** 75-85.

Michaelis C, Weeks G (1992). Isolation and characterization of a cdc 2 cDNA from Dictyostelium discoideum. *Biochim Biophys Acta* **1132:** 35-42.

Michaelis C, Weeks G (1993). The isolation from a unicellular organism, Dictyostelium discoideum, of a highly-related cdc2 gene with characteristics of the PCTAIRE subfamily. *Biochim Biophys Acta* **1179:** 117-124.

Millar JB, Blevitt J, Gerace L, Sadhu K, Featherstone C, Russell P (1991). p55CDC25 is a nuclear protein required for the initiation of mitosis in human cells. *Proc Natl Acad Sci U S A* **88:** 10500-10504.

Miyagishima SY, Kuwayama H, Urushihara H, Nakanishi H (2008). Evolutionary linkage between eukaryotic cytokinesis and chloroplast division by dynamin proteins. *Proc Natl Acad Sci U S A* **105:** 15202-15207.

Morgan DO (1995). Principles of CDK regulation. *Nature* **374:** 131-134.

Mortazavi A, Williams BA, McCue K, Schaeffer L, Wold B (2008). Mapping and quantifying mammalian transcriptomes by RNA-Seq. *Nat Methods* **5:** 621-628.

Mueller PR, Coleman TR, Kumagai A, Dunphy WG (1995). Myt1: a membrane-associated inhibitory kinase that phosphorylates Cdc2 on both threonine-14 and tyrosine-15. *Science* **270:** 86-90.

Muller GA, Quaas M, Schumann M, Krause E, Padi M, Fischer M *et al* (2011). The CHR promoter element controls cell cycle-dependent gene transcription and binds the DREAM and MMB complexes. *Nucleic Acids Res*.

Muramoto T, Chubb JR (2008). Live imaging of the Dictyostelium cell cycle reveals widespread S phase during development, a G2 bias in spore differentiation and a premitotic checkpoint. *Development* **135:** 1647-1657.

Murray AW, Hunt T (1993). *The cell cycle : an introduction*. W.H. Freeman: New York.

Musacchio A, Salmon ED (2007). The spindle-assembly checkpoint in space and time. *Nat Rev Mol Cell Biol* **8:** 379-393.

Nag DK, Tikhonenko I, Soga I, Koonce MP (2008). Disruption of four kinesin genes in dictyostelium. *BMC Cell Biol* **9:** 21.

Nakayama K, Nagahama H, Minamishima YA, Miyake S, Ishida N, Hatakeyama S *et al* (2004). Skp2-mediated degradation of p27 regulates progression into mitosis. *Dev Cell* **6:** 661-672.

Nellen W, Silan C, Firtel RA (1984). DNA-mediated transformation in Dictyostelium discoideum: regulated expression of an actin gene fusion. *Mol Cell Biol* **4:** 2890-2898.

Nieduszynski CA, Blow JJ, Donaldson AD (2005). The requirement of yeast replication origins for pre-replication complex proteins is modulated by transcription. *Nucleic Acids Res* **33:** 2410-2420.

Nikolic M, Dudek H, Kwon YT, Ramos YF, Tsai LH (1996). The cdk5/p35 kinase is essential for neurite outgrowth during neuronal differentiation. *Genes Dev* **10:** 816-825.

Norbury C, Blow J, Nurse P (1991). Regulatory phosphorylation of the p34cdc2 protein kinase in vertebrates. *Embo J* **10:** 3321-3329.

Novitch BG, Spicer DB, Kim PS, Cheung WL, Lassar AB (1999). pRb is required for MEF2-dependent gene expression as well as cell-cycle arrest during skeletal muscle differentiation. *Curr Biol* **9:** 449-459.

Ohmori T, Maeda Y (1987). The developmental fate of Dictyostelium discoideum cells depends greatly on the cell-cycle position at the onset of starvation. *Cell Differ* **22:** 11-18.

Ohtani K, DeGregori J, Nevins JR (1995). Regulation of the cyclin E gene by transcription factor E2F1. *Proc Natl Acad Sci U S A* **92:** 12146-12150.

Pagano M, Tam SW, Theodoras AM, Beer-Romero P, Del Sal G, Chau V *et al* (1995). Role of the ubiquitin-proteasome pathway in regulating abundance of the cyclin-dependent kinase inhibitor p27. *Science* **269:** 682-685.

Pardee AB (1989). G1 events and regulation of cell proliferation. *Science* **246:** 603-608.

Parikh A, Miranda ER, Katoh-Kurasawa M, Fuller D, Rot G, Zagar L *et al* (2010). Conserved developmental transcriptomes in evolutionarily divergent species. *Genome Biol* **11:** R35.

Pfaffl MW (2001). A new mathematical model for relative quantification in real-time RT-PCR. *Nucleic Acids Res* **29:** e45.

Pfleger CM, Kirschner MW (2000). The KEN box: an APC recognition signal distinct from the D box targeted by Cdh1. *Genes Dev* **14:** 655-665.

Pines J, Rieder CL (2001). Re-staging mitosis: a contemporary view of mitotic progression. *Nat Cell Biol* **3:** E3-6.

Pink RC, Wicks K, Caley DP, Punch EK, Jacobs L, Carter DR (2011). Pseudogenes: pseudo-functional or key regulators in health and disease? *RNA* **17:** 792-798.

Puig O, Caspary F, Rigaut G, Rutz B, Bouveret E, Bragado-Nilsson E *et al* (2001). The tandem affinity purification (TAP) method: a general procedure of protein complex purification. *Methods* **24:** 218-229.

Rabinovich A, Jin VX, Rabinovich R, Xu X, Farnham PJ (2008). E2F in vivo binding specificity: comparison of consensus versus nonconsensus binding sites. *Genome Res* **18:** 1763-1777.

Riabowol K, Draetta G, Brizuela L, Vandre D, Beach D (1989). The cdc2 kinase is a nuclear protein that is essential for mitosis in mammalian cells. *Cell* **57:** 393-401.

Robinson MD, McCarthy DJ, Smyth GK (2010). edgeR: a Bioconductor package for differential expression analysis of digital gene expression data. *Bioinformatics* **26:** 139-140.

Rogers GC, Rogers SL, Schwimmer TA, Ems-McClung SC, Walczak CE, Vale RD *et al* (2004). Two mitotic kinesins cooperate to drive sister chromatid separation during anaphase. *Nature* **427:** 364-370.

Rot G, Parikh A, Curk T, Kuspa A, Shaulsky G, Zupan B (2009). dictyExpress: a Dictyostelium discoideum gene expression database with an explorative data analysis web-based interface. *BMC Bioinformatics* **10:** 265.

Russell P, Nurse P (1986). cdc25+ functions as an inducer in the mitotic control of fission yeast. *Cell* **45:** 145-153.

Russell P, Nurse P (1987). Negative regulation of mitosis by wee1+, a gene encoding a protein kinase homolog. *Cell* **49:** 559-567.

Saeki M, Irie Y, Ni L, Yoshida M, Itsuki Y, Kamisaki Y (2006). Monad, a WD40 repeat protein, promotes apoptosis induced by TNF-alpha. *Biochem Biophys Res Commun* **342:** 568-572.

Sage J, Miller AL, Perez-Mancera PA, Wysocki JM, Jacks T (2003). Acute mutation of retinoblastoma gene function is sufficient for cell cycle re-entry. *Nature* **424:** 223-228.

Sambrook J, Fritsch EF, Maniatis T (1989). *Molecular Cloning: A Laboratory Manual*: New York.

Santamaria D, Barriere C, Cerqueira A, Hunt S, Tardy C, Newton K *et al* (2007). Cdk1 is sufficient to drive the mammalian cell cycle. *Nature* **448:** 811-815.

Satyanarayana A, Kaldis P (2009). Mammalian cell-cycle regulation: several Cdks, numerous cyclins and diverse compensatory mechanisms. *Oncogene* **28:** 2925-2939.

Schulkes CC, Verkerke-van Wijk I, Schaap P (1995). Transformation with vectors harboring the NEOR selection marker induces germination-specific adenylylcyclase activity in Dictyostelium cells. *Exp Cell Res* **220:** 505-508.

Schulz I, Erle A, Graf R, Kruger A, Lohmeier H, Putzler S *et al* (2009). Identification and cell cycle-dependent localization of nine novel, genuine centrosomal components in Dictyostelium discoideum. *Cell Motil Cytoskeleton* **66:** 915-928.

Sgarlata C, Perez-Martin J (2005). Inhibitory phosphorylation of a mitotic cyclin-dependent kinase regulates the morphogenesis, cell size and virulence of the smut fungus Ustilago maydis. *J Cell Sci* **118:** 3607-3622.

Sherr CJ, Roberts JM (1999). CDK inhibitors: positive and negative regulators of G1-phase progression. *Genes Dev* **13:** 1501-1512.

Soll DR, Yarger J, Mirick M (1976). Stationary phase and the cell cycle of Dictyostelium discoideum in liquid nutrient medium. *J Cell Sci* **20:** 513-523.

Sternfeld J, David CN (1982). Fate and regulation of anterior-like cells in Dictyostelium slugs. *Dev Biol* **93:** 111-118.

Stevense M, Chubb JR, Muramoto T (2011). Nuclear organization and transcriptional dynamics in Dictyostelium. *Dev Growth Differ* **53:** 576-586.

Szekely L, Jiang WQ, Bulic-Jakus F, Rosen A, Ringertz N, Klein G *et al* (1992). Cell type and differentiation dependent heterogeneity in retinoblastoma protein expression in SCID mouse fetuses. *Cell Growth Differ* **3:** 149-156.

Tanaka T, Veeranna, Ohshima T, Rajan P, Amin ND, Cho A *et al* (2001). Neuronal cyclin-dependent kinase 5 activity is critical for survival. *J Neurosci* **21:** 550-558.

Tavtigian SV, Simard J, Teng DH, Abtin V, Baumgard M, Beck A *et al* (2001). A candidate prostate cancer susceptibility gene at chromosome 17p. *Nat Genet* **27:** 172-180.

Thomas DM, Carty SA, Piscopo DM, Lee JS, Wang WF, Forrester WC *et al* (2001). The retinoblastoma protein acts as a transcriptional coactivator required for osteogenic differentiation. *Mol Cell* **8:** 303-316.

Thompson CR, Kay RR (2000a). Cell-fate choice in Dictyostelium: intrinsic biases modulate sensitivity to DIF signaling. *Dev Biol* **227:** 56-64.

Thompson CR, Kay RR (2000b). The role of DIF-1 signaling in Dictyostelium development. *Mol Cell* **6:** 1509-1514.

Toma JG, El-Bizri H, Barnabe-Heider F, Aloyz R, Miller FD (2000). Evidence that helix-loop-helix proteins collaborate with retinoblastoma tumor suppressor protein to regulate cortical neurogenesis. *J Neurosci* **20:** 7648-7656.

Toyoshima H, Hunter T (1994). p27, a novel inhibitor of G1 cyclin-Cdk protein kinase activity, is related to p21. *Cell* **78:** 67-74.

Tsai LH, Takahashi T, Caviness VS, Jr., Harlow E (1993). Activity and expression pattern of cyclin-dependent kinase 5 in the embryonic mouse nervous system. *Development* **119:** 1029-1040.

Ueda M, Graf R, MacWilliams HK, Schliwa M, Euteneuer U (1997). Centrosome positioning and directionality of cell movements. *Proc Natl Acad Sci U S A* **94:** 9674-9678.

Uhlmann F, Wernic D, Poupart MA, Koonin EV, Nasmyth K (2000). Cleavage of cohesin by the CD clan protease separin triggers anaphase in yeast. *Cell* **103:** 375-386.

Urlinger S, Baron U, Thellmann M, Hasan MT, Bujard H, Hillen W (2000). Exploring the sequence space for tetracycline-dependent transcriptional activators: novel mutations yield expanded range and sensitivity. *Proc Natl Acad Sci U S A* **97:** 7963-7968.

van den Heuvel S (2005). Cell-cycle regulation. *WormBook***:** 1-16.

Veltman DM, Keizer-Gunnink I, Haastert PJ (2009). An extrachromosomal, inducible expression system for Dictyostelium discoideum. *Plasmid* **61:** 119-125.

Vernon AE, Devine C, Philpott A (2003). The cdk inhibitor p27Xic1 is required for differentiation of primary neurones in Xenopus. *Development* **130:** 85-92.

Vernon AE, Philpott A (2003). A single cdk inhibitor, p27Xic1, functions beyond cell cycle regulation to promote muscle differentiation in Xenopus. *Development* **130:** 71-83.

Vicente JJ, Galardi-Castilla M, Escalante R, Sastre L (2008). Structural and functional studies of a family of Dictyostelium discoideum developmentally regulated, prestalk genes coding for small proteins. *BMC Microbiol* **8:** 1.

Wang M, Aerts RJ, Spek W, Schaap P (1988). Cell cycle phase in Dictyostelium discoideum is correlated with the expression of cyclic AMP production, detection, and degradation. Involvement of cyclic AMP signaling in cell sorting. *Dev Biol* **125:** 410-416.

Watts DJ, Ashworth JM (1970). Growth of myxameobae of the cellular slime mould Dictyostelium discoideum in axenic culture. *Biochem J* **119:** 171-174.

Weeks G, Weijer CJ (1994). The Dictyostelium cell cycle and its relationship to differentiation. *FEMS Microbiol Lett* **124:** 123-130.

Weijer CJ, Duschl G, David CN (1984). A revision of the Dictyostelium discoideum cell cycle. *J Cell Sci* **70:** 111-131.

Weinert TA, Kiser GL, Hartwell LH (1994). Mitotic checkpoint genes in budding yeast and the dependence of mitosis on DNA replication and repair. *Genes Dev* **8:** 652-665.

Winckler T (1998). Retrotransposable elements in the Dictyostelium discoideum genome. *Cell Mol Life Sci* **54:** 383-393.

Wood SA, Ammann RR, Brock DA, Li L, Spann T, Gomer RH (1996). RtoA links initial cell type choice to the cell cycle in Dictyostelium. *Development* **122:** 3677-3685.

Zacksenhaus E, Jiang Z, Chung D, Marth JD, Phillips RA, Gallie BL (1996). pRb controls proliferation, differentiation, and death of skeletal muscle cells and other lineages during embryogenesis. *Genes Dev* **10:** 3051-3064.

Zada-Hames IM, Ashworth JM (1978). The cell cycle and its relationship to development in Dictyostelium discoideum. *Dev Biol* **63:** 307-320.

Zimmerman W, Weijer CJ (1993). Analysis of cell cycle progression during the development of Dictyostelium and its relationship to differentiation. *Dev Biol* **160:** 178-185.

6. APPENDICES

Table S1 Microsoft Excel file containing data on *rblA*-repressed genes as well as a number of additional genes included for comparison. This table contains raw data on regulation by RblA, developmental regulation, and regulation in the cold-synchronization experiment. Macros are included to assist the user in graphing the expression profiles and calculating error bars. Gene IDs are linked to Dictybase. (.xls)